PhD-FSTC-2014-19
The Faculty of Sciences, Technology and Communication

DISSERTATION

Defense held on 07/07/2014 in Luxembourg

to obtain the degree of

DOCTEUR DE L'UNIVERSITÉ DU LUXEMBOURG

EN INFORMATIQUE

by

Dimitrios CHRISTOPOULOS
Born on 29 October 1986 in Athens, (Greece)

MULTIBEAM JOINT PROCESSING IN SATELLITE COMMUNICATIONS

Dissertation defense committee

Dr Björn Ottersten, dissertation supervisor
Professor and Director of SnT, University of Luxembourg

Dr Symeon Chatzinotas
Research Scientist, SnT, University of Luxembourg

Dr Peter Ryan, Chairman
Professor, University of Luxembourg

Dr Jens Krause
Senior Manager, Satellite Telecommunications Systems, SES

Dr. Riccardo De Gaudenzi, Vice Chairman
Head of Radio Frequency Systems, Payload and Technology Division., European Space Agency

Multibeam Joint Processing in Satellite Communications

Dimitrios Christopoulos

ISBN: 978-2-87971-135-5

Abstract

Cooperative Satellite Communications (SatComs) involve multi-antenna satellites enabled for the joint transmission and reception of signals. This joint processing of baseband signals is realized amongst the distinct but interconnected antennas. Advanced signal processing techniques –namely precoding and Multiuser Detection (MUD)– are herein examined in the multibeam satellite context. The aim of this thesis is to establish the prominence of such methods in the next generation of broadband satellite networks. To this end, two approaches are followed. On one hand, the performance of the well established and theoretically concrete MUD is analysed over the satellite environments. On the other, optimal signal processing designs are developed and evaluated for the forward link.

In more detail, the present dissertation begins by introducing the topic of multibeam joint processing. Thus, the most significant practical constraints that hinder the application of advanced interference mitigation techniques in satellite networks are identified and discussed. Prior to presenting the contributions of this work, the multi-antenna joint processing problem is formulated using the generic Multiuser (MU) Multiple Input Multiple Output (MIMO) baseband signal model. This model is also extended to apply in the SatComs context. A detailed presentation of the related work, starting from a generic signal processing perspective and then focusing on the SatComs field, is then given. With this review, the main open research topics are identified.

Following the comprehensive literature review, the first contribution of this work, is presented. This involves the performance evaluation of MUD in the Return Link (RL) of multiuser multibeam SatComs systems. Novel, analytical expressions are derived to describe the information theoretic channel capacity as well as the performance of practical receivers over

realistic satellite channels. Based on the derived formulas, significant insights for the design of the RL of next generation cooperative satellite systems are provided.

In the remaining of this thesis, the focus is set on the Forward Link (FL) of multibeam SatComs, where precoding, combined with aggressive frequency reuse configurations, are proposed to enhance the offered throughput. In this context, the alleviation of practical constraints imposed by the satellite channel is the main research challenge. Focusing on the rigid framing structure of the legacy SatCom standards, the fundamental frame-based precoding problem is examined. Based on the necessity to serve multiple users by a single transmission, the connection of the frame-based precoding and the fundamental signal processing problem of physical layer multigroup multicasting is established. In this framework and to account for the power limitations imposed by a dedicated High Power Amplifier (HPA) per transmit element, a novel solution for multigroup multicasting under Per Antenna Constraints (PACs) is derived. Therefore, the gains offered by multigroup multicasting in frame-based systems are quantified over an accurate simulation setting. Finally, advanced multicast and interference aware scheduling algorithms are proposed to glean significant gains in the rich multiuser satellite environment.

The thesis concludes with the main research findings and the identification of new research challenges, which will pave the way for the deployment of cooperative multibeam satellite systems.

To my father's great heart.

Acknowledgements

Firstly, I would like to thank my teacher, Prof. Björn Ottersten for enabling a wonderful three year journey towards new knowledge horizons. His continuous pursue for excellence has been the utmost inspiration towards shaping and fulfilling my goals. Secondly, I would like to thank my immediate supervisor, Dr. Symeon Chatzinotas, research scientist in the SnT, for his continuous support. His supervision helped discipline my research methods and encouraged me to overcome the day-to-day barriers. Thirdly, my most sincere gratitude is owed to my industrial supervisor, Dr. Jens Krause from SES, who substantiated the practical aspects of my work. With his involvement, a realistic value has been added in my research results. Besides by supervision committee, , I feel the need to thank Dr. Pantelis-Daniel Arapoglou, communications systems engineer in the ESA, for introducing me to the fascinating world of Satellite Communications. His immense interest in satcoms greatly motivated my work while our constructive discussions shaped interesting open problems. As result of these discussions I had the opportunity to experience three months in the ESA, invited by Dr. Alberto Ginesi Head of the Communication - TT&C Systems & Techniques Section of the ESA, whom I also thank for his immediate supervision. Finally, I would like to thank Dr. Riccardo de Gaudenzi, Head of RF Payload Systems Division, for serving as external reviewer of the present thesis and examiner during my defense. His interest in my work has been more than an honor, while his thorough examination enhanced my research. Finally, my colleagues in the SnT have created a professional everyday environment, that anyone would envy. Special thanks are dedicated to each and every member of the Signal Processing and Communications group of the SnT, and to the colleagues that helped with the proof reading of this thesis.

Besides the professional experience, this journey has greatly affected my personal life. For this I thank all the people that have been close to me during these years. It comes without saying, that I owe all my accomplishments to the support and love of my family. My father, Athanasios, my mother Aikaterini and my sister Maria. My childhood friends, who stayed close to me even from far away need to be thanked for helping me in good and bad moments. An unimaginable gratitude is owed to the people that came into my life while living in Luxembourg. People I never though I would ever come across and will always cherish in my heart.

Contents

List of Tables

List of Figures

Nomenclature

$[\cdot]_{ij}$	The i,j-th element of a matrix
$\lambda_{max}(\mathbf{X})$	Principal eigenvalue of matrix $\mathbf{X}$
$\lfloor\cdot\rfloor, \lceil\cdot\rceil$	Floor and Ceiling operations
$\mathbb{C}$	The set of complex numbers
$\mathbb{R}^+$	The set of real positive numbers
$\mathbf{X}$, $\mathbf{x}$	Matrices, Column vectors
$\mathcal{E}(\cdot)$	Expectation
$\mathrm{Tr}(\cdot)$	Trace
$\max_x, \min_x$	Maximum and minimum cost values over variable x
$\odot$	Hadamard product (element-wise product)
$\otimes$	Kronecker product
$\prod_{\mathbb{P}}$	Projection onto set $\mathbb{P}$
$\emptyset$	The empty set
$(\cdot)^\dagger$	Conjugate transpose
$(\cdot)^{\mathrm{T}}$	Transpose

Acronyms

ACM	Adaptive Coding and Modulation. 27, 35
APSK	Amplitude Phase Shift Keying. 35
ASI	Adjacent Satellite Interference. 163, 172
AWGN	Additive White Gaussian Noise. 40, 42
BC	Broadcast Channel. 40, 44
BS	Base Station. 49–51
CSI	Channel State Information. 31–33, 36, 50, 60, 87, 164, 170, 173, 177
DAS	Distributed Antenna System. 60
DPC	Dirty Paper Coding. 44–46, 53, 60
DVB – RCS2	second generation of Digital Video Broadcasting, return link over satellite. 32, 35
DVB – S2	second generation standard for Digital Video Broadcasting over Satellite. 27, 34
FEC	Forward Error Correction. 130
FL	Forward Link. 6, 29, 32, 33, 37, 40, 42, 60, 164, 176
FSS	Fixed Satellite Services. 33, 130
GEO	Geostationary. 130, 142, 162
GW	Gateway. 29–33, 36, 65, 76, 77, 79, 81, 137, 164, 167, 173
HPA	High Power Amplifier. 6, 33
HTS	High Throughput Satellite. 175, 176
LDPC	Low Density Parity Check. 35
LMS	Land Mobile Satellite. 57
LoS	Line-of-Sight. 39, 43, 88

MAC	Multiple Access Channel. 40, 42, 67
MC	Monte Carlo. 71, 77, 85
MF − TDMA	Multi-frequency Time Division Multiple Access. 32
MIMO	Multiple Input Multiple Output. 5, 39–44, 57, 58
MISO	Multiple Input Single Output. 30, 51, 52
MMSE	Minimum Mean Square Error. 42, 43, 47, 49, 57–59, 77–79, 176
MRC	Minimum Rate Constraint. 61
MSS	Mobile Satellite Services. 65
MUD	Multiuser Detection. 5, 42, 43, 79, 175
MU	Multiuser. 5, 40, 42–44, 57, 58, 67, 86, 176
NP	non polynomial in complexity. 126
PAC	Per Antenna Constraint. 6, 46, 48, 60, 61, 87–89, 109, 166
PHY	Physical Layer. 27, 28, 31, 33–35, 39, 50, 60
QCQP	Quadratically Constrained Quadratic Problem. 45
QoS	Quality of Service. 45, 88
R − ZF	Regularized Zero Forcing. 46, 47, 49, 58, 60
RL	Return Link. 5, 6, 29, 32, 33, 35, 37, 39, 42, 57–59, 65, 175, 176
RTT	Round Trip Time. 130
SDR	Semi-Definite Relaxation. 45
SIC	Successive Interference Cancellation. 42, 57, 59, 77–79, 82, 83
SIMO	Single Input Multiple Output. 67, 86, 176
SINR	signal-to-interference-plus-noise ratio. 44–47, 87, 152, 166
SNR	Signal-to-noise ratio. 42, 46, 60, 70, 77, 79, 171, 172
SPC	Sum Power Constraint. 51
SR	Sum Rate. 46, 48, 53, 61, 88, 105, 107, 129, 133, 152, 166, 171, 172
SSPA	Solid State Power Amplifier. 34
SoA	State-of-the-Art. 27, 31, 35, 39, 89, 176
TDD	Time Division Duplex. 49
TDMA	Time Division Multiple Access. 164

TDM	Time Division Multiplexing. 35
TWTA	Travelling Wave Tube Amplifier. 33, 34, 132
ULA	Uniform Linear Array. 60, 88
VSAT	Very Small Apperture Terminal. 35
ZF	Zero Forcing. 46, 48, 53, 58, 60, 164, 166, 171
SatCom	Satellite Communications. 5, 6, 27, 28, 31, 32, 34–37, 41, 56, 58–61, 130, 134, 142, 155–157, 175, 176

Chapter 1

Introduction

Existing SatCom standards, such as the second generation standard for Digital Video Broadcasting over Satellite (DVB − S2), operate under efficient Adaptive Coding and Modulation (ACM) schemes thus making significant progress in improving the spectral efficiencies of satellite networks. However, the constantly increasing demand for broadband and interactive satellite links emanates more aggressive reuse of the available resources, striving towards terabit throughput. As this reuse is bound to increase the intra-system interference, novel interference mitigation techniques are substantiated. In this direction, the objective of the present thesis is to investigate multiuser joint processing techniques for multibeam satellite systems.

The State-of-the-Art (SoA) in high throughput SatCom systems relies on multibeam antennas. These multibeam architectures allow for a significant boost in capacity by reusing the available Physical Layer (PHY) resources (i.e. frequency and/or polarization) several times within the coverage area. Typically three or four color frequency reuse schemes are employed to mitigate the inter-beam (intra-system) interference. Consequently, multibeam satellites exploit the reuse of the scarce PHY resources to achieve hundreds of Gbps capacity. Predominantly in the higher frequency bands, a large number of recent satellite procurements have clearly confirmed the multibeam trend as a broadband reference system architecture. Examples include systems such as Wildblue-1 [1] and Anik F2 [2] (66 Ka-band spot beams) covering parts of America and Kasat (82 Ka-

band spot beams) for mainly fixed two-way (i.e., interactive) broadband applications as well as the GlobalExpress system designed for a new generation of mobile services in Ka-band over Europe [3]. Interactive broadband services, in particular, benefit from these architectures since a finer partitioning of the coverage area facilitates parallel data stream transmissions. This allows for the most recently deployed systems, like Viasat-1 (72 spot beams in Ka-band) [4], to offer more than 100 Gbps of total capacity. In spite of the already deployed systems, the foreseeable future requirements in satellite capacity are beyond the capabilities of conventional multibeam communications payload of a satellite (hereafter simply referred to as payload unless stated otherwise). On one hand, these systems are limited by self-interference (i.e. inter-beam interference). As a result, limitations on the reuse of the available PHY resources are introduced. On the other hand, the number of beams required to cover a specific area cannot be arbitrarily increased since the diffraction rules of the signals propagating through the atmosphere impose a minimum radius of each antenna footprint. Hence, the necessity to explore novel system architectures arises.

Next generation SatComs networks are striving for terabit capacity [5–9]. They are expected to deliver high throughput, interactive services to low cost, spectrally efficient terminals. Since the realization of the terabit satellite by the means of conventional frequency/polarization reuse schemes is inhibited by intra-system interference, fractional resource reuse over the multiple beams is evidently not the solution for the terabit satellite [10]. Therefore, more aggressive reuse is emanated towards covering the expected demand in connectivity via satellite. To the end of managing the resulting interference, novel interference mitigation techniques are considered a promising new tool for the design of future SatComs.

The present thesis discusses the application of novel baseband signal processing techniques, referred to as multibeam joint processing, over envisaged full frequency compatible multibeam satellite payloads. These techniques are capable of managing interference via the spatial degrees of freedom offered by the multiple antennas, thus enabling aggressive frequency reuse schemes. As it will be shown, the application of such techniques in multibeam satellite systems, operating in more aggressive frequency reuse configurations, paves the way towards extremely high throughput SatComs. In this direction, this work attempts to bridge some of the substantial gaps between information theoretic results [11]

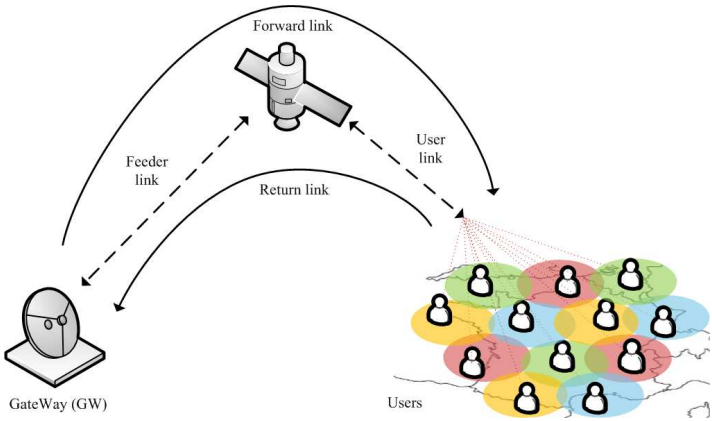

Figure 1.1: Multibeam Satellite System

and practical implementation of multibeam joint processing.

1.1 Multibeam Satellite Networks

In satellite networks, information is transmitted either from the Gateway (GW) to the users, i.e. the FL, or from the users back to the GW, i.e. the RL. Each of these paths is comprised of two wireless links, namely the uplink, connecting a ground segment (GW or user terminal) with the satellite and the downlink, vice versa. A diagram of a typical satellite network is given in Fig. 1.1, where the wireless links of issue are illustrated. The notion of a feedback link is also given, which can be established either over the wireless RL uplink or over other networks (e.g. terrestrial networks can offer low rate links).

The focus of the present work is on increasing the offered throughput of the satellite network. The bottleneck of this network lies in the user link where a large number of users are competing over a limited amount of resources. A first step to reduce this obstacle has been the introduction of multibeam antennas that facilitate frequency reuse, by spatially separating co-channel users. Due to the antenna imperfections however, residue interference still limits the system. A simple example of an on-board

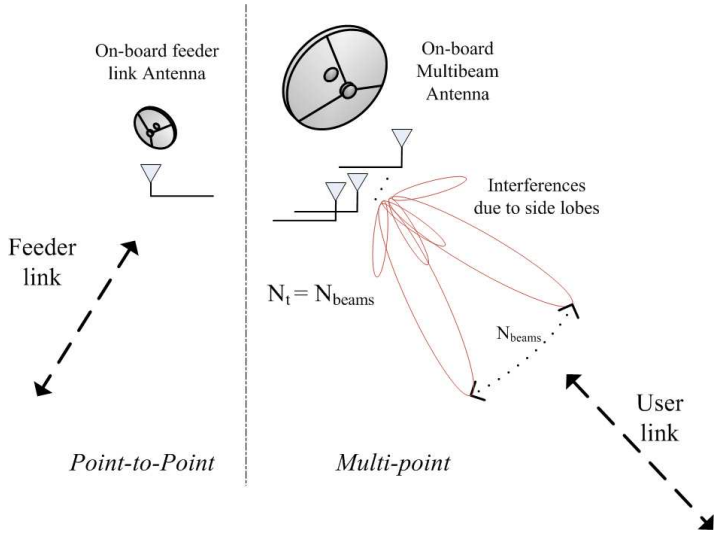

Figure 1.2: Multibeam Antenna

multibeam antenna is presented in Fig. 1.2

In a multibeam system, the fundamental attribute of the user link is the existence of multiple antennas at the satellite that are simultaneously serving multiple users over the coverage. Therefore, a multiuser multiple antenna channel is realized. In the return link, it can be viewed as a multiuser single input (single antenna users are assumed) multiple output (the multibeam antenna is the receiver) channel. In the forward link, as a Multiple Input Single Output (MISO) channel. Under this perspective, the present work proposes realistic solutions for the enhancement of the multiuser multi-antenna user link.

It should be pointed out, that a real satellite system is limited by the capacity of the feeder link (i.e. the link between the satellite and the GW). Since the feeder link is a point to point link, frequency multiplexing is necessary. Subsequently, an increase in the user sum-rate, requires proportional increase in the bandwidth of the feeder link. Higher frequency bands (e.g. Q/V bands) for this case are being considered in the design of

the future terabit satellite [12–14]. However, the study of this wireless link is beyond the purposes of the present work and will be therefore assumed ideal.

The key advantage of applying multiple antenna signal processing in SatComs lies in the inherent nature of multibeam satellite networks: a large number of antennas are illuminating a vast coverage area, while all return link signals are processed in one or more central locations, namely the GWs. A transparent multibeam satellite illuminating central Europe with 12 beams is given in Fig. 1.1. For a typical multibeam satellite covering Europe, more than 200 beams are expected to be deployed. The SoA techniques developed and evaluated in the present thesis are motivated by the inherent characteristics of satellite communications which impose specific constraints. An overview of these constraints is given in following sections.

1.1.1 Practical Constraints

Albeit the throughput enhancement provided by cooperative techniques in satellite networks, as in detail presented in the following, several issues arise with the adoption of these techniques in SatComs and need to be addressed. These practical constraints are identified as follows:

1. Channel State Information (CSI) is a requisite for the application of multibeam joint processing. A discussion on CSI acquisition is given in Sec. 1.2.

2. Aggressive reuse of the PHY resources proportionally increases the on-board payload requirements, as developed in Sec. 1.3.

3. An increase in the capacity of the user link of the multibeam system can only be enabled by a proportional increase in the capacity of the feeder link. The need to deploy multiple GWs to cover the feeder link requirements is discussed in Sec. 1.5.

4. The rigid framing structure of SatCom standards introduces constraints in the application of signal processing in SatComs. More details on this will are presented in 1.4

5. The effect of the non-linear satellite channel over multibeam joint processing methods. This topic is considered the most prominent future extension of this work.

More details on these practical constraints are given in the following sections.

1.2 Channel State Acquisition

CSI is one of the most important enablers for the application of the multibeam joint processing techniques. In the context of SatComs, channel knowledge can be acquired at the end-user ground stations and then fed back to the GW. More specifically, CSI should be available at the GW so that multiuser precoding can be performed for the FL and joint decoding at the RL. Current standards are using pilot sequences, either available within the standard as an optional feature (i.e., for DVB-S2 [16]) or defined within the specified requirements for the transmission burst structure of the Multi-frequency Time Division Multiple Access ($MF-TDMA$) return channel. For instance, for the second generation of Digital Video Broadcasting, return link over satellite ($DVB-RCS2$) [17]. The current state of the art reference transmission standards are well suited for the adaptation of the proposed multibeam satellite systems. In more detail, CSI is acquired by broadcasting pilot signals through the FL to all terminals which in turn measure them and feed the quantized measurements back to the GW through the RL. In most cases, FL and RL operate in different frequency bands and thus the described process yields the FL CSI. Nevertheless, it is often assumed that the two link are reciprocal (especially if they are adjacent in frequency) and as a result the measured CSI can be also used for the RL. Furthermore, the CSI acquisition process in SatComs introduces a long delay which may result in outdated CSI. This complication is especially acute for the FL where CSI is needed before transmission in order to calculate the precoding vectors. In the RL, CSI is only needed for decoding and therefore it can be transmitted by the terminals along with their data.

Based on this discussion, in the following sections we focus on fixed terminals for the FL (slow-varying channel) and mobile terminals for the RL. In the latter case, the joint decoding techniques can be applied either for fixed or mobile satellite services. As a matter of fact, the slow fading channel would even lead to simpler practical implementation since CSI is easier to acquire. However, this distinction has been made in order to point out one main difference between the forward and the return links. In the RL, the channel estimates can be sent along with the transmitted

data. This introduces much less delay when compared to FL case, where the pilot signal needs to be transmitted and fed back to the GW before the precoding matrix can be calculated, leading to approximately double time delay compared to the RL case. This substantial difference in the CSI acquisition procedure, leads to the definition of the specific scenarios. Nevertheless, the proposed analysis is straightforwardly applicable to Fixed Satellite Services (FSS), by omitting the shadowing coefficients in the definition of the channel matrix.

1.3 Aggressive Frequency Reuse Payloads

Conventional payloads, typically employ Travelling Wave Tube Amplifiers (TWTAs) as on-board HPAs. Despite its reliability, this equipment significantly burdens the multibeam satellite in terms of weight and power requirements. To optimize the payloads, multiple beams are amplified by a single HPA. In more detail, a four color frequency reuse scheme is commonly realized by splitting the available frequency/polarization resources into four colors: half the available bandwidth and one circular polarization (right hand-RHCP or left hand - LHCP) define one color. Then adjacent beams are allocated a different color (i.e. polarization and frequency combination), so that an adequate signal to interference plus noise ratio can be attained at the receive side. As a result, an x number of beams will reuse $x/4$ times the available PHY resources. In this configuration, since half of the total user link bandwidth is used in each beam, a single TWTA can be dedicated to every two beams. By advancing to more aggressive reuse schemes, e.g. 2 color reuse, some of the adjacent beams will be operating over the same resources, thus greatly increasing the intra-system interference. In this case, x beams will provide $x/2$ times the PHY resources at the expense of requiring two TWTAs per beam, one for each polarization. By pushing the reuse to the extreme, a full frequency reuse scheme provides the highest possible linear increase of the PHY resources with the number of antennas, since x beams will reuse all resources x times. Nevertheless, all adjacent beams will be co-channel and interference will tremendously increase. Also, two TWTAs per beam will be necessary. The only plausible realization of such scenarios is via joint multibeam signal processing as it will be shown in the following.

Since signal processing methods will be designed to mitigate the increased interference, the second fundamental limitation for the applica-

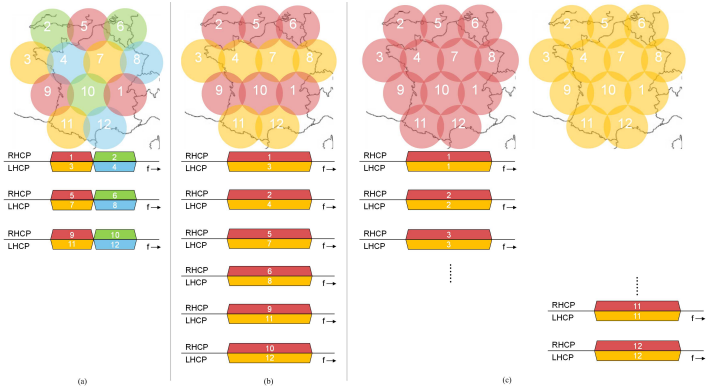

Figure 1.3: Payload complexity increase due to aggressive frequency reuse.

tion of aggressive frequency reuse, namely the added on-board complexity, needs to be addressed. The heavy TWTAs hinder the deployment of full frequency reuse payloads that accommodate a large number of antennas. Nevertheless, future multibeam payloads compatible with full frequency are enabled by the already developed low cost, efficient, reliable and low weight Solid State Power Amplifier (SSPA) [18].

The payload complexity increase is illustrated in Fig. 1.3

1.4 SatCom Standards

The PHY design of SatCom standards encompasses long forward error correction codes to cope with noise limited channels and long propagation delays. Besides block coding, synchronization issues and fade mitigation techniques that rely on an adaptive link layer design (ACM) also necessitate this structure. More specifically, DVB − S2 is the latest generation standard for SatComs enabling broadband and interactive services via satellite [19]. It has been designed for broadcasting services (standard and high definition TV), internet and professional services such as TV contribution links and digital satellite news gathering [16]. During the formulation of DVB − S2, three main concepts were carefully considered: (a) best transmission performance approaching the Shannon limit, (b)

total flexibility and (c) reasonable receiver complexity [20]. High performance and low complexity iterative decoding schemes like Low Density Parity Check (LDPC) codes along with high order Amplitude Phase Shift Keying (APSK) modulations were adopted for efficient operation over the nonlinear satellite channel in the quasi error free region. Compared to previous standards, the second generation standard attains 20–35% capacity increase or alternatively 2–2.5 dB more robust reception for the same spectrum efficiency by virtue of the advanced waveforms. Furthermore, to facilitate the provision of interactive services, the standard features operation under a great range of ACM parameters. When used for interactive services, ACM allows optimization of the transmission parameters adaptive to varying path conditions [21,22]. The optimization of the transmission parameters is also possible in combination with Time Division Multiplexing (TDM) data for multiple receivers. Transmission parameters can change instantaneously one a frame-by-frame basis. Hence, resources are optimally exploited, since operation under a constant fading margin according to a worst case scenario design, is no longer necessary.

Focusing on the the most recent extensions of the second generation digital video broadcasting for satellite standard, DVB − S2X [23], specific modifications allow for the application of signal processing techniques. The introduction of a framing constraint in the precoding design is plausible due to the latest evolution of SatCom standards [23], where PHY frames can be perfectly aligned in time over the beams. Consequently, precoding needs to be applied without changing the optimized PHY design[1]. However, the unequal data payloads that correspond to each user, along with the variable number of users per frame, hinder the calculation of a precoding matrix on a user-by-user basis. Therefore, despite the optimality, in the channel capacity sense, of channel-by-channel precoding, practical system implementations impose a frame based precoding design.

As far as the RL is concerned, DVB − RCS2 is the new generation, Very Small Apperture Terminal (VSAT) standard that has recently been approved by the DVB technical module as common PHY standard. This standard improves the existing mature DVB-RCS by including SoA channel coding and highly efficient modulation schemes. Hence, the efficiency and the flexibility of the return channel operational modes is enhanced.

[1] It should be noted that the PHY design is optimized to cope with the inherent attributes of the satellite channel such as long propagation delay and low signal power and is therefore challenging to modify it in favor of the signal processing methods.

All of these standards have been devised for large multiuser satellite two-way systems and can be adapted to the proposed multibeam processing techniques.

1.5 Multiple Gateways

High throughput satellite systems have to be supported by multiple GWs. Due to feeder link limitations, one single GW cannot accommodate the total number of employed beams thus necessitating multiple GWs to serve large multibeam systems. In the present work, to perform multibeam joint processing, both for the forward and the return links, a centralized precoder and decoder respectively is assumed. This theoretical assumption can be supported by a real system implementation via two approaches. One solution would be the exploitation of higher frequency bands for the feeder link (optical feeder links), assuming that such a system can be practically employed. As a result, a single GW could serve the multibeam satellite system. Alternatively, another approach is the full interconnection amongst the multiple GWs so that they all share the same data (CSI and data). The second approach is easier to implement if we consider the bandwidth capabilities of broadband cable networks. Of course, the added delay is an issue to be considered, especially in the SatComs context where delay is already a major issue. Subsequently, both approaches lead to the verification of the simplistic assumption of cooperative system that utilizes a central precoder/decoder. Additionally, although this contribution does not tackle the subject of decentralized precoding/decoding, works in the existing literature examine the performance degradation effects of the adoption of decentralized precoder designs, for the case where full GW interconnection cannot be assumed. An example of such an approach for multibeam satellite systems can be found in [24] where the level of cooperation amongst GWs is examined and the most promising technique is shown to be partial data and CSI exchange among the interconnected GWs.

1.6 Scope

The scope of the present thesis is twofold. Firstly it is meant to provide an overview of the application of multibeam joint processing techniques in the forward and return link of satellite networks. These techniques

have the potential of being incorporated in future satellite payloads with minor modifications on the state of the art equipment. To this end, the performance gains of multibeam joint processing techniques are derived under realistic assumptions.

Secondly, novel signal processing methods –inspired by the inherent attributes of SatComs– are developed, towards enabling the adoption of joint processing over satellite. Therefore, the main practical constraints in current systems that may inhibit the application of precoding are identified and tackled. Thus, the current state of the art in signal processing techniques are extended to account for practical constraints that are of utmost importance for SatComs.

The present thesis is structured as follows. In Ch. 2 the problem under investigation is analytically formulated. A detailed description of the applicable system model is presented, the related state of the art is discussed and the contributions over it are explicitly given. Following this, the technical contributions are described in Ch. 3, 4, 5 and 6, while Ch. 7 concludes the findings of this thesis.

In more detail, Ch. 3 presents closed-form derivations that describe the capacity of the RL of multibeam joint decoding satellites, under realistic channel assumptions. In Ch. 4, the extension of a fundamental signal processing problem, namely the multigroup multicasting, to account for individual constraints on the per-antenna transmit power is given. Moreover, the application of precoding in the FL of aggressive frequency reuse multibeam satellites is investigated under realistic system level assumptions in Ch.5. Therein, novel signal processing methods are developed for precoding over satellite. Following this, Ch. 6 proposes the exploitation of user scheduling towards further enhancing the performance of the multibeam satellite transmitter. In this direction, novel scheduling algorithms are presented. Finally, the results of the thesis are summarized in Ch. 7, along with the way forward.

Chapter 2

Problem Formulation

Multibeam Joint Processing is tackled in the present thesis from a PHY perspective. In the present chapter, the problem of multibeam joint processing is formally defined. The problem formulation is based on the baseband MIMO signal model. In this context, the main point of reference is the so-called channel matrix **H**. Towards accurately modeling the inherent attributes of the satellite channel, the present work proposes a generalized multibeam satellite channel model. Thus, the channel matrix **H** will include the inherent attributes of the baseband memoryless satellite channel. This model has the flexibility to include (a) the multibeam antenna characteristics, (b) the rank deficiencies introduced by the Line-of-Sight (LoS) signal components and the antenna correlation, (c) the shadowing due to user mobility and (d) the rain fading. In parallel with the problem formulation, previous related works that are based on similar models are also described in the present chapter. The contributions of this thesis over these SoA works, will conclude the chapter.

2.1 Multiuser MIMO communications

Starting from the early years of the past decade, MIMO communications are nowadays established as the most promising transmission method for the future broadband wireless communications. The concept of jointly processing the signals at the multi-antenna array of the receiver and/or the transmitter, is enabling the conversion of the interference RL and/or

FL channels of the MIMO system into a Broadcast Channel (BC) and/or Multiple Access Channel (MAC) respectively. Before proceeding to the transceiver architectures, the general vector channel model of MIMO communications will be introduced.

2.1.1 Signal Model

When multiple independent user terminals (herein refereed to as users) communicate with a single multi-antenna transceiver, then a MU MIMO system is realized. Let N_t denote the number of transmit antennas and N_u the total number of users simultaneously served. Under the assumption of multiple single antenna users up-linking to a multi-antenna receiver, the received signal at the at the j-th receive antenna is given as

$$y_j = \mathbf{h}_{j,UL}^{\dagger}\mathbf{x} + n_j, \tag{2.1}$$

where $\mathbf{h}_{j,UL}$ is a $N_u \times 1$ vector composed of the baseband channel coefficients (i.e. channel gains and phases) between the N_u users and the j-th antenna of the receiver, $\mathbf{x}$ is the $N_u \times 1$ vector of the transmitted symbols and n_j is the independent complex circular symmetric (c.c.s.) independent identically distributed (i.i.d) zero mean Additive White Gaussian Noise (AWGN), measured at the j-th receive antenna. Equivalently, assuming a multiple antenna transmitter and multiple single antenna receivers, the received signal at the i-th user reads as

$$y_i = \mathbf{h}_{i,DL}^{\dagger}\mathbf{x} + n_i, \tag{2.2}$$

where $\mathbf{h}_{i,DL}$ is a $N_t \times 1$ vector composed of the baseband channel coefficients between the i-th user and the N_t antennas of the transmitter, while $\mathbf{x}$ is the $N_t \times 1$ vector of the transmitted symbols and n_i is the AWGN, measured at the i-th user's receive antenna.

Clearly, the general input output signal model of MIMO communications can apply for the forward and the return links. By collecting all user channels in one channel matrix, the general linear signal model in vector form reads as

$$\mathbf{y} = \mathbf{H}\mathbf{x} + \mathbf{n}, \tag{2.3}$$

where the vector dimensions depend on the link under study. Therefore, the channel matrix $\mathbf{H}$ constitutes the main point of references in the baseband modeling of the physical layer of MIMO communications.

Under the assumption of channel reciprocity, a channel matrix can model either the return or the forward link of the multi-antenna channel by a simple transposition. However, focusing on SatComs, different frequency bands are commonly adopted for the two links thus invalidating the reciprocity assumption. Despite the fact that the UL and DL indices will be hereafter dropped for ease of notation, different coefficients will be typically employed for the modeling of $\mathbf{h}_{i,DL}$ and $\mathbf{h}_{n,UL}$. To facilitate the reader, the dimensions of the channel vectors and the way their elements are generated will be explicitly defined, in each section. The state-of-the-art on MIMO receiver and transmitter architectures will be in detail described in the following sections.

2.2 Receiver Architectures

When a single or even multiple MIMO receivers cooperate to serve multiple users over the same coverage area, multicell joint processing architectures can be realised. Multicell joint decoding was firstly introduced by [25, 26]. Since then, the initial results have been extended for more practical propagation environments, transmission techniques and backhaul infrastructures in an attempt to better quantify the joint processing performance gain. More specifically, it was demonstrated in [27] that fading promotes multiuser diversity which is beneficial for the ergodic capacity performance. Following that, realistic path-loss models and user distribution were investigated in [28, 29], where closed-form capacity expressions based on the cell size, path loss exponent and user spatial probability density function (p.d.f.) were provided. The beneficial effect of MIMO links was established in [30, 31], where a linear scaling with the number of BS antennas was proven. However, the correlation between multiple antennas has an adverse effect as shown in [32], especially when it affects the BS-side. Imperfect backhaul connectivity has also a negative effect on the capacity performance as quantified in [33]. Finally, limited or partial CSI availability will result in degraded performance, as proven in [34–36].

2.2.1 Multiuser Detection in the MIMO MAC

Successive Interference Cancellation

When multiple users are jointly processed by a hyper-receiver then a MIMO MAC is realized and MUD is performed. With respect to the MIMO MAC, Successive Interference Cancellation (SIC) performed at the receive side is proven to be the sum-rate capacity achieving strategy [27,37,38]. In more detail, the capacity of the independent identically distributed (i.i.d.) AWGN MIMO channels was first calculated in [39]. As a result, the well celebrated $\log - \det$ formula provides the mutual information of a Gaussian linear vector memoryless channel conditioned on the channel matrix [37]. Thus, channel capacity can be practically calculated by averaging the mutual information over many realizations of a probabilistic matrix that contains the channel gain coefficients between each user and each antenna [40]. If we assume that in the MU-MIMO MAC system, each user transmits at the same power (uniform power allocation), then the ergodic capacity is given by [39]

$$\mathrm{C}_{\mathrm{erg}} = \mathcal{E}\left\{\log_2 \det\left(\mathrm{I}_{N_r} + \gamma \mathbf{H}\mathbf{H}^{\dagger}\right)\right\}, \tag{2.4}$$

in bits/sec/Hz (bps/Hz). In the following, for notational simplicity and since the number of receive antennas in the RL, N_r is equal to the number of transmit antennas in theFL, N_t the later notation will only be employed. Hence, and since the focus is on the return link, $\mathbf{H} \in \mathbb{C}^{N_t \times N_u}$. Eq. (2.4) assumes no coordination among transmit antennas, so every user transmits at the same transmit Signal-to-noise ratio (SNR), also denoted as γ), which represents the ratio of the power transmitted by every user over the equivalent noise power at each receive antenna.

MMSE Receivers

A more practical receiver implementation which only considers Minimum Mean Square Error (MMSE) filtering of the received signals followed by singe user decoding. The reduced-complexity linear receiver [41, 42] aims at minimizing the mean squared error between the transmitted and the detected signal with the use of MMSE filters conditioned on the channel. The outputs of the filters are subsequently fed into conventional single-

user decoders. In this case, the spectral efficiency reads as

$$\mathrm{C}_{\mathrm{mmse}} = \frac{1}{N_u}\mathcal{E}\left\{\sum_{i=1}^{N_u} -\log_2\left[\left(\mathrm{I}_{N_u} + \gamma\mathbf{H}^{\dagger}\mathbf{H}\right)^{-1}\right]_{ii}\right\}. \tag{2.5}$$

The main limitation of the MMSE receiver is that the number of users that can be effectively filtered is limited by the rank of the channel matrix, which is at most equal to the total number of receive antennas in the system. This limitation applies for all linear signal processing techniques, and it originates from the linear dependence of the row vectors forming an overloaded channel matrix. In simpler words, when receive dimensions are less than the transmit then channel inversion is not possible since some of the channel vectors are bound to be linearly dependent. During the last decade, extensive research in terrestrial cellular systems employing MUD techniques has proved that substantial capacity gains exist, amid Rayleigh fading and antenna correlation [28,32]. The aforementioned contributions use free probabilistic methods and asymptotic analysis over the eigenvalues of the channel matrices. Under relevant channel assumptions, closed form capacity formulas, also using asymptotic analysis and deterministic equivalents were derived in [43]. The first result for the capacity of a joint-processing system can be found in [27] where multipath fading is proven to be beneficial. Attempts to incorporate the effect of LoS components can be found in [44] while the addition of lognormal shadowing was firstly introduced in [45]. Lognormal fading was also incorporated in the channel model leading to a composite Rayleigh/lognormal channel model in [46], where tight lower ergodic capacity bounds were derived. Rayleigh lognormal fading was also considered in [47–49]. Finally, several other fading combinations were considered, such as Nakagami-lognormal MIMO [50] and generalized-K composite fading channels [51, 52].

2.3 Transmitter Architectures

Advanced interference mitigation techniques are enabled by MU MIMO communications. In this context, the exploitation of transmit spatial degrees of freedom towards precanceling the multiuser interference, is known as precoding (or equivalently transmit beamforming).

2.3.1 Precoding in the MIMO BC

Precoding is a multiuser signal processing technique that separates user data streams in different beamforming directions [53]. Let us denote s_k, $\mathbf{w}_k$ as the unit power symbol and the $N_t \times 1$ transmit precoding vector corresponding to the k-th user. For now, the assumption of a one to one correspondence between the transmit symbols and the users is made. This assumption will hereafter be referred to as unicasting. The precoded transmit signal reads as

$$\mathbf{x} = \sum_{k=1}^{N_u} \mathbf{w}_k s_k \tag{2.6}$$

Subsequently, when beamforming is employed, (2.2) will become

$$y_k = \mathbf{h}_k^\dagger \mathbf{w}_k s_k + \mathbf{h}_k^\dagger \sum_{j \neq k} \mathbf{w}_j s_j + n_k, \tag{2.7}$$

where $\mathbf{h}_k$ is an $N_t \times 1$ complex vector. The first term of the summation refers to the useful signal and the second to the interference. The column vector $\mathbf{w}_k$ with $1 \times N_t$ dimensions is the k-th user's precoding vector, that is the k-th column of a total precoding matrix $\mathbf{W} = [\mathbf{w}_1, \mathbf{w}_2, \ldots, \mathbf{w}_k]$. The signal-to-interference-plus-noise ratio (SINR) at each user is given by

$$\mathrm{SINR}_k = \frac{|\mathbf{h}_k^\dagger \mathbf{w}_k|^2}{\sum_{j \neq k} |\mathbf{h}_k^\dagger \mathbf{w}_j|^2 + 1}. \tag{2.8}$$

When beamforming is employed, determining the optimal precoding vectors is tedious in practice. In the following paragraph the optimal in the channel capacity sense precoding scheme is presented.

Dirty Paper Coding

Dirty Paper Coding (DPC) is known to be the sum-rate capacity-achieving technique in MU MIMO downlink. In other words, the capacity of the MIMO BC channel can be achieved by DPC as shown in [54, 55]. Hence, it is used as an upper bound for the suboptimal, linear techniques. As a non-linear technique, DPC is based on the idea of known interference precancelation while serially encoding user signals. More specifically, DPC allows for the cancelation of the interference of the previously, serially encoded users, thus causing no interference to the following users. Let us

now assume that $\pi_0 = \{1, 2, ..., K\}$ is a trivial user encoding order. Then, the received SINR at user k is

$$\mathrm{SINR}_k^{\mathrm{DPC}} = \frac{|\mathbf{h}_k^\dagger \mathbf{w}_k|^2}{\sum_{j>k} |\mathbf{h}_k^\dagger \mathbf{w}_j|^2 + 1}. \tag{2.9}$$

With DPC, the throughput maximization problem under individual power constraints has been solved using the principles of duality [56]. converting it into a dual uplink with sum power constraint across users and uncertain noise and employing an interior-point algorithm . It should be noted that although the sum-rate capacity can be achieved by all user encoding orders, the individual user rates will vary. As a result, the employed encoding order can only affect the individual user rates. However, the implementation complexity of dirty paper coding [55] led to the development of less complex, linear techniques.

Linear Precoding

Focusing on generic linear precoding methods, the transmitter is given the flexibility to design the precoding matrix with a given optimization goal under well defined constraints. Thus, the precoding matrix is not constrained to a specific structure but it can be calculated as the solution of an optimization problem that achieves predefined targets. Formally, the generic linear precoding problem is defined as

$$\boxed{\begin{aligned} &\max_{\{\mathbf{W}\}} \ f\left(\mathrm{SINR}_k\right) \\ &\text{s.t.} \quad g\left(\mathbf{W}\right) \leq C_k, \end{aligned}}$$

where functions f, g and the constraints C_k are problem dependent. The optimal downlink transmission strategy, in the sense of minimizing the total transmit power under guaranteed per user Quality of Service (QoS) constraints, was given in [57, 58]. Therein, the powerful tool of Semi-Definite Relaxation (SDR) reduced the non-convex Quadratically Constrained Quadratic Problem (QCQP) into a relaxed semi-definite programming instance by changing the optimization variables and disregarding the unit-rank constraints over the new variable. The relaxed solution was proven to be optimal. In the same direction, the multiuser downlink beamforming problem that aims at maximizing the minimum over all

users SINR, was optimally solved in [59]. The goal of the later formulation is to increase the fairness of the system by boosting the SINR of the user that is further away from a targeted performance. Hence, the problem is commonly referred to as *max–min fair*. The more elaborate transmit beamforming problem under per-antenna power constraints (PACs) was formulated and solved in [60]. Finally, the derivation of the optimal in the sum rate maximization sense (max Sum Rate (SR)) is a considerably complicated problem [61].

Some well known solutions of the linear precoding optimization problem are presented in the following.

Zero Forcing

A linear precoding technique with reasonable computational complexity that still achieves full spatial multiplexing and multiuser diversity gains, is ZF precoding [53, 62, 63]. The ability of Zero Forcing (ZF) to fully cancel out multiuser interference makes it useful for the high SNR regime. However, it performs far from optimal in the noise limited regime. Also it can only simultaneously serve at most equal to the number of transmit antennas, single antenna users. A common solution for the ZF precoding matrix is the pseudo-inverse of the $N_u \times N_t$ channel matrix $\mathbf{H} = [\mathbf{h}_1, \mathbf{h}_2 \ldots, \mathbf{h}_k]^\dagger$. Under a total power constraint, channel inversion is the optimal precoder choice in terms of maximum SR and maximum fairness [64]. However, according to the same authors, when PACs are assumed, optimization over the parameters of a generalized inverse has to be performed. Finally, when $N_u = N_t$, a symmetrical system simplifies the calculation of the precoding matrix, i.e. $\mathbf{W} = \mathbf{H}^{-1}$. Following the complete mitigation of interference, the SINR at the k-th user will read as $\mathrm{SINR}_k^{ZF} = |\mathbf{h}_k^\dagger \mathbf{w}_k|^2$.

Regularized Zero Forcing (MMSE precoding)

Although glsZF is asymptotically optimal in the high SNR regime, the drawback of ZF precoding is that the throughput does not grow linearly with N_u [65]. Besides ZF, the implementation complexity of DPC motivated the investigation of other linear precoding techniques with reduced complexity such as Regularized Zero Forcing (R − ZF) precoding. R-ZF was proposed as a simple precoding technique with substantial performance. This method introduces a regularization parameter that takes into account the noise effect. Thus, the resulting throughput is proven to

grow linearly with N_u [66]. More specifically the precoding vector $\mathbf{w}_k$ is taken from the normalized k-th column of

$$\mathbf{W} = \left(\mathbf{H}^{\dagger}\mathbf{H} + \alpha \mathbf{I}_{N_t}\right)^{-1} \mathbf{H}^{\dagger}, \tag{2.10}$$

where α is the regularization factor that needs to be carefully chosen to achieve good performance and $\mathbf{H} \in \mathbb{C}^{N_u \times N_t}$. Based on the large system analysis, the optimal α (in the statistical sense) to maximize the SINR is given in [67]. R − ZF beamforming is also refereed to as MMSE precoding in existing literature, a fact clearly justified by observing (2.10).

Power Constraints

In the above mentioned works, the common assumption of power sharing amongst the transmit antennas is typically adopted. However, PACs are motivated from the practical implementation of systems that rely on precoding. The lack of flexibility in sharing energy resources amongst the antennas of the transmitter is usually the case, since a common practice in multi-antenna systems is the use of individual amplifiers per antenna. Despite the fact that flexible amplifiers could be incorporated in multi-antenna transmitters, specific communication systems cannot afford this design. Typical per antenna power limited systems can be found in multi-beam satellite communications [68], where flexible on board payloads are difficult to implement and in cooperative multicell systems (also known as distributed antenna systems, DAS), where the physical co-location of the transmitting elements is not a requisite and hence power sharing might be infeasible. Formally, total power radiated from the antenna array is equal to

$$P_{tot} = \sum_{k=1}^{N_t} \mathbf{w}_k^{\dagger}\mathbf{w}_k = \text{Trace}\left(\mathbf{W}\mathbf{W}^{\dagger}\right), \tag{2.11}$$

where $\mathbf{W} = [\mathbf{w}_1, \mathbf{w}_2, \dots \mathbf{w}_{N_t}]$. The power radiated by each antenna element is a linear combination of all precoders and reads as [60]

$$P_n = \left[\sum_{k=1}^{N_t} \mathbf{w}_k \mathbf{w}_k^{\dagger}\right]_{nn} = \left[\mathbf{W}\mathbf{W}^{\dagger}\right]_{nn}, \tag{2.12}$$

where $n \in \{1 \dots N_t\}$ is the antenna index. The flexibility provided by generic linear precoding allows for a per antenna power constrained optimization. Extending the above mentioned works, the practical PACs were considered in [60]. Generalized power constraints, including sum power, per-antenna power and per-antenna array power constraints were considered in [69], where the proposed max-min fair solution was derived on an extended duality framework.

The Power Perplexity

A very common confusion stems from the frequent use of the word power. Typically, real valued variables, e.g. the norm of a vector, are also refereed to as power, regardless of the fact that they might not represent an actual physical parameter of the system. Having previously defined the power radiated by each transmit element, which actually represents a physical attribute of the system, in the present section we present the so-called "power allocation" problem. The main goal is to clarify that the power radiated by each antenna and the power of each precoder, as it will be defined hereafter, are two inherently different variables in the precoding problem, only connected by the precoding matrix.

A simplified approach, to optimize the linear precoding design is based on normalizing the precoders and solving an optimization problem over the real valued amplitude of the precoding vectors, commonly referred to as the power of the precoders. Let us denote as $\mathbf{v}_k$ the $N_t \times 1$ normalized transmit precoding vector and p_k the real scaling factor corresponding to the k-th precoder. As before, the unicasting assumption holds. The precoded transmit signal now reads as

$$\mathbf{x} = \sum_{k=1}^{N_u} \sqrt{p_k}\mathbf{v}_k s_k. \tag{2.13}$$

The benefits of such a consideration stem for the reduced complexity in solving the decoupled problem. For instance, a SR maximization problem can be posed as follows. Firstly, the ZF precoders can be calculated and then normalized. Then a SR maximization problem under per antenna

power constraints can be defined as

$$\begin{aligned} &\max_{\{p_k\}} \sum_{k=1}^{N_u} \log_2(1+\mathrm{SINR}_k^{ZF}), \\ &\text{s.t.} \left[\sum_{k=1}^{N_t} p_k \mathbf{v}_k \mathbf{v}_k^{\dagger}\right]_{nn} \leq P_n,\ n=1,\cdots,N_t, \end{aligned} \tag{2.14}$$

where $P_n = P_{tot}/N_t$, for every n, since we assume that all satellite antennas have identical RF chains. The power allocation optimization problem is a standard convex optimization problem [70], [60] which can be solved using common convex optimization tools [71].

Another example can be found in $\mathrm{R}-\mathrm{ZF}$ precoding. In this case, the throughput maximization problem can be posed as a power allocation

$$\begin{aligned} &\max_{\{p_k\}} \sum_{i=1}^{N_u} \log_2\left(1+\mathrm{SINR}_i^{\mathrm{R-ZF}}\right) \\ &\text{s.t.} \left[\sum_{k=1}^{N_t} p_k \mathbf{v}_k \mathbf{v}_k^{\dagger}\right]_{nn} \leq P_n, n=1,\cdots,N_t, \end{aligned} \tag{2.15}$$

with the beamforming directions given by (2.10). Subsequently, by applying $\mathrm{R}-\mathrm{ZF}$, the power and precoding matrix optimization problems are separated and a solution can be found. Although the constraints are linear, the throughput is non-convex with respect to the power vector and therefore finding the optimal solution is non-trivial. To overcome this restrain, the use of simple gradient-based algorithms, such as the steepest descent algorithm, can be employed to find a locally optimal solution for the power allocation problem [105].

When multiple MIMO transmitter cooperate to cover a specific area, a multicell joint precoding architecture is realized. Several multi-cell processing methods for the downlink of terrestrial systems were devised in [36, 72, 73]. In particular, assuming data sharing, the authors in [72] studied the design of transmit beamforming by recasting the downlink beamforming problem into an MMSE problem. However, the required signalling between the Base Stations (BSs) is too high and global convergence is not guaranteed. Later, in [36], a distributed design in Time

Division Duplex (TDD) systems was proposed, using only local CSI and demonstrating that performance close to the Pareto bound can be obtained. However, the main issue with [36, 72] is that both methods require data sharing between the BSs. Hence, their use with limited backhaul throughput is prohibited. Finally, a distributed multicell processing scheme without data or CSI sharing was proposed, in [73], only requiring moderate control signalling among BSs.

2.3.2 Multicasting

A fundamental consideration of the aforementioned works is that independent data is addressed to multiple users. However, the new generation of multi-antenna communication standards has to adapt the physical layer design to the needs of the higher network layers. Examples of such cases include highly demanding applications (e.g. video broadcasting) that stretch the throughput limits of multiuser broadband systems. In this direction, physical layer (PHY) multicasting [1] has the potential to efficiently address the nature of future traffic demand and has become part of the new generation of communication standards.

By introducing a common data assumption, the aforementioned unicast solutions no longer apply. Therefore, the PHY multicasting problem was proposed and proven NP-hard in [76]. Therein, the NP-hard multicast problem was accurately approximated by SDR and Gaussian randomization. The natural extension of the multicast concept lies in assuming multiple interfering groups of users. Considering a multi-antenna transmitter that conveys independent sets of common data to distinct groups of users, the model known as PHY multicasting to multiple co-channel groups is realized. PHY multicasting to multiple co-channel groups can provide the theoretically optimal precoders when a multi-antenna transmitter conveys independent sets of common data to distinct groups of users. In each group, each user receives a stream of common data. However, independent symbols are addressed to different groups and inter-group interference comes into play. A unified framework for physical layer multicasting to multiple co-channel groups, where independent sets of common data are transmitted to groups of users by the multiple antennas, was

[1] The multi-antenna multicast problem was originally proposed in [74], where the maximization of the average SNIR over all users was the goal, without however guaranteeing some QoS at the user side.

given in [75, 77]. Therein, the QoS and the fairness problems were formulated, proven NP-hard and solved for the sum power constrained multicast multigroup case. In parallel to [77], the independent work of [78] involved complex dirty paper coding methods. Also, a convex approximation method was proposed in [79] that exhibits superior performance as the number of users per group grows. Finally, in [80] the multicast multigroup problem under a Sum Power Constraint (SPC), was solved based on approximations and uplink-downlink duality [59]. In the context of coordinated multicast multicell systems, max–min fair beamforming with per BS constraints has been considered in [81] where each BS transmits to a single multicast group. Hence, a power constraint over each precoder was imposed while no optimization weights were considered. This formulation still considers power sharing amongst the multiple antennas at each transmitter.

Remark 2.1. PHY *multicasting is relevant for the application of beamforming without changing the framing structure of standards. Such a scenario can be found in satellite communications where the communication standards are optimized to cope with long propagation delays and guarantee scheduling efficiency by framing multiple users per transmission [68].*

Multicast Problem Formulation

Herein, the focus is on a MU MISO multicast system. Assuming a single transmitter, the input-output analytical expression will read as in (2.2). Focusing on a multigroup multicasting scenario with N_u users, let there be a total of $1 \leq G \leq N_u$ multicast groups with $\mathcal{I} = \{\mathcal{G}_1, \mathcal{G}_2, \dots \mathcal{G}_G\}$ the collection of index sets and $\mathcal{G}_k$ the set of users that belong to the k-th multicast group, $k \in \{1 \dots G\}$. Each user belongs to only one group, thus $\mathcal{G}_i \cap \mathcal{G}_j = \mathbf{O}$,$\forall i, j \in \{1 \cdots G\}$. Let $\mathbf{w}_k \in \mathbb{C}^{N_t \times 1}$ denote the precoding weight vector applied to the transmit antennas to beamform towards the

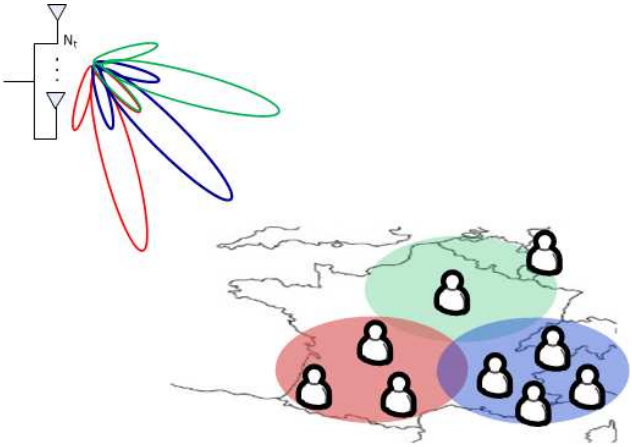

Figure 2.1: Multicast multigroup beamforming to 3 separate groups of co-channel users. Different colors **do not** represent different frequency segments.

k-th group. The PAC weighted max-min fair problem is defined as

$$\max_{t,\ \{\mathbf{w}_k\}_{k=1}^{G}} \quad t$$

$$\text{subject to } \frac{1}{\gamma_i}\frac{|\mathbf{w}_k^\dagger \mathbf{h}_i|^2}{\sum_{l\neq k}^{G}|\mathbf{w}_l^\dagger \mathbf{h}_i|^2+\sigma_i^2} \geq t, \qquad (2.16)$$

$$\forall i \in \mathcal{G}_k, k, l \in \{1\dots G\},$$

$$\text{and to } \left[\sum_{k=1}^{G}\mathbf{w}_k\mathbf{w}_k^\dagger\right]_{nn} \leq P_n, \qquad (2.17)$$

$$\forall n \in \{1\dots N_t\},$$

where $\mathbf{w}_k \in \mathbb{C}^{N_t}$ and $t \in \mathbb{R}^+$. A multicast multigroup MISO transmitter is given in Fig. 2.1

More details on this problem are given in Ch. 4.

2.3.3 Multiuser Scheduling

Multiuser scheduling can glean the multiuser gains offered by the BC channel. The transmitter, by choosing which combinations of users to simultaneously serve can maximize the system performance by reducing the interference and increasing the useful signal power at the receive side. In general, linear ZF beamforming is suboptimal compared to the capacity achieving DPC. However, *Yoo et al* [53, 82] proved that via user selection, ZF can achieve asymptotically optimal SR performance. Moreover, an iterative user selection algorithm that allows ZF to achieve the performance of non-linear precoding [55] when the number of available for selection users grows to infinity was proposed in [82]. This iterative, heuristic semi-orthogonal user selection algorithm accounts for the level of orthogonality of each user over the set of the already selected users. By rejecting users that have high cross user correlation between their vector channels a large set of random users is reduced. Subsequently, out of the users that are left, the most orthogonal ones are iteratively chosen to form a group of users equal to the number of transmit elements. Specifically, if user channels are perfectly orthogonal to each other, ZF will attain maximum performance. Under the assumption of large random user sets, the probability of orthogonal users increases. By recalling that ZF creates equivalent orthogonal channels, it is intuitive to conclude that when the selected users are already orthogonal to each other, the precoding performance will be drastically enhanced. In [82] it was proven that the proposed scheduling method achieves nearly optimal performance as the number of random users grows to infinity. This result is expected since at the limit of infinite users, one can find perfectly orthogonal channels and perform ZF without any orthogonalization losses. Hence, despite their suboptimality, when compared to DPC, linear precoding methods can still achieve asymptotically optimal performance under specific conditions, as proven in [53, 72, 82]. More details on this topic are given in the dedicated Ch. 6.

2.4 Multibeam Satellite Channel

The differences between the satellite and the terrestrial wireless channels are fundamental. The first includes contributions from the multibeam satellite antenna, the propagation medium (rain fading) and the satellite

payload as a non linear relay. In the present section, an attempt to capture most of these effects in the channel matrix **H** is presented. As it be will shown, the channel matrix can be formulated as a proper combination of separate matrices, each modeling a different effect.

The most significant contribution in the total channel matrix is that of the multibeam antenna gains. The effects of the multibeam radiation pattern will be captured by matrix **B**. Beam gain for each satellite antenna–user pair, depends on the spotbeam antenna pattern and on the user position. Assuming that user position does not change considerably in the duration of a codeword, **B** reduces to a deterministic real positive matrix, composed of the square roots of the channel coefficients.

Based on the assumptions of each section, these coefficients can either models the position dependant beam gain, or the carrier to noise ration of each satellite antenna user pair. The latter model applies when some of the link budget parameters are included in the coefficients. To avoid any confusions, despite the fact that a single symbol will be used to describe the satellite channel matrix **B**, the real coefficients that compose **B** in each case are explicitly defined hereafter.

2.4.1 Approximated Multibeam Antenna Pattern

Bessel Function Approximations

In this case, the matrix $\mathbf{B}_b$ is composed of the square roots of the gain coefficients calculated using the well accepted method of Bessel functions [83]:

$$g_{ij}(\theta_{ij}) = G_{\max}\left(\frac{J_1(u)}{2u} + 36\frac{J_3(u)}{u^3}\right)^2, \tag{2.18}$$

where $u = 2.07123 \sin\theta / \sin\theta_{3dB}$, and J_1, J_3 are the Bessel functions of the first kind, of order one and three respectively. The j^{th} user corresponds to an off-axis angle θ_{ij} with respect to the boresight of the i^{th} beam where $\theta_i = 0^\circ$. This beamgain is plotted versus an off axis angular distance, for two different beam sizes in Fig. 2.2.

It should be clarified that the present section for simplicity purposes, the earth curvature and the satellite orbit geometry are not accounted for in the channel model. Subsequently, the variations in the distances of the beam centers and the distance between the satellites are not modeled.

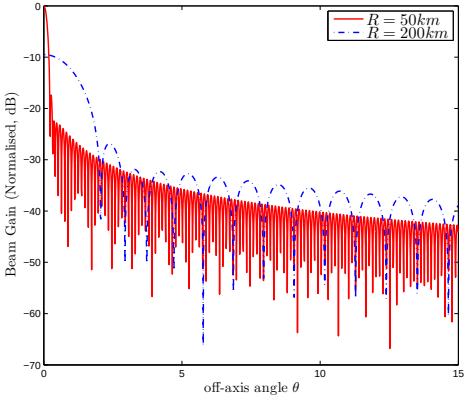

Figure 2.2: Main and secondary radiation lobes for different beam sizes, based on the Bessel function approximation

The assumption that the centers of all beams are equidistant from the satellite can be supported only for small coverage areas.

2.4.2 Measured Multibeam Antenna Pattern

Towards providing more accurate results a realistic antenna pattern is also employed. A 245 beam pattern that covers Europe is employed [84], as presented in Fig. 2.3. A complex channel matrix that models the link budget of each UT as well as the phase rotations induced by the signal propagation is employed [84] [85]. The real matrix $\mathbf{B} \in \mathbb{R}^{N_u \times N_t}$ models the satellite antenna radiation pattern, the path loss, the receive antenna gain and the noise power. Its i, j-th entry is given by [84]:

$$b_{ij} = \left(\frac{\sqrt{G_R G_{ij}}}{4\pi (d_j \cdot \lambda^{-1}) \sqrt{\kappa T_{cs} B_u}} \right), \tag{2.19}$$

with d_j the distance between the k-th UT and the satellite (slant-range), λ the wavelength, κ the Boltzman constant, T_{cs} the clear sky noise temperature of the receiver, B_u the user link bandwidth, G_R the receiver

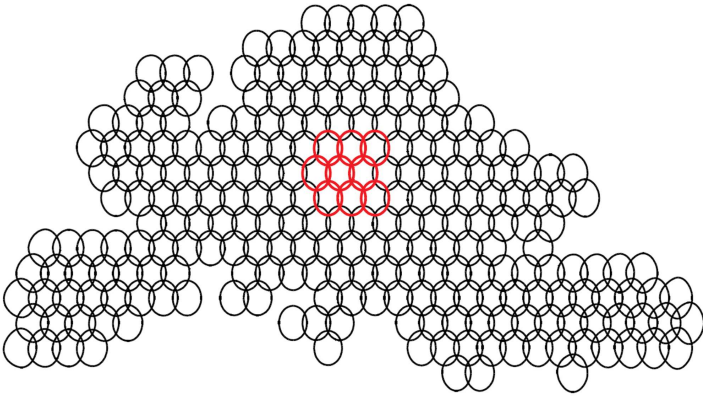

Figure 2.3: Beam pattern covering Europe, provided by [84]

antenna gain and G_{ij} the multibeam antenna gain between the i-th single antenna user and the j-th on board antenna (= feed). Hence, the beam gain for each satellite antenna- user pair, depends on the antenna pattern and on the user position. The link budget parameters are problem dependent and will be defined explicitly for each examined scenario.

2.4.3 Correlation

An inherent characteristic of SatComs is the high correlation among the signals at the satellite side. Total absence of scatterers on the space side renders the received signals highly correlated. In addition, an adequate antenna separation is practically impossible due to on-board size limitations. The assumption of signal correlation, shall impose the multiplication with a diagonal matrix [86, 87]. Depending on the considered link, the multiplication is over the right or the left side of the beamgain matrix.

2.5 Multi-beam Joint Processing

2.5.1 Multiuser Detection over Satellite

First attempts to study multibeam joint processing in the RL, onwards referred to as multibeam joint decoding, have been carried out in [87–89]. The RL of a satellite system employing multibeam joint decoding was studied via simulations in [89]. Therein, MMSE and optimal multiuser receivers were considered, on a simplistic channel model basis. A considerable improvement in both availability and throughput was demonstrated. The first analytic investigation of the uplink capacity of a multibeam satellite system was done by [87], where closed-form expressions were derived for the capacity of multibeam Rician channels. Asymptotic analysis methods for the eigenvalues of the channel matrix were used in [90] to determine upper bounds for the ergodic capacity and calculate the outage probability of a MIMO Land Mobile Satellite (LMS) channel. Similarly, in [91] the statistics of minimum and maximum eigenvalues were derived for Rician fading with Gamma distributed LoS component. Moreover, it should be noted that a multiuser decoding algorithm was presented in [88]. Finally user mobility was considered only in [90].

Linear MMSE receivers are more difficult to analyze compared to the optimal capacity achieving SIC techniques. MU linear MMSE receivers have been extensively studied for various channels in [92]. More recently, numerous contributions examined the asymptotic performance of these architectures by employing random matrix theory methods described in [40] and the references therein. In the same field, the work of [93] is also noted. Focusing on SatComs, the performance of linear MMSE receivers is not trivial to characterize analytically. In the existing literature, two different modeling approaches have been considered. The authors of [90] have modeled fading as the sum of two random matrices, each following a specific distribution, without however reporting results for linear receivers. The other approach, namely the multiplicative model, was introduced in [87], where the performance of optimal non-linear and linear receivers was given as a function of matrix arguments, with high computational complexity, for theoretical channel models. Finally, the incorporation of rain fading has been tackled in [94], using an identical channel model, in which asymptotic closed form expressions for the system's capacity and the MMSE were derived. To this end, the information theoretic, link

between the channel mutual information and the MMSE given in [95], is exploited[2].

The basic characteristic of the RL multibeam satellite channel is the high receive correlation among the channels at the satellite side, resulting from the total lack of scatterers, as well as the practical collocation of the multibeam antenna feeds, at the satellite side. As a result, all the receive antennas experience identical fading instances from a specific user. The first attempts to derive the ergodic capacity of the satellite RL in closed form can be found in [87]. The ergodic capacity of rank deficient MIMO satellite channels in general was also investigated by the authors of [97].

2.5.2 Precoding over Satellite

Following the early works of [98–101], the SatComs literature on MU MIMO precoding is intensifying lately [84,85,102–104] demonstrating very high precoding gains by mainly evaluating various linear and non-linear precoding techniques over the multibeam fixed satellite channel. In terms of precoding techniques selection, it turns out that simple linear techniques already grasp the largest part of the potential multi-user gains with manageable complexity and deliver improvements that double the throughput of existing systems. More specifically, Tomlinson Harashima precoding (THP) was studied in [83, 101], while linear precoding schemes such as ZF and R − ZF were evaluated in [83, 99]. Furthermore, authors in [85] investigated generic linear precoding algorithms under realistic power constraints for single and dual polarized satellite channels. The effect of flexible power constraints rising from flexible and multi-port amplifiers was evaluated in [103] and an energy efficient scheme for MMSE beamforming was proposed in [102]. Finally, authors in [100] have considered an opportunistic beamforming technique based on a codebook of ortho-normal precoders and low-rate feedback.

[2]For completeness we also mention the work of [96] that provides an analytic framework for linear MMSE receivers, which however does not cover the case studied herein.

2.6 Contributions

2.6.1 Return Link

Identifying the gaps in the aforementioned literature, the present work has focused on the investigation of the capacity of multibeam joint decoding satellites under realistic channel assumptions. In this direction, the derivation of closed form formulas provides insights on the system performance with respect to important system parameters. The following works have been published as part of this thesis.

In [86], the determination of the capacity gains for the uplink of a multibeam satellite that jointly decodes mobile user signals from all beams is performed. Therein, the multiplicative model of [87] has been extended to apply for composite, realistic channels. Also, a novel, simple lower bound for the channel capacity has been deduced. To assist this investigation, the lower bound of the theoretical ergodic capacity of such a system, is derived. Tight lower bounds are crucial in evaluating the novel techniques, since overestimation is avoided. Additionally, analytical formulas facilitate the investigation of the impact of the model parameters on the channel capacity.

In [105], the achievable RL throughput by the means of non-linear SIC and of linear MMSE mobile receivers is calculated through simulations. The novelty of this work is the consideration of a multibeam antenna pattern based on Bessel approximations, with a variable beam overlap.

In [106] the MMSE performance of the generalized satellite channel is investigated. Therein, the mutual information is analytically described through tight bounds. More specifically, a closed form expression is derived to describe the linear MMSE performance of multiuser channels that exhibit full receive correlation: an inherent attribute of the RL of multibeam SatComs. Analytic, tight approximations on the MMSE performance are proposed for the cases where closed form solutions are not available in the existing literature. The proposed framework is generic, in the sense that it is straightforwardly extendable to include various fading models over channels that exhibit full receive correlation. Simulation results are provided to show the tightness of the proposed approximation with respect to the available transmit power.

Finally, in [107] the performance of the RL of a SatCom system serving mobile users that are jointly decoded at the receiver is evaluated. In this

context, the throughput performance of the assumed system is compared to that of a conventional one, under the constraint of equal PHY resource utilization; thus the comparison can be regarded as fair. Results under a fair comparison show that significant gains can be realized, especially in the high SNR region. Finally, existing analytical formulas are also employed to provide closed form descriptions of the performance of clustered systems, thus introducing insights on how the performance scales with respect to the system parameters.

2.6.2 Forward Link

In [105], the achievable FL throughput of full frequency reuse multibeam satellites that rely on linear (ZF and R − ZF) and non linear (DPC) precoding methods is assessed by simulations. Therein, the Bessel functions based, multibeam antenna pattern with variable beam overlap is considered. The performance is compared to conventional frequency reuse scenarios versus an increasing beam overlap, thus providing useful insights for the design of the multibeam antenna pattern of future full frequency reuse multibeam systems.

Towards the incorporation of linear precoding techniques in broadband multibeam SatComs, practical constraints imposed by the inherent characteristics of the satellite channel need to be addressed, as presented in [68]. Therein, the focus involves two fundamental constraints, namely the rigid framing structure of SatCom standards and the cost efficient, non flexible on-board payloads that prevent power sharing amongst the beams.

The rigid framing structure of SatCom standards inspires the investigation of PHY multicasting. In this context, the optimal multicast multigroup precoders when a maximum limit is imposed on the transmitted power of each antenna have been derived in [108]. Extending this, a consolidated solution for the weighted max–min fair multicast multigroup beamforming under PACs has been presented in [109]. Therein, practical system design insights are given by examining the implications of the PACs on multicast multigroup Distributed Antenna Systems (DASs), modulation constrained systems and uniform linear array Uniform Linear Array (ULA) transmitters. Also, a robust to erroneous CSI multicast multigroup design under PACs is proposed.

By acknowledging the connection of the multicast multigroup precod-

ing with the frame based precoding problem, the application the max–min fair solutions over an accurate SatCom scenario is presented in [110].

A natural extension of the fairness based solutions is given in [111], where the focus is set on maximizing the total throughput of the multicast multigroup system under PACs. To this end, the *max sum rate* (SR) multigroup multicast problem under PACs is formulated and solved.

The application of the max SR multigroup multicast under PACs solution over a multibeam satellite operating in full frequency reuse configuration is given in [112]. Towards further addressing the practical constraints of multibeam SatComs, the max SR problem is extended to account for Minimum Rate Constraints (MRCs). Moreover, a novel modulation aware max SR optimization that considers the discretized throughput function of the receive useful signal power is proposed. A heuristic optimization algorithm is derived for the solution of this elaborate optimization problem. Finally, in order to glean the multiuser gains of the SatCom system, a low complexity user scheduling algorithm that considers the multicast multigroup nature of the system is envisaged.

Lastly, the optimal user allocation in a dual satellite scenario has been considered in [113]. The novelty of the proposed work lies in the fact that user selection and allocation, not only optimizes the ZF performance of each system but also considers the interaction between the two transmitters, i.e. the inter-satellite interference.

2.6.3 Publication outline

The following publications have appeared or are under in the review process of international peer-reviewed

- Patents [140]
- journals [106], [105], [109], [112], [114],
- conferences [86], [107], [113], [68], [108], [111], [110], [115], [116], [117], and
- book chapters [118, 119].

2.6.4 Publication List

Patents

- P.-D. Arapoglou, A. Ginesi, G. Taricco, D. Christopoulos, S. Chatzinotas, B. Ottersten, M.-Á. Vzquez, A.-I. Pérez-Neira, S. Andrenacci, A. Vanelli-Coralli "Joint Transmitter Signal Processing in Multi-Beam Satellite Systems," in *European Space Agency Patent: 641-05628EP TE/BD*, 2014

Journals

- D. Christopoulos, S. Chatzinotas, and B. Ottersten, "Weighted fair multicast multigroup beamforming under per-antenna power constraints," *IEEE Trans. Signal Process.*, vol. 62, no. 19, pp. 5132–5142, Oct. 2014.

- D. Christopoulos, S. Chatzinotas, and B. Ottersten, "Multicast Multigroup Precoding and User Scheduling for Frame-Based Satellite Communications," *IEEE Trans. Wireless Commun.*, vol. PP, no. 99, pp. 1–1, 2015, *DOI: 10.1109/TWC.2015.2424961.*

- D. Christopoulos, S. Chatzinotas, G. Zheng, J. Grotz, and B. Ottersten, "Linear and non-linear techniques for multibeam joint processing in satellite communications," *EURASIP J. on Wirel. Commun. and Networking 2012, 2012:162.* [Online]. Available: `http://jwcn.eurasipjournals.com/content/2012/1/162`

- D. Christopoulos, J. Arnau, S. Chatzinotas, C. Mosquera, and B.-Ottersten, "MMSE performance analysis of generalized multibeam satellite channels," *IEEE Commun. Lett.*, vol. 17, no. 7, pp. 1332–1335, 2013.

Conferences

- D. Christopoulos, S. Chatzinotas, M. Matthaiou, and B. Ottersten, "Capacity analysis of multibeam joint decoding over composite satellite channels," in *Proc. of 45th Asilomar Conf. on Signals, Systems and Computers*, Pacific Grove, CA, Nov. 2011, pp. 1795 –1799.

- D. Christopoulos, S. Chatzinotas, J. Krause, and B. Ottersten, "Multiuser detection for mobile satellite systems: A fair performance evaluation," in *Proc. of 77th IEEE Vehic. Technol. Conf.*, 2013.

- D. Christopoulos, S. Chatzinotas, and B. Ottersten, "User scheduling for coordinated dual satellite systems with linear precoding," in *Proc. of IEEE Int. Commun. Conf.*, 2013.

- D. Christopoulos, P.-D. Arapoglou, S. Chatzinotas, and B. Ottersten, "Linear precoding in multibeam SatComs: Practical constraints," in *31st AIAA International Communications Satellite Systems Conference (ICSSC)*, Florence, IT, Oct. 2013.

- D. Christopoulos, S. Chatzinotas, and B. Ottersten, "Multicast multigroup beamforming under per antenna power constraints," in *Proc. of IEEE Int. Commun. Conf.*, Sydney, AU, Jul. 2014, *preprint:* arXiv:1407.0004 [cs.IT].

- D. Christopoulos, S. Chatzinotas, and B. Ottersten, "Frame based precoding in satellite communications: A multicast approach," in *Proc. of ASMS Conf.*, Livorno, IT, Sep. 2014,
preprint: arXiv:1406.6852 [cs.IT].

- D. Christopoulos, S. Chatzinotas, and B. Ottersten, "Sum rate maximizing multigroup multicast beamforming under per-antenna power constraints," in *Proc. of IEEE Global Commun. Conf.*, 2014, Austin,TX, USA, Dec. 2014, *preprint:* arXiv:1407.0005 [cs.IT].

Book Chapters

- D. Christopoulos, S. Chatzinotas, G. Taricco, M. A. Vazquez, A.Perez-Neira, P.-D. Arapoglou, and A. Ginesi, *Cooperative and Cognitive satellite systems.* Elsevier, 2014, ch. Multibeam Joint Precoding: Frame Based Design.

- D. Christopoulos, S. Chatzinotas, and B.-Ottersten, *Cooperative and Cognitive satellite systems.* Elsevier, 2014, ch. User Scheduling in Cooperative Satellite Systems.

2.6.5 Publications not included in this thesis

- J. Arnau, D. Christopoulos, S. Chatzinotas, C. Mosquera, and B.-Ottersten, "Performance of the multibeam satellite return link with correlated rain attenuation," *IEEE trans. in Wirel. Commun.*, to appear.

- A. Zohair, B. Shankar, D. Christopoulos, and P.-D. Arapoglou, "Timing and frequency synchronisation for multiuser detection on the return link of interactive mobile satellite networks," in *31st AIAA International Communications Satellite Systems Conference (ICSSC)*, Florence, IT, Oct. 2013.

- S. K. Sharma, D. Christopoulos, S. Chatzinotas, and B. Ottersten, "New generation cooperative and cognitive dual satellite systems: Performance evaluation," in *32nd AIAA International Communications Satellite Systems Conference (ICSSC)*, San Diego, US, Sep. 2014.

- S. Chatzinotas, D. Christopoulos, and B. Ottersten, "Coordinated multi-point decoding with dual-polarized antennas," in *Proc. of 7th Int. Wirel. Commun. and Mobile Comput. Conf.*, Jul. 2011, pp. 157 –161.

Chapter 3

Capacity Limits of Multiuser Detection

In the present chapter, the ergodic capacity bounds for the return link of a multibeam satellite employing multiuser detection shall be analytically evaluated. Important insights gained by the closed form derivations are used to propose possible ways for the incorporation of joint detection methods in the next generation of multibeam satellite channels. In the return link, channel reporting is relatively simpler when compared to the forward link, since one less hop is necessary to acquire the channel state at the transmitter side. Therefore, multiuser detection methods have the potential of being incorporated in Mobile Satellite Services (MSS) systems. Consequently, the proposed analytical expressions are generalized to include user mobility assumptions. Nonetheless, the results reported hereafter, are applicable to any general satellite channel.

3.1 The Multibeam Return Channel Capacity

The present section investigates the ergodic capacity bounds for the RL of a multibeam satellite where full frequency reuse is employed and user signals are jointly processed at the GW.

3.1.1 Composite Multibeam Channel

The proposed model incorporates correlated satellite antennas over Rician channels which represent some inherent characteristics of satellite communications. Additionally, the effects of shadowing caused by user mobility, are modeled via the classical lognormal distribution. Hence, a composite Rician/lognormal fading channel with fully correlated receive antennas is investigated. Novel, lower bounds on the ergodic capacity are analytically deduced and verified through simulations. Channel matrix $\mathbf{H}$ reads as

$$\mathbf{H} = \mathbf{B} \odot \mathbf{H}_R \mathbf{\Xi}_d^{1/2}. \tag{3.1}$$

Note that the matrix $\mathbf{B}$ models the satellite antenna gain using the Bessel approximation model presented in Sec. 2.4.1. Each user-receiver antenna pair has a different gain due to the antenna radiation pattern, hence $\mathbf{B}$ is multiplied element-wise (i.e. Hadamard product) with the small-scale, fading matrix $\mathbf{H}_R$. The latter matrix consists of random i.i.d. nonzero mean Gaussian elements and models the Rician fading component as follows [87]

$$\mathbf{H}_R = \sqrt{\frac{K_r}{K_r+1}}\bar{\mathbf{H}}_R + \sqrt{\frac{1}{K_r+1}}\tilde{\mathbf{H}}_R, \tag{3.2}$$

where K_r is the Rician factor, $\bar{\mathbf{H}}_R$ is a deterministic full rank matrix modeling the LoS signal component and $\tilde{\mathbf{H}}_R$ is a complex random matrix representing the scattered components. The effects of antenna correlation are considered using the Kronecker correlation model [40]. Hence, a realization of $\tilde{\mathbf{H}}_\mathbf{R}$ is generated according to

$$\tilde{\mathbf{H}}_R = \mathbf{R}_r^{1/2} \mathbf{H}_w \mathbf{R}_t^{1/2}, \tag{3.3}$$

where $\mathbf{H}_w \sim \mathbb{CN}(0, \mathbf{I}_n)$. An inherent characteristic of SatCom is the high correlation among the received signals. Hence, unit rank receive correlation is assumed, such that $\mathbf{R}_r^{1/2} = \mathbb{I}_{n\times n}$. On the other hand, the effects of correlation can be ignored on the transmit side; this implies that $\mathbf{R}_t^{1/2} = \mathbf{I}_n$. As a result, the Rayleigh component of the total channel matrix is

$$\tilde{\mathbf{H}}_R = \mathbb{I}_n \mathbf{H}_w \mathbf{I}_n = \mathbb{I}_n \mathbf{H}_w. \tag{3.4}$$

As far as the large-scale fading matrix $\mathbf{\Xi}_d$ is concerned, we first note that its entries are modeled via the classical lognormal distribution [46]. In addition, due to the collocation of the on board antennas, possible

obstructions affect equally all received signals. Thus, $\mathbf{\Xi}_d$ is a diagonal matrix composed of random elements that represent shadowing due to user mobility: The probability density function of the random fading coefficients ξ_m reads as

$$p\left(\xi_m\right) = \frac{1}{\xi_m \sqrt{2\pi\sigma_m^2}} \exp\left(-\frac{\left(\ln \xi_m - \mu_m\right)^2}{2\sigma_m^2}\right), \quad \xi_m \geq 0. \tag{3.5}$$

where μ_m and σ_m are the mean and standard deviation of the variable's natural logarithm, respectively.

An important observation that simplifies the theoretical analysis is the transformation of (3.1) into a more tractable form. In particular, we notice that the receive correlation imposes rank deficiency on the matrix $\tilde{\mathbf{H}}_R$. According to (3.4), $\tilde{\mathbf{H}}_R$ is a matrix with identical rows, as can be easily verified. Likewise, $\bar{\mathbf{H}}_R$ has by assumption identical rows: Each user has the same LoS component towards the receiver, since the distance between satellite antennas is infinitesimal compared to the user-satellite propagation path. The sum of unit-rank matrices with identical rows leads to a total channel matrix $\mathbf{H}_R$ with identical rows and thus unit rank: $\operatorname{rank}\left(\mathbf{H}_R\right) = 1$. The Hadamard product between two matrices can be transformed into matrix product in the special case where the latter is a unit rank matrix with identical rows. Then, the Hadamard product between the initial matrices is equivalent to the product between the first one and a diagonal matrix containing row elements of the unit-rank matrix[1]. Taking this observation into consideration, (3.1) can be transformed into

$$\mathbf{H} = \mathbf{B}\mathbf{H}_d\mathbf{\Xi}_d^{1/2}, \tag{3.6}$$

where $\mathbf{H}_d$ is a diagonal matrix containing i.i.d. non-zero mean complex circularly symmetric elements.

3.1.2 Ergodic Capacity Closed form Analysis

The considered system is a MU Single Input Multiple Output (SIMO) MAC, hence capacity is calculated by the *log-det* formula (2.4). According

[1] In the channel derivations this property is used in more than one occasions [120]. It results from the assumption that channel coefficients between each user and every receive antenna are identical.

to [46, 121], a capacity lower bound for a symmetric $n \times n$ system reads as

$$C_{\text{erg}} \geqslant n \log_2 \left(1 + \gamma \exp\left(\frac{1}{n}\mathcal{E}\{\ln\left(\det\left(\mathbf{H}^{\dagger}\mathbf{H}\right)\right)\}\right)\right). \tag{3.7}$$

Considering $\mathbf{H}$ as in (3.6) and by exploiting the symmetrical nature of the system, (3.7) yields

$$\mathrm{C}_{\text{erg}} \geqslant n \log_2 \left(1 + \gamma \exp\left(\Omega_1\right)\right), \text{where} \tag{3.8}$$

$$\Omega_1 = \frac{1}{n}\left(\mathcal{E}\{\ln\left(\det\left(\mathbf{B}\cdot\mathbf{B}^{\dagger}\right)\right)\} + \mathcal{E}\{\ln\left(\det \boldsymbol{\Xi}_{\mathbf{d}}\right)\} + \mathcal{E}\{\ln\left(\det|\mathbf{H}_d|^2\right)\}\right)$$

Since $\mathbf{B}$ is deterministic, the remaining non deterministic terms of (3.8) need to be calculated. The expectation of the shadowing matrix is

$$\mathcal{E}\left\{\ln\left(\det \boldsymbol{\Xi}_d\right)\right\} = \sum_{m=1}^{n} \mathcal{E}\left\{\ln\left(\xi_m\right)\right\} = \sum_{m=1}^{n} \mu_m, \tag{3.9}$$

where μ_m *(dB)* and σ_m *(dB)* have been defined in (3.5)[2]. Finally, to deduce an analytical expression for the term $\mathcal{E}\{\ln\left(\det|\mathbf{H}_d|^2\right)\}$, the procedure described hereafter is necessary. The diagonal matrix $|\mathbf{H}_d|^2$ is composed of Rician elements, i.e. $\mathbf{H}_d = \text{diag}\{\mathbf{h}\}$, where $\mathbf{h} = [h_1, h_2 \ldots h_n]$. Each element of vector $\mathbf{h}$ is given by $h_i = \sqrt{\frac{K_r}{K_r+1}}\bar{h}_{ii} + \sqrt{\frac{1}{K_r+1}}\tilde{h}_{ii}$, where $\bar{h}$ is complex deterministic and $\tilde{h} \sim \mathcal{CN}(0,1)$, representing the LoS and the Rayleigh components of the signal respectively. Let us consider the following algebra

$$\begin{aligned}
&\mathcal{E}\left\{\ln\left(\det|\mathbf{H}_d|^2\right)\right\} = \\
&= \mathcal{E}\left\{\ln\left(\prod_{i=1}^{n}\left|\sqrt{\frac{K_r}{K_r+1}}\bar{h}_{ii} + \sqrt{\frac{1}{K_r+1}}\tilde{h}_{ii}\right|^2\right)\right\} \\
&= \sum_{i=1}^{n}\mathcal{E}\left\{\ln\left|\sqrt{\frac{K_r}{K_r+1}}\bar{h}_{ii} + \sqrt{\frac{1}{K_r+1}}\tilde{h}_{ii}\right|^2\right\} \\
&= -n\ln\left(K_r+1\right) + \sum_{i=1}^{n}\mathcal{E}\left\{\ln\left|\sqrt{K_r}\bar{h}_{ii} + \tilde{h}_{ii}\right|^2\right\}.
\end{aligned} \tag{3.10}$$

[2]It should be noted here that this equality holds for large systems

Hence, the last term of (3.10) needs to be deduced. From [87], the elements of $|\mathbf{H}_d|^2$ follow a non-central chi-squared (χ^2) distribution and the exact analytical calculation of this term will be discussed further on. According to [122,123], the expectation of the natural logarithm of a random variable following the χ^2 distribution can be calculated as follows:

$$\mathcal{E}\left\{\ln\sum_{j=1}^{m}|U_j+w_j|^2\right\}=g_m\left(s^2\right), \tag{3.11}$$

where $U\sim\mathcal{CN}(0,1)$, w is a deterministic complex number, $2m$ are the degrees of freedom of the χ^2 distribution (i.e. the number of squared normal random variables summed)[3] and s^2 is the distribution's non-centrality parameter, given by

$$s^2=\sum_{j=1}^{m}|w_j|^2. \tag{3.12}$$

Function g_m is defined as [123]

$$g_m\left(s^2\right)\triangleq\begin{cases}\ln(s^2)-Ei(-s^2)+\sum_{j=1}^{m-1}(-1)^j\cdot\\ \cdot\left[e^{-s^2}(j-1)!-\frac{(m-1)!}{j(m-1-j)!}\right]\left(\frac{1}{s^2}\right)^j, & s^2>0\\ \psi(m), & s^2=0.\end{cases} \tag{3.13}$$

where $Ei(x)$ denotes the exponential integral function, and $\psi(x)$ is Euler's digamma function.

An important variation of the present analytical contribution from [87] lies on the number of squared normal random variables added to form one element of the diagonal matrix. In [87], there are m channel coefficients added and since each random complex number is the sum of two normal random variables, each element of the diagonal channel matrix follows a $\chi-$squared distribution with $2m$ degrees of freedom. By examining (3.10) and (3.11), $m=1$ complex channel coefficients are added, thus $|\mathbf{H}_d|^2$ follows a χ^2-distribution with two degrees of freedom, (i.e. $|\mathbf{H}_d|^2\sim\chi_2^2(s^2)$). For $m=1$ and with $w_i=\sqrt{K_r}\bar{h}_{ii}$ and $U_i=\tilde{h}_{ii}$, the last term

[3] Of particular interest is the case of even number of degrees of freedom since not only it leads to closed form solutions but is also realistic. The squared norm of complex random variables distributed as $\mathcal{CN}(0,1)$ leads to an even number of total squared normal variables.

of (3.10) can be calculated using (3.11)[4]:

$$\mathcal{E}\{\ln\left(\det|\mathbf{H}_d|^2\right)\} = -n\ln\left(K_r+1\right) + \sum_{i=1}^{n} g_2\left(s^2{}_i\right), \tag{3.14}$$

where $s^2{}_i = |w_i|^2 = K_r|\bar{h}_{ii}|^2$. Hence, the analytically deduced lower bound for a symmetrical $n \times n$ multibeam joint processing system operating in composite Rician/lognormal channel with correlated receive antennas reads as

$$\mathrm{C}_{\mathrm{erg}} \geqslant n\log_2\left(1+\gamma\exp\left(\Omega\right)\right), \text{where} \tag{3.15}$$

$$\Omega_2 = \frac{1}{n}\left(\ln\left(\det\left(\mathbf{B}\cdot\mathbf{B}^{\dagger}\right)\right) + \sum_{m=1}^{n}\mu_m - n\ln\left(K_r+1\right) + \sum_{i=1}^{n} g_2\left(s^2{}_i\right)\right).$$

Numerical Evaluation of the Closed Form Solution

Simulations were carried out to calculate the expectation of the channel mutual information, that is the channel capacity, given by (2.4). The results are visualized in Fig. 3.1, with respect to a large range of transmit SNR. In the same figure, the analytically deduced lower bound is compared to the theoretical capacity. Finally, the achievable capacity of multibeam systems employing frequency reuse, over identical channel assumptions, is also plotted for the case of a four color frequency reuse scheme, in order to assist the quantification of the potential capacity gain. The simulation parameters can be found in Tab. 3.1. In the same table, the link budget of the assumed system has been calculated. The behavior of the proposed bounds in the extreme cases of low and high SNR can provide important insights. The performance is given versus increasing transmit power over normalized receive noise, also referred to as transmit SNR. For comparison, also the capacity of a conventional system employing a four color frequency reuse scheme is given. Amid the lack of tightness in the low transmit SNR region, it is proven that the bound converges for SNR values more than 30 dB. However, the link budget calculations included in Tab. 6.1 show that a low SNR analysis is necessary in order to provide tighter bounds in the area of practical interest (i.e. [-5

[4]It should be clarified that the summation is not included in the logarithm, hence the use of a different summation index. Subsequently, the distribution still has two degrees of freedom.

Table 3.1: Mobile Satellite System Return Link Budget Parameters

Parameter	Value
Orbit	GEO
Frequency Band	S (2.2 GHz)
User Link Bandwidth B_u	15 MHz
Mobile terminal RF power	[-3 – 24.5] dBW
Receiver noise power N	-133 dBW
Free Space Loss L	190 dB
Atmospheric Loss	0.5 dB
Polarization Loss	3 dB
Mobile Antenna Gain G_T	3 dBi
Max satellite antenna gain G_R	52 dBi
Fading Margin	3 dB
Transmit SNR	[-5 – 25] dB
Beam Radius	350km
Area Radius	1000km
Number of Beams	7
Rician factor K_r	13 dB
Lognormal Shadowing μ_m, σ_m	-2.62dB, 1.6dB
Monte Carlo (MC) Iterations	1000

– 20] dB). Furthermore, according to Fig. 3.1, the gain over a traditional frequency reuse system is more than threefold at the high SNR region and approximately twofold for lower SNR values. This result indicates that potential operation in higher SNR regions, will increase the gain of MUD techniques in a satellite communications network, especially at the point where conventional techniques reach a saturation point due to inter-beam interference (i.e. over 40 dB).

The behavior of the deduced formula was also examined for variable Rician factors. The results are depicted in Fig. 3.2 for a specific SNR value (i.e. 25 dB) versus a typical range of the Rician factor in a satellite channel [124]. According to these results, the bound remains exact with respect to the Rician factor and can thus be used for various satellite scenarios.

3.2 MMSE Performance Analysis

3.2.1 MMSE Closed Form Analysis

The purpose of the present contribution is to extend the results of [86] and [94] for the case of linear MMSE receivers, thus providing an analytic framework that covers the generalized type of channels with full receive correlation. The performance of linear multiuser detection (MUD) is evaluated via the achievable SINR_k after MMSE detection at the kth user,

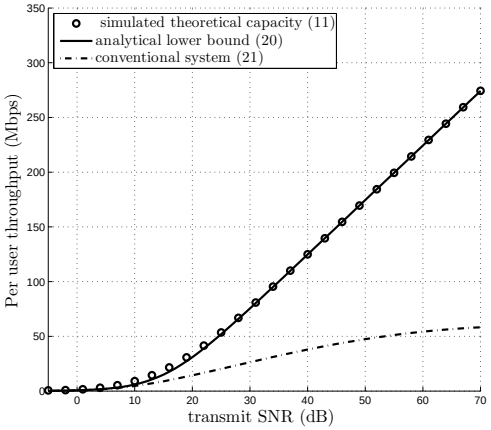

(a)

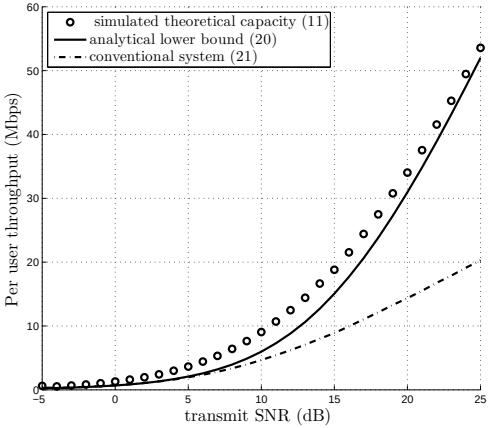

(b)

Figure 3.1: Theoretical and analytical results versus a large range of transmit power over normalized noise. The performance of a conventional four color frequency reuse system is also shown.

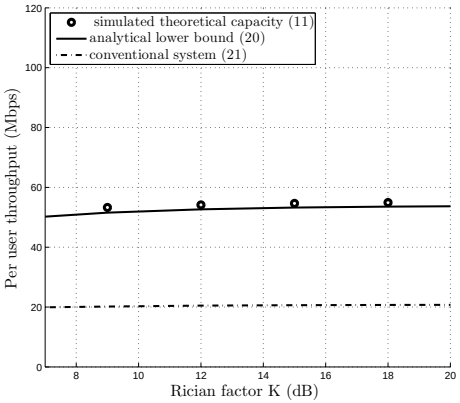

Figure 3.2: Theoretical and analytical results versus a typical range of the Rician factor.

given by [125]

$$\gamma_{\mathrm{mmse},k} = \frac{1}{\left[\left(\mathbf{I}_K + \gamma \mathbf{H}^{\dagger}\mathbf{H}\right)^{-1}\right]_{kk}} - 1. \tag{3.16}$$

Averaged over the users and all channel instances, the system spectral efficiency, is given by [125]

$$\mathrm{C}_{\mathrm{mmse}}(\gamma) = \mathcal{E}_{\mathbf{H}}\left\{ I_{\mathrm{mmse}} \right\} = \mathcal{E}_{\mathbf{H}}\left\{ \frac{1}{K} \sum_{i=1}^{K} \log_2\left(1 + \gamma_{\mathrm{mmse},k}\right) \right\}, \tag{3.17}$$

in bits/sec/Hz. By combining (3.16) and (3.17) and directly applying the Jensen's inequality the following stands

$$\mathrm{C}_{\mathrm{mmse}} \geq \mathcal{E}_{\mathbf{H}} \left\{ -\log_2 \left(\frac{1}{K} \operatorname{trace} \left(\left(\mathbf{I}_K + \gamma \mathbf{H}^{\dagger}\mathbf{H} \right)^{-1} \right) \right) \right\}. \tag{3.18}$$

Thus, in common practice, another measure, namely the instantaneous, per user, minimum mean square error, is also adopted [40, 95]

$$\epsilon^2 = \frac{1}{K} \operatorname{trace} \left(\left(\mathbf{I}_K + \gamma \mathbf{H}^{\dagger}\mathbf{H} \right)^{-1} \right). \tag{3.19}$$

It should be clarified, that the above metric provides a lower bound when used to calculate the average system throughput, i.e. $C_{mmse} \geq \log_2(\epsilon^2)$, simply deduced by applying Jensen's inequality over the convex sum of negative logarithm. The error's covariance matrix $\mathbf{Q}$ is given by

$$\mathbf{Q} = \left(\mathbf{I} + \gamma \mathbf{H}^H \mathbf{H}\right)^{-1}. \tag{3.20}$$

The presence of the inverse of a matrix sum in (3.18) hinders the computation of ϵ^2 when the eigenvalue distribution of $\mathbf{H}^\dagger\mathbf{H}$ cannot be computed analytically. To solve this problem, we propose to use the approximation defined in the following lemma.

Lemma 3.1. The instantaneous per user MMSE of an uplink MU SIMO system can be approximated by

$$\hat{\epsilon}^2 = \left(1 + \gamma \exp\left(\frac{1}{K} \ln\det\left(\mathbf{H}^\dagger\mathbf{H}\right)\right)\right)^{-1}. \tag{3.21}$$

Proof. In [95], an explicit relationship between the channel mutual information $\mathrm{I}_e = \log_2\det\left(\mathbf{I} + \gamma\mathbf{H}^\dagger\mathbf{H}\right)$ in bits/sec/Hz and ϵ^2 is derived by differentiating with respect to the SNR. This result is easily extended for vector channels yielding [40]

$$\gamma\frac{\partial}{\partial\gamma}\mathrm{I}_e(\gamma) = K - \mathrm{trace}\left(\left(\mathbf{I}_K + \gamma\mathbf{H}^\dagger\mathbf{H}\right)^{-1}\right) \tag{3.22}$$

$$= K(1-\epsilon^2). \tag{3.23}$$

Furthermore, with the use of Minkowski's inequality, the following bound on I_e has been derived in [121]

$$\mathrm{I}_e \geq \mathrm{I}_{lb} \ = K\log_2\left(1 + \gamma\det\left(\left(\mathbf{H}^\dagger\mathbf{H}\right)^{1/K}\right)\right). \tag{3.24}$$

The above bound is known to be tight and becomes exact for large SNR values. By differentiation with respect to γ we get the following:

$$\gamma\frac{\partial}{\partial\gamma}\mathrm{I}_{lb} = \frac{\gamma K\det\left(\left(\mathbf{H}^\dagger\mathbf{H}\right)^{1/K}\right)}{1+\gamma\det\left(\left(\mathbf{H}^\dagger\mathbf{H}\right)^{1/K}\right)} \overset{(10)}{\Longrightarrow}$$

$$\hat{\epsilon}^2 = \left(1 + \gamma\det\left(\left(\mathbf{H}^\dagger\mathbf{H}\right)^{1/K}\right)\right)^{-1}. \tag{3.25}$$

Finally (3.25) can be rewritten as in (3.21). Q.E.D.

Since the differentiation does not preserve the direction of the bound, the characteristics of this approximation will be studied in more detail in the following lemma.

Lemma 3.2. Let $\hat{\epsilon}^2$ be the derived approximation of ϵ^2, then $\hat{\epsilon}^2$ and ϵ^2 as functions of γ, have a crossing point.

Proof: Denoting as λ_i the ordered eigenvalues of $\mathbf{H}^\dagger\mathbf{H}$, let us define the function $D(\gamma) \doteq \mathrm{I}_e(\gamma) - \mathrm{I}_{lb}(\gamma)$, where $I_e(\gamma) = \sum_i \log(1+\gamma\lambda_i)$ and $I_{lb}(\gamma) = \log\left(1+\gamma\left(\prod_i \lambda_i\right)^{1/K}\right)$, with the following properties: 1) $D(0) = 0$. 2) For γ_o sufficiently large, but finite, we have that $D(\gamma_o) = 0$. From properties 1 and 2, a straightforward application of Cauchy's mean-value theorem yields that there will be at least one point $\gamma^* \in (0, \gamma_o)$, with zero derivative and subsequently a crossing point between the approximation and the actual function.

Lemma 3.3. The average (over the channel realizations), per user MMSE, $\mathcal{E}_{\mathbf{H}}\left\{\hat{\epsilon}^2\right\}$, can be bounded by

$$\left(1+\gamma\exp\left(\frac{1}{K}\mathcal{E}_{\mathbf{H}}\left\{\ln\det\left(\mathbf{H}^\dagger\mathbf{H}\right)\right\}\right)\right)^{-1} \tag{3.26}$$

Proof. Let us consider the function $\phi(x) = ((1+\exp(x)))^{-1}$ which is convex for $x<0$ and concave for $x>0$. By applying Jensen's inequality over the two regions we get that

$$\mathcal{E}_{\mathbf{H}}\left\{\hat{\epsilon}^2\right\} = \begin{cases} \geq a, & x \leq 0 \\ \leq a, & x > 0 \end{cases} \tag{3.27}$$

for $a = \left(1+\gamma\exp\left(\frac{1}{K}\mathcal{E}_{\mathbf{H}}\left\{\ln\det\left(\mathbf{H}^\dagger\mathbf{H}\right)\right\}\right)\right)^{-1}$
and $x = 1/K \cdot \ln\det(\left(\mathbf{H}^\dagger\mathbf{H}\right)) + \ln\gamma$. Q.E.D.

Lemma 3.4. The average per user MMSE approximation, for the composite multibeam satellite channel, is analytically described by

$$\mathcal{E}_{\mathbf{H}}\left\{\hat{\epsilon}^2_{\mathrm{comp}}\right\} = \tag{3.28}$$
$$\left(1+\gamma\exp\left(\frac{1}{K}\log\left(\det\mathbf{B}^2\right)+\mu_m+g_2\left(s^2\right)-\log\left(K_r+1\right)\right)\right)^{-1},$$

where μ_m (dB) is the mean of the normal distribution, K_r the Rician factor, the g_2 function is given as $g_2(s^2) = \log s^2 + E_i(s^2)$ (as defined in [86]), E_i is the exponential integral and $s^2 = K_r$ is the non-centrality parameter of the associated χ^2-distribution.

Proof. The expectation of the logarithm of the determinant of the specific channel matrix has been derived in [86]. Direct application of these calculations on (3.26) concludes the proof. Q.E.D.

Lemma 3.5. The average, per user MMSE approximation, for the rain faded multibeam channel, is analytically described by

$$\mathcal{E}_{\mathbf{H}}\left\{\hat{\epsilon}^2_{\text{rain}}\right\} = \left(1 + \gamma \exp\left(\frac{1}{K}\ln\left(\det \mathbf{B}^2\right) + \mu_l\right)\right)^{-1}, \tag{3.29}$$

where μ_l the mean of the equivalent log-normal distribution.

Proof. Following the steps of the previous proofs, an analytical bound on $\mathcal{E}_{\mathbf{H}}\left\{\hat{\epsilon}^2_{\text{rain}}\right\}$ will read as

$$\left(1 + \gamma \exp\left(\frac{1}{K}\mathcal{E}_{\mathbf{H}}\left\{\ln\det\left(\mathbf{B}^2\mathbf{L}_d\right)\right\}\right)\right)^{-1} \tag{3.30}$$

where $\ln\det(\mathbf{B}^2\mathbf{L}_d) = \ln\left(\det\mathbf{B}^2\right) + \ln\det\mathbf{L}_d$ since the matrices are square and

$$\mathcal{E}\left\{\ln\left(\det\mathbf{L}_d\right)\right\} = \sum_{i=1}^{K}\mathcal{E}\left\{\ln l_i\right\} = K\cdot\mu_l\mathcal{E}\left\{\ln\left(\det\mathbf{L}_d\right)\right\} = \sum_{i=1}^{K}\ln l_i \ = K\cdot\mu_l$$

The parameter μ_l is the mean of the related log-normal distribution given by $\mu_l = \exp(\mu_m + \sigma^2/2)$. As before, μ_m and σ are the mean and variance of the associated normal distribution. Since $\mathbf{B}$ is a deterministic matrix, from the above analysis, (3.29) is deduced. Q.E.D.

Realistic beam patterns from multibeam coverage over Europe are chosen to provide accurate results for the system performance, as presented in Sec. 2.4.2. In multibeam systems, multiple GWs -each only serving a fraction of the total number of beams- are deployed due to limitations in the feeder link bandwidth. In order to focus on a specific GW, only a part of the total beam pattern (i.e. 7 beams) has been considered in the

analysis as presented in Fig. 3.1. These beams correspond to the beams served by a specific GW over which MUD will be performed in a distributed GWs scenario. Monte Carlo simulations have been performed to calculate the exact performance over the random channel. The analytic results derived in the present section provide deterministic approximations on the system performance with respect to γ and are compared to the MC results to illustrate the tightness of the deduced formulas.

In Fig. 3.3, the simulated expectation of the MMSE given by (3.19) over 1000 channel instances for the composite and the rain faded channels, is presented with star markers. The results are based on the measured antenna pattern of 2.4.2, normalized by the total number of beams and for a rician factor K_r = 10dB. Also the lognormal parameters chosen are μ_m = -2.63, σ=0.5. In the same figure, circle markers represent the simulated expectation of the proposed approximation, given by (3.21). The analytic formulas presented in (3.28) and (3.29), are plotted with continuous lines. It is clear that the analytical expressions precisely fit the expected values of the proposed approximation, thus providing a strong analytic performance evaluation tool. In the same figure, the tightness of the proposed approximation with respect to the actual performance, as calculated by monte carlo simulations on (3.19), is also evident. Over the entire SNR region, the maximum deviation from the actual MMSE value is no more than 1.5dB for the composite fading case, while for the rain fading, the deviation is less than 1dB. Especially for the SNR regions around 12.5 dB and 2dB for the two cases respectively approximation becomes almost exact. In practical systems, these regions are of main interest. Consequently, the proposed expressions are very tight for systems with finite users and conventional link budgets, in contrast to asymptotic results based on large system dimensions or high SNR approaches.

3.3 System Design

3.3.1 Beam Overlap

A sensitivity analysis to deduce the optimal beam overlap in a throughput maximizing sense is included in this section. The RL scenario follows the parameters of Tab. 6.1. The goal of the simulations is twofold. Firstly, it serves as a benchmark to measure the gain of the theoretical SIC given by (2.4) and the more realistic MMSE method given by (2.5), over the

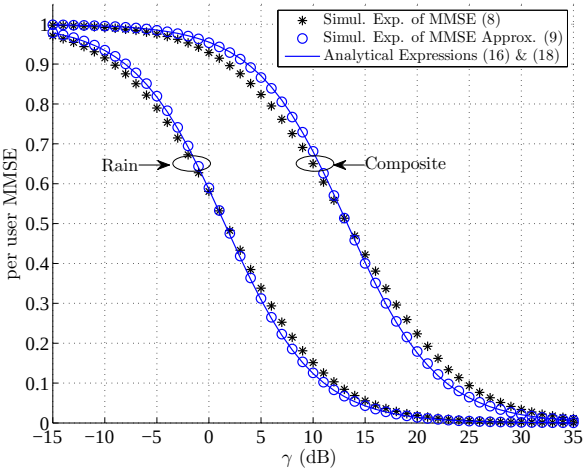

Figure 3.3: MMSE versus increasing transmit power.

conventional four color frequency reuse schemes. Amid the theoretical nature of (2.4) and (2.5), of practical interest is the relative performance of these techniques rather than the absolute numbers of the achievable bit-rate. Secondly, the effect of beam overlapping on the performance of the system is investigated. Thus the achievable per user throughput is plotted in Figures 3.4 and 3.5, for the three different receiver implementations, as the percentage of beam overlap changes. The independent variable is normalized over the nominal 3 dB beam size. For beam size less than one, the satellite receives less than half of the maximum gain from each user, hence gaps appear between beams in the coverage area. For more than one, beams overlap and the satellite is receiving more useful as well as interfering signal power. The metric utilized is average per user achievable throughput, expressed in Mbps.

In Figure 3.5, mobile users are assumed on the cell edge. In this worst case scenario, results indicate that multibeam joint decoding techniques with SIC can theoretically achieve more than twofold gain over conventional techniques. More realistic receiver implementation techniques with linear MMSE filtering still achieve two times more throughput than the

four color frequency reuse scheme. Additionally, system optimality is as expected very close to the nominal value of the beam size. In the same figure, we notice that for high beam separation (i.e., values of normalized beam overlap less than 0.6) linear MMSE performs the same to the SIC. This is justified by the fact that when beams do not overlap, interference becomes negligible. Taking into account that a characteristic of LMMSE is its optimality at the noise limited regime, the above observation is justifiable. Furthermore, when the SNR increases, interference becomes important and linear MMSE techniques prove suboptimal compared to SIC. However, they still manage to maintain a twofold gain over the conventional systems. Finally, an important observation is that the performance of conventional schemes quickly degrades as they are highly affected by interference. Alternatively, the proposed schemes show higher tolerance to interference, hence making them appropriate for a real system implementation where practical restrictions prevent ideal multibeam coverage areas.

According to Figure 3.4, when users are randomly allocated within each beam, then the optimal solution is to incorporate highly directive antennas that better serve users close to the beam center. Hence, optimal throughput is achieved for 0.2 of the nominal beam size. As expected, achievable throughput is higher, compared to the worst case scenario with cell edge users. Again, more than twofold gain can be realized of conventional schemes.

3.3.2 Conventional Payloads

In the present paragraph, a sub-optimal in terms of performance, system design that utilizes exactly the same on board resources, is assumed. From another perspective, interference mitigation techniques are applied over conventional fractional frequency reuse payloads. The purpose is to quantify the potential gains of MUD without necessitating an increase in the payload complexity.

The proposed solution is based on clustering all the co-channel[5] beams and treating each cluster as a smaller full resource reuse system in which multibeam MUD is employed. Since each cluster is served by one GW in the case of multi-GW systems, the necessity of inter-GW cooperation

[5] by the term co-channel we will refer to beams sharing the shame orthogonal dimension, i.e. identical spectrum segment and polarization.

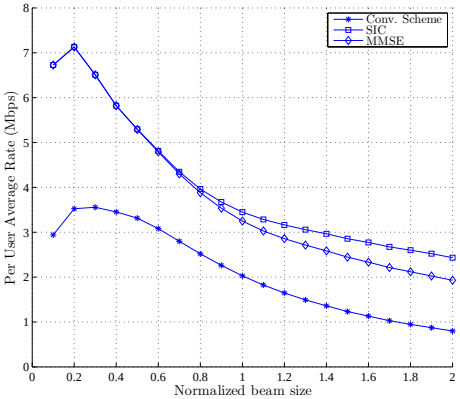

Figure 3.4: Average per user rate in the RL for uniformly distributed users.

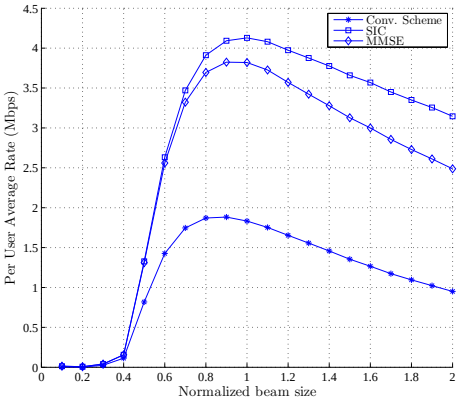

Figure 3.5: Average per user rate in the RL for beam edge users.

is also alleviated. Subsequently, the proposed system utilizes the same resources, in terms of payload, feeder link bandwidth and GW interconnection, as conventional systems.

Beam Clustering

Beam clustering is achieved by assuming beam gain matrices that contain all the co-channel beams. Consequently, in the first proposed scenario (Fig. 3.6), hereafter referred to as *scenario 1*, a conventional frequency and polarization allocation pattern is assumed, where the user link bandwidth is divided in two parts and each one is reused in two polarizations, a Right Hand Circular and a Left Hand Circular Polarization (RHCP and LHCP, respectively). Identical orthogonal dimensions (i.e. colors) are allocated to spatially separated beams, as depicted in Fig. 3.6 and they are handled by the same GW. In (*scenario 2*, depicted in Fig. 3.7) the frequency allocation pattern is altered. All co-channel beams are made adjacent thus increasing the aggregate received power at the receive side. This scenario is inspired from cooperative terrestrial networks where the interference has a beneficial effect on the system throughput performance [26,27]. Subsequently, the composite multibeam satellite channel,

Figure 3.6: Beam clustering with conventional frequency and polarization allocation(*scenario 1*).

firstly proposed in [86], is extended to model the uplink of the clustered

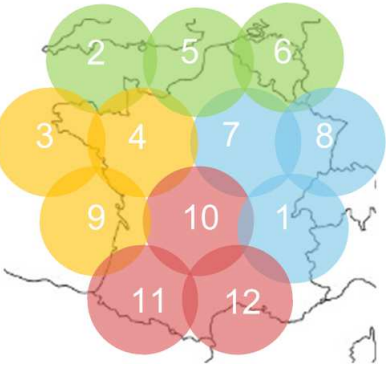

Figure 3.7: Beam clustering with adjacent co-channel beams (*scenario 2*).

system. Herein we will refer to systems that employ MUD over clusters of beams as *clustered systems*, to identify them from conventional single user decoding systems or full resource reuse systems.

Capacity Analysis

In this section, existing results on the capacity of the multibeam composite satellite channel, as achieved by full resource reuse and SIC at the receive side, are briefly reviewed. To assist the investigation of the multibeam composite Rician/lognormal fading channel, the analytical lower bound that has been introduced in (3.7) will serve as a worst case upper bound.

$$C_{\text{erg}} = \sum_{i=1}^{N_c} \mathcal{E}\left\{\log_2 \det\left(\mathrm{I}_n + \gamma \mathbf{H}_i^{\dagger}\mathbf{H}_i\right)\right\}, \tag{3.31}$$

where $\mathbf{H}_i$ is the channel matrix corresponding to each cluster and N_c is the number of available orthogonal resources in frequency and polarization (i.e. $N_c = 4$ in Figs 3.6, 3.7). Extending (3.15) for the clustered system

case is straightforward

$$C_{\text{clus}} = \sum_{i=1}^{N_c} n \log_2 \left(1 + \gamma \exp\left(\frac{1}{n} \cdot \ln\left(\det\left(\mathbf{B}_i \cdot \mathbf{B}_i^{\dagger}\right)\right)\right.\right.$$
$$\left.\left. + \mu_m - \ln\left(K_r + 1\right) + g_1\left(K_r\right)\right)\right). \tag{3.32}$$

The achievable spectral efficiency of conventional multibeam systems employing a frequency reuse scheme is given by

$$C_{\text{conv}} = \tag{3.33}$$
$$\mathcal{E}\left\{N_c^{-1} \sum_{i=1}^{n} \log_2\left(1 + \frac{|h_{ii}|^2}{\sum_{j \neq i, j \in A_C^i} |h_{ij}|^2 + \left(N_c \cdot \gamma\right)^{-1}}\right)\right\},$$

where h_{ij} are the channel coefficients, γ has been defined in (2.4), A_C^i is the set of co-channel beams to the i-th beam and N_c has been defined in (3.31).

Performance Results

To the end of investigating the potential gains of multibeam joint decoding under realistic and accurate assumptions, parameters from existing S-band Geostationary (GEO) satellite systems are used in the simulation model. In Tab. (6.1), the link budget of such a system is presented. According to these values, the expressions for the achievable spectral efficiency presented in Section 3.1.2, are employed to calculate the total achievable throughput of the return link. Monte Carlo simulations (1000 iterations) where carried out to evaluate the average spectral efficiency of the random channels.

According to Fig. 3.8, the upper bound for the achievable throughput is achieved by SIC and full resource (i.e. frequency and polarization) reuse. As already proven in [86, 105], this capacity achieving decoding strategy can provide more than twofold gain over conventional systems, around the SNR region of operation and even higher gains in as the transmit power increases. The performance of the less complex clustered system is presented in the same figure. Results indicate that in the SNR region of operation of current systems, i.e. [5–25]dB, a gain is achieved

by the clustered system. However, it should be clarified that the comparison is made over equal physical layer resource utilization, while as a technology, it requires minor modifications on existing satellite systems. For larger values of received signal power (i.e. over 30dB), this gain becomes substantial. This originates from the logarithmic dependence of the throughput of conventional systems with respect to γ (dB), due to the increase of interference. Controversially, MUD techniques, exploiting the added spatial degrees of freedom, exhibit linear increase of the throughput with γ (dB), in the high SNR region, as depicted in Fig. 3.8. As far

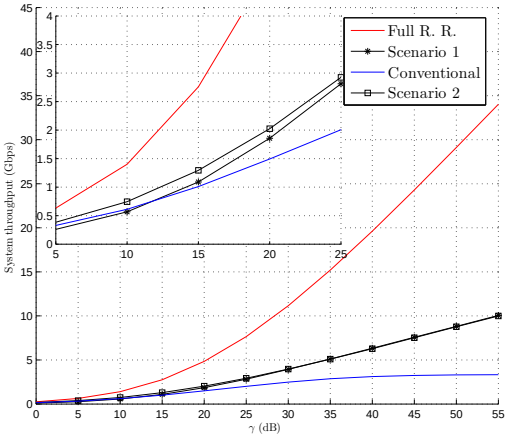

Figure 3.8: Achievable throughput of the proposed and the conventional systems. The Full Resource Reuse (F.R.R.) curves are also included to provide an upper bound on the performance

as the comparison between the possible frequency allocation is concerned (as discussed in the previous paragraphs), the following observations from Fig. 3.8 are made. For less than 25dB, the system proposed in *Scenario 2* marginally outperforms the one proposed in *Scenario 1.* However, as the received power grows larger, the two schemes perform almost equivalently. Consequently, when comparing the two assumed scenarios, we can conclude that little is gained by reallocating the co-channel beams, in the low transmit power region. Although intuitively unexpected, since the

increase of interference should significantly increase the performance of joint decoding techniques according to [26,27], this result is in accordance with the more realistic modeling approaches. As proven in [87], when all interfering tiers are taken into account in the system model, as it is the case in the present work, the increase of interference leads to a degradation of the system performance. This is especially observed in the high SNR region. Thus, the present results are explicitly justified. Consequently, if the clustered MUD systems maintain the same levels of transmit power as existing systems, then the beam reallocation should be considered to offer approximately 2dB gain. Otherwise, if power is to be increased, then the beam pattern should follow the conventional standards.

The results presented hitherto, were based on MC simulations. In order to gain more insight on the implications of the system parameters, analytical calculations firstly introduced in [86] are extended and employed. Eq. (3.15) is used to lower bound the optimal capacity of the full resource reuse system and (3.32) that of the clustered system. Results are presented in Fig. 3.9. As far as the full resource reuse system is concerned, the bound proves exact in the high SNR region but becomes loose in the region [5–25]dB. However, it never exceeds the theoretical performance, thus it can be employed if worst case results need to be produced. Furthermore, an important insight provided by these formulas is the high SNR slope of each system, evaluating the exact throughput for higher values of γ. For example, the throughput of the optimal system will behave exactly as

$$C_{\text{h-SNR}} = N \log_2(\gamma) + \frac{1}{\ln 2}\Big(\ln\big(\det\left(\mathbf{B}\cdot\mathbf{B}^{\dagger}\right)\big) + N\mu_m - N\cdot\big(\ln(K_r+1) - g_1(K_r)\big)\Big). \tag{3.34}$$

The above high SNR slope shows that the capacity grows linearly with respect to γ (in dB) and the inclination of the slope is calibrated by the number of users. Subsequently, the large number of the jointly decoded users benefits the system. Also, the negative effect of the high line of sight is also notable by taking into account that $g_1(K_r) = \ln(K_r) - Ei(K_r)$ is positive and increasing with K_r. The same observations are made for the clustered MUD system, as presented in Fig. 3.9.

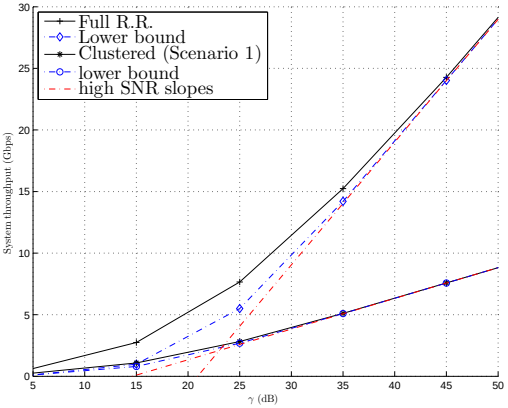

Figure 3.9: Analytical lower bounds and high SNR asymptotes for the proposed techniques. The Full Resource Reuse (F.R.R) curves are also included to provide an upper bound on the performance

3.4 Summary

The capacity of a MU-SIMO channel has been analytically studied under various realistic system parameters. This analysis has been associated to a multibeam satellite communication system where multiple mobile users are transmitting and the received signals at the multibeam satellite antenna, are jointly decoded by an ideal hyper receiver. Indicative per user throughput results are provided for realistic scenarios while comparison with conventional frequency reuse schemes quantifies the potential gain of the proposed techniques.

A new, accurate approximation for the MMSE of a MU SIMO channel that exhibits full receive correlation has been derived, under an analytic framework that generalizes to various fading distributions. The proposed analytic expressions provide accurate approximations of the expected value of the system MMSE, valid for finite system dimensions and over a large SNR region.

Chapter 4

Multicast Multigroup Precoding

A multi-antenna transmitter that conveys independent sets of common data to distinct groups of users is considered in the present chapter. This model is known as physical layer multicasting to multiple co-channel groups. In general, the term multicasting refers to transmitting a single symbol to multiple users. The generalization of multicasting, namely multigroup multicasting, allows multiple symbols each addressed to a group of users. In the multicast multigroup context, the practical constraint of a maximum permitted power level radiated by each antenna is tackled herein, in conjunction with the following fundamental optimization problems.

Firstly, the per-antenna power constrained system is optimized in a maximum fairness sense with respect to a set of predetermined quality of service weights. The term fairness is related to the maximization of the minimum SINR over the coverage area. In other words, the worst user in terms of receive SINR is boosted. The more elaborate, weighted fairness term is introduced to express the flexibility to serve each user (or group of users in the multicast multigroup scenario) with a different service level. This is achieved by maximizing the weighted SINR of each user. A detailed solution to tackle this weighted max-min fair multicast multigroup problem under PACs is therefore derived. The implications of the novel constraints are investigated via prominent applications and paradigms. Additionally, robust to imperfect CSI per-antenna constrained multicast multigroup solutions are proposed. Finally, an extensive performance

evaluation quantifies the gains of the proposed algorithm over existing solutions and exhibits its accuracy over per-antenna power constrained systems.

Secondly, the present chapter also presents a novel multicast multigroup under PACs design that aims at maximizing the total achievable sum rate. To this end, the available power resources are re-allocated to well conditioned groups of users by the means of sub-gradient based power allocation. A detailed solution to tackle the elaborate SR maximization multicast multigroup problem under PACs is therefore derived. Numerical results are presented to quantify the gains of the proposed algorithm over heuristic solutions. As in the fairness case, besides Rayleigh faded channels, the solution is also applied to ULA transmitters operating in the far field[1], where LoS conditions are realized. In this setting, a sensitivity analysis with respect to the angular separation of co-group users is included. Finally, a simple scenario providing important intuitions for the sum rate maximizing multicast multigroup solutions is elaborated.

4.1 Introduction

The spatial degrees of freedom offered by multiple antenna arrays are a valuable resource towards efficiently reusing the available spectrum. Advanced transmit signal processing techniques are currently employed to optimize the performance of the multi-antenna transmitters without compromising the complexity of single antenna receivers. These precoding (or equivalently beamforming) techniques efficiently manage the co-channel interference to achieve the targeted service requirements, herein referred to as QoS targets. As a result, conventional frequency reuse schemes are no longer necessary and the available spectrum is efficiently utilized towards increasing the system throughput. As always, however, the benefits of these advanced schemes come with a cost. The fundamental requisite for the application of precoding is the accurate knowledge of the CSI at the transmitter.

The optimal transmit beamforming in the minimum total transmit power sense, assuming independent –over the users– data transmission (hereafter referred to as unicasting), was initially derived in [57,58]. PACs

[1] In the far field of ULA transmitters, a Rician channel model manifestation is of issue.

were subsequently considered in [60]. The motivation for the PACs originates from the practical implementation of systems that rely on precoding. The lack of flexibility in sharing energy resources amongst the antennas of the transmitter is usually the case since a common practice in multi-antenna systems is the use of individual amplifiers per antenna. Despite the fact that flexible amplifiers could be incorporated in multi-antenna transmitters, specific communication systems cannot afford this design. Typical per antenna power limited systems can be found in multibeam satellite communications [68], where flexible on board payloads are difficult to implement. The PACs are also relevant in cooperative multicell systems (also known as distributed antenna systems, DAS), where the physical co-location of the transmitting elements is not a requisite and hence power sharing is infeasible[2].

The momentum in the application of multiuser multiple input multiple output (MIMO) antenna wireless communications substantiates the consideration of inherent system level attributes. Thus, in several cases the new generation of multi-antenna communication standards has to adapt the physical layer design to the needs of the higher network layers. Examples of such cases include highly demanding applications (e.g. video broadcasting) that stretch the throughout limits of multiuser broadband systems. In this direction, physical layer (PHY) multicasting has the potential to efficiently address the nature of traffic demand in future systems and has become part of the new generation of communication standards. Additionally, towards enhancing the PHY multicasting functionality, multiple multicast co-channel groups have been considered. In this multicast multigroup scenario, the system design is proven to be quite challenging and is connected with fundamental optimization problems [75–77]. An in depth literature review of the SoA in multigroup multicasting will be presented in the following sections.

Lastly, PHY multicasting can be employed when the goal is to optimize full frequency reuse multi-antenna transmitters without changing the framing structure of communication standards. For instance, specific PHY designs are optimized to cope with noise limited channels with long propagation delays [19, 19]. Also, the framing of multiple users per trans-

[2]For the sake of clarity, the difference between the proposed cooperative multicell networks and the coordinated case of [81] is pointed out. In the latter case, each base station (BS) transmits to a single multicast group. On the other hand, in a cooperative multicast multicell system, all BSs jointly transmit to multicast groups.

mission is emanated to guarantee scheduling efficiency when long forward error correction codes are employed. Thus, beamforming techniques in such systems cannot be based on the conventional precoding design that assumes independent symbols, each addressed to a different single user, and multicasting needs to be considered. This problem will be the focus of the next chapter.

4.2 QoS and Fairness: Two related problems

In the multicast multigroup literature, two fundamental optimization criteria have been considered until now, namely the sum power minimization under specific QoS constraints and the maximization of the minimum SNIR (*Max-Min Fair*) under SPC.

The optimal downlink transmission strategy in the sense of minimizing the total transmit power whilst guaranteing specific QoS targets at each user, was given in [57, 58]. Therein, the tool of Semi-Definite Relaxation (SDR) reduced the non-convex quadratically constrained quadratic problem (QCQP) into a relaxed semi-definite programming instance by changing the optimization variables and disregarding the rank-1 constraints over the new variable. The solution of the relaxed problem was proven to be optimal. The multiuser downlink beamforming problem in terms of maximizing the minimum SNIR, was optimally solved in [59]. The goal of the later formulation is to increase the fairness of the system by boosting the SNIR of the user that is further away from a targeted performance. Hence, the problem is commonly referred to as *max–min fair*. In [59], this problem was solved using the principles of uplink/downlink duality. Therein, the authors developed a strongly convergent iterative alternating optimization algorithm for the equivalent uplink problem. In the same work, the power minimization problem of [57] was also solved by acknowledging its inherent connection with the max-min fair problem. Consequently, a significantly less complex framework to solve the optimal *max–min fair* beamforming problem was established.

Power Minimization under QoS Constraints

A fundamental consideration in [57, 58] is the unicast assumption, where independent data are addressed to the multiple users. Under this assumption, the SDR guarantees an optimal solution to the QCQP problem [57].

In other words, the relaxation is always tight. Based on the principles of SDR, the QoS problem in a physical layer multicasting scenario[3] was tackled in [76]. One inherent difference over the prior consideration of transmitting independent data to each user substantiated the new formulation. Specifically, in the physical layer multicasting problem, *common* symbols are addressed to all the users. This assumption renders the beamforming problem NP-hard [76]. Hence, when the goal is to transmit common information to multiple users with different channels, the optimal solution is not obtainable in polynomial time. In order to derive a low complexity and accurate approximate solution[4] to the multicast problem, SDR was combined with Gaussian randomization in [76]. A detailed review of this method can be found in [126]. Finally, the feasibility of the original problem can be guaranteed by a simple rescaling of the random Gaussian solutions, without affecting the beamforming directions [76].

The natural extension of the physical layer multicasting lies in assuming multiple co-channel groups of users. In each group, each user receives a stream of common data. However, independent symbols are addressed to different groups and inter-group interference comes into play. A unified framework for physical layer multicasting to multiple interfering groups, where independent sets of common data are transmitted to multiple interfering groups of users by the multiple antennas, was given in [75, 77]. This general problem was also shown to be NP-hard to solve, since it includes multicasting as a special case [75]. Despite the existence of an optimal solution for the independent data beamforming, via the SDR, and the existence of a high accuracy approximation of the multicasting case, via the Gaussian randomization, a general solution to the multicast multigroup scenario is more complicated. The combination of SDR and Gaussian randomization is only the first step. The difficulties arise due to the coupling between the multicast groups. More specifically, the issue of intergroup interference emerges due to the independent data being transmitted to different groups over the same channels. Hence, after obtaining candidate solutions from the Gaussian randomization process, the feasibility of the initial QCQP cannot be guaranteed by a simple re-

[3]The multi-antenna multicast problem was originally proposed in [74], where the maximization of the average SINR over all users was the goal, without however guaranteeing some QoS at the user side.

[4]In SDR, accuracy refers to the ability of a rank-1 approximation to approach the relaxed upper bound, that is the optimal value of the problem without any rank constraints.

scaling of the randomized precoding vectors, in contrast to the multicast case. Rescaling the power of one precoder affects the co-channel groups, since they are coupled by interference. To the end of solving the elaborate multicast multigroup problem, an additional step following the Gaussian randomization was proposed in [75]. This step consisted of a new linear programming optimization problem, namely the *multicast multigroup power control* (MMPC) problem, that converted the candidate solutions into feasible solutions of the original problem [75, 77].

For the sake of completeness, in parallel to [77], the independent work presented in [78] is also mentioned. Despite the use of the SDR method combined with Gaussian randomization to solve the QoS multicast multigroup problem, the authors of [78] rely on dirty paper coding (DPC) to successively precancel intergroup interference. Thus the co-channel groups are decoupled and the power allocation process is simplified at the expense of high implementation complexity.

Fairness under SPC

The maximization of the minimum SINR received by any of the available users in the coverage area, subject to a SPC at the transmitter is closely related to the previously described QoS problem. The goal of the max–min formulation is to increase the fairness of the system by boosting the SINR of the user that is further away from a targeted performance. Initially, in [76] it was proven that a QoS problem with equal SINR constraints is equivalent to the max-min fair problem up to scaling. Towards extending this, the maximum scaled fairness optimization was formulated, proven NP-hard and accurately approximated, for a multicast multigroup case in [75]. This weighted max–min formulation allowed for per user SINR targets. In more detail, a bisection search method over the relaxed power minimization problem provided candidate solutions to the initial weighted fairness optimization of [75]. Then, an additional power allocation guaranteed the feasibility of the original problem. The complication in the fairness scenario, however, was that the *multicast multigroup power control* MMPC problem does not admit a linear program reformulation and thus its solution is not trivial[5]. To overcome this, a one dimensional bisection search was again performed, this time over the power control of

[5]It can however be reformulated as a geometric problem (GP) and solved efficiently with interior point methods [75]. Either methods can be used alternatively.

the QoS problem.

In optimization terminology, the fact that the SDR can provide a global optimum for the original unicast problem shows that strong duality holds. In other words, a zero duality gap between the two problems is observed. In this light, the authors of [80], tackled the multicast multigroup problem under SPC, based on the framework of uplink-downlink duality [59]. However, since in the multicast multigroup case one precoder needs to apply for multiple users conventional duality is not straightforward. Thus, approximations were employed, leading to the low complexity *multicast-aware* solutions of [80]. These solutions were shown to tradeoff the low complexity with the inferior performance in terms of BER (i.e. minimum SINR) compared to [75], under numerically exhibited convergence.

Finally, a different approach was followed in [79], where an iterative algorithm based on the convex approximation of the original non-convex problem was proposed. This method was shown to perform equivalently to [75] when the number of users per group is relatively small (e.g. 3 users per group) but exhibit superior performance as the number of users per group grows. This improved performance is also given at a reduced complexity cost.

In the context of coordinated multicast multicell systems, the solution of a max–min fair problem with per base-station (BS) constraints and equal SINR targets has been derived in [81]. In this scenario, a sum power constraint is no longer applicable and the QoS problem is no longer related to the max–min fair problem. Therefore, a solution of the new optimization problem was given following the well established framework of bisection over a modified related problem. Nevertheless, in each BS a single group of receivers was assumed. Hence, a power constraint over each precoder was imposed. Additionally, no optimization weights were considered.

Amid the extensive literature on multicast multigroup beamforming, a per antenna power constrained system has yet to be considered. Therefore, a consolidated solution for the weighted max–min fair multicast multigroup beamforming under PACs is hereafter presented.

4.3 Per-antenna Constrained Fairness Optimization

Towards deriving the optimal multicast multigroup precoders when a maximum limit is imposed on the transmitted power of each antenna, a new optimization problem with one constraint per transmit antenna needs to be formulated. Amid the extensive literature on multicast multigroup

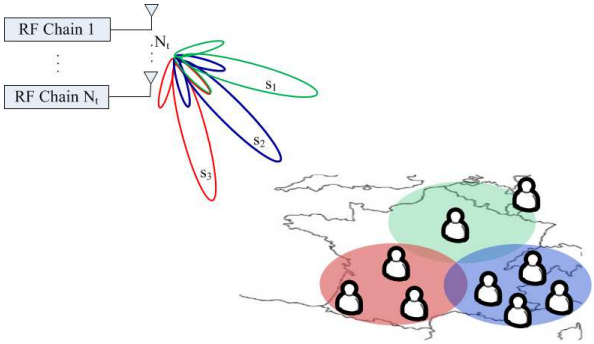

Figure 4.1: Multicast multigroup beamforming for a transmitter with N_t antennas driven by individual amplifiers.

beamforming, the PACs have yet to be considered. Therefore, a consolidated solution for the weighted max–min fair multicast multigroup beamforming under PACs is hereafter presented. The contributions of this thesis adding to the literature on multicast precoding, are summarized in the following points:

- The PAC weighted fair multicast multigroup problem is formulated and solved.
- Practical system design insights are given by examining the implications of the PACs on multicast multigroup distributed antenna systems (DAS), modulation constrained systems and uniform linear array (ULA) transmitters.
- A robust to erroneous CSI, multicast multigroup design under PACs is proposed.

- The performance of all solutions is evaluated through extensive numerical results under various system setups.
- The max SR multicast multigroup problem under PACs is formulated and solved for the first time.

4.3.1 Weighted Fair Optimization

The PAC weighted max-min fair problem is defined as

$$\mathcal{F}: \max_{t,\ \{\mathbf{w}_k\}_{k=1}^{G}} t$$

$$\text{subject to } \frac{1}{\gamma_i}\frac{|\mathbf{w}_k^{\dagger}\mathbf{h}_i|^2}{\sum_{l\neq k}^{G}|\mathbf{w}_l^{\dagger}\mathbf{h}_i|^2+\sigma_i^2}\geq t, \quad \forall i\in\mathcal{G}_k, k, l\in\{1\dots G\}, \tag{4.1}$$

$$\text{and to } \left[\sum_{k=1}^{G}\mathbf{w}_k\mathbf{w}_k^{\dagger}\right]_{nn}\leq P_n, \quad \forall n\in\{1\dots N_t\}, \tag{4.2}$$

where $\mathbf{w}_k\in\mathbb{C}^{N_t}$ and $t\in\mathbb{R}^{+}$. The parameters of the above formulations are in detail described in Ch. 2 and are avoided herein for shortness. Different service levels between the users can be acknowledged in this weighted formulation. Problem $\mathcal{F}$ receives as inputs the PACs vector $\mathbf{p}=[P_1,P_2\dots P_{N_t}]$ and the target SNIRs vector $\mathbf{g}=[\gamma_1,\gamma_2,\dots\gamma_{N_u}]$. Its goal is to maximize the slack variable t while keeping all SNIRs above this value. Thus, it constitutes a max-min problem that guarantees fairness amongst users. Following the common in the literature notation for ease of reference, the optimal objective value of $\mathcal{F}$ is denoted as $t^*=\mathcal{F}(\mathbf{g},\mathbf{p})$ and the associated optimal point as $\{\mathbf{w}_k^{\mathcal{F}}\}_{k=1}^{G}$. Of particular interest is the case where the co-group users share the same target i.e. $\gamma_i=\gamma_k,\ \forall i\in\mathcal{G}_k, k\in\{1\dots G\}$.

Remark 4.1. *The difference of the present formulation with respect to the weighted max-min fair problem with* SPC *presented in [75, 76] lies in the N_t power constraints over each individual radiating element. Additionally, this formulation differs from the coordinated multicell multicasting Max-Min formulation of [81] since the constraint is imposed on the n-th*

diagonal element of the summation of the correlation matrices of all precoders,i.e. 4.2, while weights on each users SNIR *are also inserted, i.e. 4.1. On the contrary, in [81], the imposed per base station constraints are translated to one power constraint per each precoder. Consequently, an inherently different problem is formulated herein, with a different number of constraints aiming to model the per-antenna limitations at the transmitter. In [109], weights to differentiate the* QoS *targets between users are also proposed. A special case of this for equal* SNIR *weights amongst the users is presented in [108].*

Per-antenna Power Minimization

The sum transmit power minimization problem under QoS constraints [57] is related to the max–min problem [127] and this relation was generalized for the multicast multigroup case in [75]. Hence by bisecting the solution of the QoS optimization, a solution to the weighted fairness problem can be derived. Nevertheless, two fundamental differences between the existing formulations and problem $\mathcal{F}$ complicate the solution. Firstly, the power constraints are not necessarily met with equality. Secondly, the absence of a related, solvable problem prohibits the immediate application of bisection. Thus a per antenna power minimization problem is proposed as

$$\begin{aligned}
\mathcal{Q}: \quad & \min_{r,\ \{\mathbf{w}_k\}_{k=1}^{G}} \quad r \\
& \text{subject to} \quad \frac{|\mathbf{w}_k^{\dagger}\mathbf{h}_i|^2}{\sum_{l\neq k}^{G}|\mathbf{w}_l^{\dagger}\mathbf{h}_i|^2+\sigma_i^2} \geq \gamma_i, \qquad (4.3) \\
& \qquad\qquad \forall i \in \mathcal{G}_k, k, l \in \{1\dots G\}, \\
& \text{and to} \quad \frac{1}{P_n}\left[\sum_{k=1}^{G}\mathbf{w}_k\mathbf{w}_k^{\dagger}\right]_{nn} \leq r, \qquad (4.4) \\
& \qquad\qquad \forall n \in \{1\dots N_t\},
\end{aligned}$$

with $r \in \mathbb{R}^+$. Problem $\mathcal{Q}$ receives as input SNIR constraints for all users, defined before as $\mathbf{g}$, as well as the per antenna power constraint vector $\mathbf{p}$ of (4.2). Subsequently, the maximum power consumption out of all antennas is minimized and this solution is denoted as $r^* = \mathcal{Q}(\mathbf{g}, \mathbf{p})$. The generic difference of the present min-max formulation and the formulation proposed in [81] lies in the per antenna constraint (4.4). Instead

of constraining the power of each antenna, the authors of [81] impose a constraint over each precoder that serves a common multicast group. In the case tackled herein, the number of constraints is increased from one to N_t, while each constraint is a function of all multigroup precoders as the summation in (4.4) reveals. The following claim reveals the relation between the described problems.

Claim 1: Problems $\mathcal{F}$ and $\mathcal{Q}$ are related as follows

$$1 = \mathcal{Q}\left(\mathcal{F}\left(\mathbf{g}, \mathbf{p}\right) \cdot \mathbf{g}, \mathbf{p}\right) \tag{4.5}$$

$$t = \mathcal{F}\left(\mathbf{g}, \mathcal{Q}\left(t \cdot \mathbf{g}, \mathbf{p}\right) \cdot \mathbf{p}\right) \tag{4.6}$$

Proof: The above claims will be proven by contradiction. Starting with (4.5), let $t^* = \mathcal{F}(\mathbf{g},\ \mathbf{p})$ denote the optimal value of $\mathcal{F}$ with associated variable $\{\mathbf{w}_k^F\}_{k=1}^G$. Also, let $\hat{r} = \mathcal{Q}\left(t^* \cdot \mathbf{g},\ \mathbf{p}\right)$ be the optimal value of $\mathcal{Q}$ at the point $\{\mathbf{w}_k^Q\}_{k=1}^G$. Then, assuming that $\hat{r} > 1$, the vectors $\{\mathbf{w}_k^F\}_{k=1}^G$ satisfy the feasibility criteria of $\mathcal{Q}$ and produce a lower optimal value thus contradicting the optimality of $\{\mathbf{w}_k^Q\}_{k=1}^G$ and opposing the hypothesis. Alternatively, assuming that $\hat{r} < 1$ then the solutions $\{\mathbf{w}_k^Q\}_{k=1}^G$ can be scaled by the non-negative $\hat{r}$. The vectors $\{\hat{r} \cdot \mathbf{w}_k^Q\}_{k=1}^G$ are feasible solutions to $\mathcal{F}$ which provide the same optimal objective value with however some remaining power budget. Therefore, the power could be scaled up until at least one of the PACs is satisfied with equality and a higher objective value would be derived thus again contradicting the hypothesis. Consequently, $\hat{r} = 1$. The same line of reasoning is followed to prove (4.6). Let $r^* = \mathcal{Q}(t \cdot \mathbf{g},\ \mathbf{p})$ denote the optimal value of $\mathcal{Q}$ with associated solution $\{\mathbf{w}_k^Q\}_{k=1}^G$. Assuming that the optimal value of $\mathcal{F}$ under constraints scaled by the solution of $\mathcal{Q}$ is different, i.e. $\hat{t} = \mathcal{F}\left(\mathbf{g},\ \mathcal{Q}\left(t \cdot \mathbf{g},\ \mathbf{p}\right) \cdot \mathbf{p}\right)$ with $\{\mathbf{w}_k^F\}_{k=1}^G$, the following contradictions arise. In the case where $\hat{t} < t$, then the precoders $\{\mathbf{w}_k^Q\}_{k=1}^G$ are feasible solutions to $\mathcal{F}$ which lead to a higher minimum SNIR, thus contradicting the optimality of $\hat{t}$. Alternatively, if $\hat{t} > t$ then the solution set $\{\mathbf{w}_k^F\}_{k=1}^G$ can be scaled by a positive constant $c = t/\hat{t} < 1$. The new solution $\{c\mathbf{w}_k^F\}_{k=1}^G$ respects the feasibility conditions of $\mathcal{Q}$ and provides a lower optimal value, i.e. $c \cdot r^*$, thus again contradicting the hypothesis. As a result, $\hat{t} = t$ $\square$.

Semidefinite Relaxation

Problem $\mathcal{Q}$ belongs in the general class of non-convex QCQPs for which the SDR technique is proven to be a powerful and computationally efficient

approximation technique [126]. The relaxation is based on the observation that $|\mathbf{w}_k^\dagger \mathbf{h}_i|^2 = \mathbf{w}_k^\dagger \mathbf{h}_i \mathbf{h}_i^\dagger \mathbf{w}_k = \mathrm{Tr}(\mathbf{w}_k^\dagger \mathbf{h}_i \mathbf{h}_i^\dagger \mathbf{w}_k) = \mathrm{Tr}(\mathbf{w}_k \mathbf{w}_k^\dagger \mathbf{h}_i \mathbf{h}_i^\dagger)$. With the change of variables $\mathbf{X}_i = \mathbf{w}_i \mathbf{w}_i^\dagger$, $\mathcal{Q}$ can be relaxed to $\mathcal{Q}_r$

$$\mathcal{Q}_r : \min_{r,\ \{\mathbf{X}_k\}_{k=1}^G} r$$

$$\text{subject to } \frac{\mathrm{Tr}\left(\mathbf{Q}_i \mathbf{X}_k\right)}{\sum_{l \neq k} \mathrm{Tr}\left(\mathbf{Q}_i \mathbf{X}_l\right) + \sigma_i^2} \geq \gamma_i, \quad \forall i \in \mathcal{G}_k, k, l \in \{1 \dots G\}, \tag{4.7}$$

$$\text{and to } \frac{1}{P_n} \left[\sum_{k=1}^G \mathbf{X}_k\right]_{nn} \leq r \quad \forall n \in \{1 \dots N_t\}, \tag{4.8}$$

$$\text{and to } \mathbf{X}_k \succeq 0,\ \forall k \in \{1 \dots G\}, \tag{4.9}$$

where $\mathbf{Q}_i = \mathbf{h}_i \mathbf{h}_i^\dagger$, $r \in \mathbb{R}^+$, while the constraint $\mathrm{rank}(\mathbf{X}_i) = 1$ is dropped. Now the relaxed $\mathcal{Q}_r$ is convex, thus solvable to an arbitrary accuracy. This This relaxation can be interpreted as a Lagrangian bi-dual of the original problem [71]. The weighted max-min fair optimization is also relaxed as

$$\mathcal{F}_r : \max_{t,\ \{\mathbf{X}_k\}_{k=1}^G} t$$

$$\text{subject to } \frac{1}{\gamma_i} \frac{\mathrm{Tr}\left(\mathbf{Q}_i \mathbf{X}_k\right)}{\sum_{l \neq k} \mathrm{Tr}\left(\mathbf{Q}_i \mathbf{X}_l\right) + \sigma_i^2} \geq t, \quad \forall i \in \mathcal{G}_k, k, l \in \{1 \dots G\}, \tag{4.10}$$

$$\text{and to } \left[\sum_{k=1}^G \mathbf{X}_k\right]_{nn} \leq P_n, \quad \forall n \in \{1 \dots N_t\}, \tag{4.11}$$

$$\text{and to } \mathbf{X}_k \succeq 0,\ \forall k \in \{1 \dots G\}, \tag{4.12}$$

which, however, remains non-convex due to (4.10), as in detail explained in [75]. However, this obstacle can be overcome by the following observation. *Claim 2: Problems $\mathcal{F}_r$ and $\mathcal{Q}_r$ are related as follows*

$$1 = \mathcal{Q}_r\left(\mathcal{F}_r\left(\mathbf{g}, \mathbf{p}\right) \cdot \mathbf{g}, \mathbf{p}\right) \tag{4.13}$$

$$t = \mathcal{F}_r\left(\mathbf{g}, \mathcal{Q}_r\left(t \cdot \mathbf{g}, \mathbf{p}\right) \cdot \mathbf{p}\right) \tag{4.14}$$

Proof: Follows the steps of the proof of *Claim 1* and is therefore omitted. □

Gaussian Randomization

Due to the NP-hardness of the multicast problem, the relaxed problems do not necessarily yield unit rank matrices. Consequently, one can apply a rank-1 approximation over $\mathbf{X}^*$. Many types of rank-1 approximations are possible depending on the nature of the original problem. The solution with the highest provable accuracy for the multicast case is given by the Gaussian randomization method [126]. In more detail, let $\mathbf{X}^*$ be a positive semidefinite solution of the relaxed problem. Then, a candidate solution to the original problem can be generated as a Gaussian random variable with zero mean and covariance equal to $\mathbf{X}^*$, i.e. $\hat{\mathbf{w}} \backsim \mathbb{CN}(0, \mathbf{X}^*)$. After generating a predetermined number of candidate solutions, the one that yields the highest objective value of the original problem can be chosen. The accuracy of this approximate solution is measured by the distance of the approximate objective value and the optimal value of the relaxed problem and it increases with the predetermined number of randomizations. Nonetheless, an intermediate problem dependent step between generating a Gaussian instance with the statistics obtained from the relaxed solution and creating a feasible candidate instance of the original problem still remains, since the feasibility of the original problem is not yet guaranteed.

Feasibility Power Control

After generating a random instance of a Gaussian variable with statistics defined by the relaxed problem, an additional step comes in play to guarantee the feasibility of the original problem. In [76], a simple power rescaling of the candidate solutions which follows the Gaussian randomization is sufficient to guarantee feasibility. Nevertheless, since in the multigroup case an interference scenario is dealt with, a simple rescaling does not guarantee feasibility. Therefore, an additional optimization step is proposed in [75] to re-distribute the power amongst the candidate precoders. To account for the inherently different PACs, a novel power control problem with per antenna power constraints is proposed herein. Given a set of Gaussian instances, $\{\hat{\mathbf{w}}_k\}_{k=1}^{G}$, the *multicast multigroup Per*

Antenna power Control (MMPAC) problem reads as

$$\mathcal{S}^{\mathcal{F}}: \max_{t,\ \{p_k\}_{k=1}^{G}} t$$

$$\text{subject to } \frac{1}{\gamma_i}\frac{|\hat{\mathbf{w}}_k^{\dagger}\mathbf{h}_i|^2 p_k}{\sum_{l\neq k}^{G}|\hat{\mathbf{w}}_l\mathbf{h}_i|^2 p_l+\sigma_i^2}\geq t, \quad \forall i\in\mathcal{G}_k, k, l\in\{1\dots G\} \tag{4.15}$$

$$\text{and to } \left[\sum_{k=1}^{G}\hat{\mathbf{w}}_k\hat{\mathbf{w}}_k^{\dagger}p_k\right]_{nn}\leq P_n, \quad \forall n\in\{1\dots N_t\}, \tag{4.16}$$

with $\{p_k\}_{k=1}^{G}\in\mathbb{R}^{+}$. Problem $\mathcal{S}^{\mathcal{F}}$ receives as input the PACs as well as the SNIR targets and returns the maximum scaled worst SNIR $t^*=\mathcal{S}(\mathbf{g},\mathbf{p})$ and is also non-convex like $\mathcal{F}$. The difference of this problem compared to [75] lies in (4.16).

Remark 4.2. *A very important observation is clear in the formulation of the power control problem. The optimization variable* $\mathbf{p}$ *is of size* G*, i.e. equal to the number of groups, while the power constraints are equal to the number of antennas,* N_t*. In each constraint, all the optimization variables contribute. This fact, can prohibit the total exploitation of the available power at the transmitter in some scenarios. Once at least one of the* N_t *constraints is satisfied with equality and remaining power budget, then the rest can not be scaled up since this would lead to at least one constraint exceeding the maximum permitted value.*

Bisection

The solution of $r^*=\mathcal{Q}_r\left(\frac{L+U}{2}\mathbf{g},\mathbf{p}\right)$ is obtained by bisecting the interval $[L,U]$ as defined by the minimum and maximum SNIR values. Since $t=(L+U)/2$ represents the SNIR, it will always be positive or zero. Thus, the bisection initiates with $L=0$. Also, if the system was interference free while all the users had the channel of the best user, then the maximum worst SNIR would be attained, thus at the first iteration of bisection, $U=\max_i\{P_{tot}\mathbf{Q}_i/\sigma_i\}$. If $r^*<1$, then the lower bound of the interval is updated with this value. Otherwise the value is assigned to the upper bound of the interval. Bisection is iteratively performed until an the

interval size is reduced to a pre-specified value ϵ. This value needs to be dependent on the magnitude of L and U so that the accuracy of the solution is maintained regardless of the region of operation. After a finite number of iterations the optimal value of $\mathcal{F}_r$ is given as the resulting value for which L and U become almost identical. This procedure provides an accurate solution to the non-convex $\mathcal{F}_r$. Following this, for each and every solution $\{\hat{\mathbf{w}}_k\}_{k=1}^G$, the power of the precoders needs to be controlled. Problem $\mathcal{S}^F$ can be solved by bisecting its convex equivalent problem, which reads as

$$\begin{aligned}
&\mathcal{S}^{\mathcal{Q}}: \min_{r,\ \{p_k\}_{k=1}^G} r \\
&\quad \text{subject to } \frac{|\hat{\mathbf{w}}_k^\dagger \mathbf{h}_i|^2 p_k}{\sum_{l\neq k}^G |\hat{\mathbf{w}}_l^\dagger \mathbf{h}_i|^2 p_l + \sigma_i^2} \geq \gamma_i, \qquad (4.17)\\
&\qquad\qquad \forall i \in \mathcal{G}_k, k, l \in \{1 \dots G\}, \\
&\quad \text{and to } \quad \frac{1}{P_n}\left[\sum_{k=1}^G \hat{\mathbf{w}}_k \hat{\mathbf{w}}_k^\dagger p_k\right]_{nn} \leq r, \qquad (4.18)\\
&\qquad\qquad \forall n \in \{1 \dots N_t\},
\end{aligned}$$

which is an instance of a linear programming (LP) problem.

Remark 4.3. *For completeness, the possible reformulation of the non-convex problem $\mathcal{S}^{\mathcal{F}}$ into the following geometric problem (*GP*) is considered, thus surpassing the need for bisection:*

$$\begin{aligned}
&\mathcal{S}_{\mathcal{GP}}^{\mathcal{F}}: \min_{t,\ \{p_k\}_{k=1}^G} t^{-1} \\
&s.\ t. \sum_{l\neq k}^G |\hat{\mathbf{w}}_l \mathbf{h}_i|^2 p_l + \sigma_i^2 \leq \frac{t^{-1}}{\gamma_i} |\hat{\mathbf{w}}_k^\dagger \mathbf{h}_i|^2 p_k, \qquad (4.19)\\
&\qquad \forall i \in \mathcal{G}_k, k, l \in \{1 \dots G\} \\
&\textit{and to } \left[\sum_{k=1}^G \hat{\mathbf{w}}_k \hat{\mathbf{w}}_k^\dagger p_k\right]_{nn} \leq P_n, \forall n \in \{1 \dots N_t\},
\end{aligned}$$

4.3.2 Complexity

An important discussion involves the complexity of the employed techniques to approximate a solution of the NP-hard, multicast multigroup problem under PACs. Focusing on the proposed algorithm (cf. Alg. 1), the main complexity burden originates from the solution of a SDP. The present work relies on the CVX tool [71] which calls numerical solvers such as SeDuMi to solve semi-definite programs. The complexity of the SDR technique has been exhaustively discussed in [126] and the references therein. To calculate the total worst case complexity of the solution proposed in the present work, the following are considered.

Initially, a bisection search is performed over $\mathcal{Q}_r$ to obtain the relaxed solution. This bisection runs for $N_{\text{iter}} = \lceil \log_2 (U_1 - L_1) / \epsilon_1 \rceil$ where ϵ_1 is the desired accuracy of the search. Typically ϵ_1 needs to be at least three orders of magnitude below the magnitudes of U_1, L_1 for sufficient accuracy. In each iteration of the bisection search, problem $\mathcal{Q}_r$ is solved. This SDP has G matrix variables of $N_t \times N_t$ dimensions and $N_u + N_t$ linear constraints. The interior point methods employed to solve this SDP require at most $\mathcal{O}(\sqrt{GN_t} \log(1/\epsilon)$ iterations, where ϵ is the desired numerical accuracy of the solver. Moreover, in each iteration not more than $\mathcal{O}(G^3 N_t^6 + G N_t^3 + N_u G N_t^2)$ arithmetic operations will be performed. The increase in complexity stems from increasing the number of constraints, i.e. $N_t + N_u$ constraints are considered instead of only N_u as in [75]. However, this increase is not significant, since the order of the polynomial with respect to the number of transmit antennas is not increased. The solver used also exploits the specific structure of matrices hence the actual running time is reduced. Next, a fixed number of Gaussian random instances with covariance given by the previous solution are generated. The complexity burden of this step is given by the following considerations. For each randomization, a second bisection search is performed this time over the LP $\mathcal{S}^{\mathcal{Q}}$. An $\epsilon-$optimal solution of this problem can be generated with a worst case complexity of $\mathcal{O}(G^{3.5} \log(1/\epsilon))$ [128] . The second bisection runs for $N_{\text{iter}} = \lceil \log_2 (U_2 - L_2) / \epsilon_2 \rceil$ iterations, which are significantly reduced since the upper bound U_2 is now the optimal value of the relaxed problem. Moreover, the Gaussian randomization is executed for a fixed number of iterations. The accuracy of the solution increases with the number of randomizations [75, 76, 126]. Finally, the complexity burden can be further reduced by the reformulation of the non-convex $\mathcal{S}^{\mathcal{F}}$

into the GP $\mathcal{S}^{\mathcal{F}}_{\mathcal{GP}}$ which is efficiently solved by successive approximations of primal-dual interior point numerical methods [71]. Thus the need for the second bisection can be surpassed.

Input: $N_{\text{rand}}, \mathbf{p}, \mathbf{g}, \mathbf{Q}_i, \sigma_i^2 \ \forall i \in \{1 \dots G\}$
Output: $\{\mathbf{w}_k^{opt}\}_{k=1}^G$, t^*_{opt} of $\mathcal{F}$
begin
  Step 1: Solve $t_{opt} = \mathcal{F}_r(\mathbf{g}, \mathbf{p})$ by bisecting $\mathcal{Q}_r\left(\frac{L+U}{2}\mathbf{g}, \mathbf{p}\right)$, (see Sec. 4.3.1). .
  if $\text{rank}(\mathbf{X}_k^{opt}) = 1, \forall\ k \in \{1 \dots G\}$ **then**
    $\{\mathbf{w}_k^{opt}\}_{k=1}^G$ and t^*_{opt} are given by $\lambda_{max}(\mathbf{X}^{opt})$.
  else
    Step 2: : Generate N_{rand} precoding vectors $\{\hat{\mathbf{w}}_k\}_{k=1}^G$, (see Sec. 4.3.1). $t^*_{(0)} = 0$;
    for $i = 1 \dots N_{rand}$ **do**
      Step 3: Solve $\mathcal{S}^{\mathcal{F}}(\mathbf{g}, \mathbf{p})$ by bisecting $\mathcal{S}^{\mathcal{Q}}\left(\frac{L+U}{2}\mathbf{g}, \mathbf{p}\right)$ to get a $\{\mathbf{w}_k^{can}\}_{k=1}^G$ with $t^*_{(i)}$.
      if $t^*_{(i)} > t_{(i-1)}$ **then**
        $t^*_{opt} = t^*_{(i)}, \{\mathbf{w}_k^{opt}\}_{k=1}^G = \{\mathbf{w}_k^{can}\}_{k=1}^G$
      end
    end
  end
end

Algorithm 1: Weighted Fair multigroup multicasting under PACs.

4.4 Per-antenna Constrained Sum Rate Maximization

In a multicast scenario, the performance of all the receivers listening to the same multicast is dictated by the worst rate in the group. A multigroup multicasting scenario, however, entails the flexibility to maximize the total system rate by providing different service levels amongst groups. The multicast multigroup max SR optimization aims at increasing the minimum SINR within each group while in parallel maximizing the sum of the rates of all groups. Intuitively, this can be accomplished by reducing the

SINR of users with better conditions than the worst user of their group. Also, groups that contain compromised users might need to be turned off and their users driven to service unavailability to save power resources and degrees of freedom. Subsequently, power is not consumed for the mitigation of poor channel conditions. Any remaining power budget is then reallocated to well conditioned and balanced in terms of performance groups.

4.4.1 Sum Rate Maximization

This section focuses on the per-antenna power constrained max SR problem, formally defined as

$$\mathcal{SR}: \quad \max_{\{\mathbf{w}_k\}_{k=1}^{G}} \sum_{i=1}^{N_u} \log_2(1+\gamma_i)$$

$$\text{subject to: } \gamma_i = \min_{m \in G_k} \frac{|\mathbf{w}_k^\dagger \mathbf{h}_m|^2}{\sum_{l \neq k}^{N_t} |\mathbf{w}_l^\dagger \mathbf{h}_m|^2 + \sigma_m^2}, \tag{4.20}$$

$$\forall i \in \mathcal{G}_k, k, l \in \{1 \dots N_t\},$$

$$\text{and to: } \left[\sum_{k=1}^{N_t} \mathbf{w}_k \mathbf{w}_k^\dagger\right]_{nn} \leq P_n, \tag{4.21}$$

$$\forall n \in \{1 \dots N_t\}.$$

Problem $\mathcal{SR}$ receives as input the per-antenna power constraint vector $\mathbf{p}_{ant} = [P_1, P_2 \dots P_{N_t}]$. Following the common in the literature notation for ease of reference, the optimal objective value of $\mathcal{SR}$ will be denoted as $c^* = \mathcal{SR}(\mathbf{p}_{ant})$ and the associated optimal point as $\{\mathbf{w}_k^{\mathcal{SR}}\}_{k=1}^{N_t}$. The novelty of the $\mathcal{SR}$ lies in the PACs, i.e. (4.21) instead of the conventional SPC proposed in [129]. To the end of solving this problem, a heuristic algorithm is proposed. By utilizing the results of Sec. 4.3, the new algorithm calculates the per-antenna power constrained precoders. More specifically, instead of solving the QoS sum power minimization problem of [75], the proposed algorithm calculates the PAC precoding vectors by solving the per-antenna power minimization problem $\mathcal{Q}$.

Power Allocation

The SR maximization problem is considerably complicated, since there is no clear way to reformulate it into a convex problem. However, its solution follows some intuitive structure [61]. In the present work, towards solving this elaborate problem, the decoupling of the beamforming directions and the power allocation is employed. The general concept of such approaches has been introduced in Sec. 2.3.1.

To proceed with the power reallocation step, let us rewrite the precoding vectors calculated from $\mathcal{Q}$ as $\{\mathbf{w}_k^{\mathcal{Q}}\}_{k=1}^G = \{\sqrt{p_k}\mathbf{v}_k\}_{k=1}^G$ with $||\mathbf{v}_k||_2^2 = 1$ and $\mathbf{p} = [p_1 \dots p_k]$. By this normalization, the beamforming problem can be decoupled into two problems. The calculation of the beamforming directions, i.e. the normalized $\{\mathbf{v}_k\}_{k=1}^G$, and the power allocation over the existing groups, i.e. the calculation of $\mathbf{p}_k$. Since the exact solution of $\mathcal{SR}$ is not straightforwardly obtained, this decoupling allows for the two step optimization. Under general unicasting assumptions, the SR maximizing power allocation with fixed beamforming directions is a convex optimization problem [130]. Nonetheless, when multigroup multicasting is considered, the cost function $C_{\mathcal{SR}} = \sum_{k=1}^G \log\left(1 + \min_{i\in\mathcal{G}_k}\{\mathrm{SINR}_i\}\right)$. is no longer differentiable due to the $\min_{i\in\mathcal{G}_k}$ operation and one has to adhere to sub-gradient solutions [129]. What is more, as in detail explained in [129], the cost function needs to be continuously differentiable, strictly increasing, with a log-convex inverse function. Although this is not the case for $\mathcal{SR}$, such assumptions can be adopted by performing the optimization over the logarithmic power vector, defined as $\mathbf{s} = \{s_k\}_{k=1}^G = \{\log p_k\}_{k=1}^G$. These lead to a suboptimal heuristic solution of an involved problem without known optimal solution. However, the heuristic solutions attain a good performance, as shown in [129, 130] and in the following. Consequently, in the present contribution, the power loading is achieved via the sub-gradient method [130], under specific modifications over [129] that are hereafter described.

The proposed algorithm, presented in Alg. 2, is an iterative two step algorithm. In each step of the process, the QoS targets $\mathbf{g}$ are calculated as the minimum target per group of the previous iteration, i.e. $\gamma_i = \min_{i\in\mathcal{G}_k}\{\mathrm{SINR}_i\}, \forall i \in \mathcal{G}_k, k \in \{1 \dots G\}$. Therefore, the new precoders require equal or less power to achieve the same system sum rate. Any remaining power is then redistributed amongst the groups to the end of maximizing the total system throughput, via the sub-gradient method

[130].

Sub-gradient Optimization

Focusing of the sub-gradient optimization method, let us denote $\mathbf{s} = \{s_k\}_{k=1}^{G} = \{\log p_k\}_{k=1}^{G}$, as the logarithmic power vector. Then, the sub-gradient search method reads as

$$\mathbf{s}(t+1) = \prod_{\mathbb{P}} \left[\mathbf{s}(t) - \delta(t) \cdot \mathbf{r}(t)\right], \tag{4.22}$$

where $\prod_{\mathbb{P}}[\mathbf{x}]$ denotes the projection operation of point $\mathbf{x} \in \mathbb{R}_G$ onto the set $\mathbb{P}$. The parameters $\delta(t)$ and $\mathbf{r}(t)$ are the step of the search and the sub-gradient of the $\mathcal{SR}$ cost function at the point $\mathbf{s}(t)$, respectively. The projection operation, i.e. $\prod_{\mathbb{P}}[\cdot]$, constrains each iteration of the sub-gradient to the feasibility set of the $\mathcal{SR}$ problem. The analytic calculation of $\mathbf{r}(t)$ is given in [129, 130] and is omitted herein for brevity. Also, $\delta(t)$ needs to carefully selected according to the specific problem. Herein, the choice is based on [129] and refined by simulations. It should also be noted, that delta needs to be non-zero for a new power allocation scheme to be calculated in each iteration, based on the sub-gradient directions.

Projection

In order to account for the more complicated PACs the projection over a per-antenna power constrained set is herein considered. The set of PACs is defined as

$$\mathbb{P} = \left\{ \mathbf{p} \in \mathbb{R}_{N_t}^{+} \middle| \left[\sum_{k=1}^{N_t} p_k \mathbf{v}_k \mathbf{v}_k^{\dagger} \right]_{nn} \leq P_n \right\}, \tag{4.23}$$

where the element of the power vector $\mathbf{p} = \exp(\mathbf{s})$ with $\mathbf{p}, \mathbf{s} \in \mathbb{R}_G$, represent the power allocated to the corresponding group. It should be stressed that this power is inherently different than the power transmitted by each antenna $\mathbf{p}_{ant} \in \mathbb{R}_{N_t}^{+}$. The connection between $\mathbf{p}_{ant}$ and $\mathbf{p}$ is given by the normalized beamforming vectors as easily observed in (4.23). Different from the sum power constrained solutions of [129], the per-antenna

constrained projection problem is given by

$$\begin{aligned} &\mathcal{P}: \min_{\mathbf{p}} ||\mathbf{p}-\mathbf{x}||_2^2 \\ &\text{subject to}: \left[\sum_{k=1}^{N_t} p_k \mathbf{v}_k \mathbf{v}_k^{\dagger}\right]_{nn} \leq P_n, \\ &\qquad \forall n \in \{1 \dots N_t\}, \end{aligned} \tag{4.24}$$

where $\mathbf{p} \in \mathbb{R}_{N_t}$ and $\mathbf{x} = \exp(\mathbf{s}(t))$. Problem $\mathcal{P}$ is a quadratic problem (QP) [71] and can thus be solved to arbitrary accuracy using standard numerical methods.[6] Subsequently, the solution of (4.22) is given as $\mathbf{s}(l+1) = \log(\mathbf{p}^*)$, where $\mathbf{p}^* = \mathcal{P}(\mathbf{p}_{ant}, \mathbf{x})$ is the optimal point of convex problem $\mathcal{P}$. To summarize the solution process, the per-antenna power constrained sum rate maximizing algorithm is presented in Alg. 2.

4.4.2 Complexity & Convergence Analysis

An important discussion involves the complexity of the proposed algorithm. The complexity of the techniques employed to approximate a solution of the highly complex, NP-hard multicast multigroup problem under PACs is presented in Sec. 4.3.1. Therein, the computational burden for an accurate approximate solution of the per-antenna power minimization problem $\mathcal{Q}$ has been calculated.

Focusing on the max SR algorithm, the main complexity burden originates from the solution of a SDP. The remaining three steps of Alg. 2 involve a closed form sub-gradient calculation as given in [130] and the projection operation, which is a real valued least square problem under N_t quadratic inequality PACs. Consequently, the asymptotic complexity of the derived algorithm is polynomial, dominated by the complexity of the QoS multicast multigroup problem under PACs.

The convergence of Alg. 1 is guaranteed given that the chosen step size satisfies the conditions given in [129,130], that is the diminishing step size. Herein, $\delta(l+1) = \delta(l)/2$.

[6] Analytical methods to solve problem $\mathcal{P}$ are beyond the scope of the present work. For more information, the reader is referred to [71].

Input: (see Tab.4.1) $\{\mathbf{w}_k^{(0)}\}_{k=1}^{N_t} = \sqrt{P_{tot}/(N_t^2)} \cdot \mathbf{1}_{N_t}$, $\mathbf{p}_{ant}$.
Output: $\{\mathbf{w}_k^{\mathcal{SR}}\}_{k=1}^{N_t}$
begin
  $j = 0$
  while *$\mathcal{SR}$ does not converge* **do**
    $j = j + 1$;
    Step 1: Solve $r^* = \mathcal{Q}(\mathbf{g}_{(j)}, \mathbf{p}_{ant})$ to calculate $\{\mathbf{w}_k^{(j)}\}_{k=1}^{N_t}$.
    The input SINR targets $\mathbf{g}_{(j)}$ are given by the minimum SINR per group, i.e.
    $\gamma_i = \min_{i \in \mathcal{G}_k} \{\mathrm{SINR}_i\}, \forall i \in \mathcal{G}_k, k \in \{1 \dots N_t\}$.
    Step 2: Initialize the sub-gradient search algorithm as:
    $\mathbf{p}^{(j)} = \{p_k\}_{k=1}^{N_t} = \{||\mathbf{w}_k^{(j)}||_2^2\}_{k=1}^{N_t}$,
    $\mathbf{s}^{(j)} = \{s_k\}_{k=1}^{N_t} = \{\log p_k\}_{k=1}^{N_t}$, $\{\mathbf{v}_k^{(j)}\}_{k=1}^{N_t} = \{\mathbf{w}_k^{(j)}/\sqrt{p_k^{(j)}}\}_{k=1}^{N_t}$.
    Step 3: Calculate t_{max} iterations of the sub-gradient power control algorithm, starting from $\mathbf{s}(0) = \mathbf{s}^{(j)}$:
    for $t = 0 \dots t_{max} - 1$ **do**
      $\mathbf{s}(t+1) = \prod_{\mathbb{P}} [\mathbf{s}(t) - \delta(t) \cdot \mathbf{r}(t)]$
    end
    $\mathbf{s}^{(j+1)} = \mathbf{s}(t_{max} - 1)$,
    Step 4: Calculate the current throughput: $c^* = \mathcal{SR}(\mathbf{p}_{ant})$ with $\{\mathbf{w}_k^{\mathcal{SR}}\}_{k=1}^{N_t} = \{\mathbf{w}_k^{(j+1)}\}_{k=1}^{N_t} = \{\mathbf{v}_k^{(j)} \exp(s_k^{(j+1)})\}_{k=1}^{N_t}$
  end
end

Algorithm 2: Sum-rate maximizing multigroup multicasting under per-antenna power constraints.

Table 4.1: Input Parameters of the Sum-rate maximizing Algorithm

Parameter	Symbol	Value
Sub-gradient Iterations	l_{max}	1
Sub-gradient step	δ	0.4
Gaussian Randomizations	N_{rand}	100
Total Power at the T_x	P_{tot}	$[-20 : 20]$ dBW
Per-antenna constraints	$\mathbf{p}_{ant}$	P_{tot}/N_t
User Noise variance	σ_i^2	$1, \ \forall i \in \{1 \dots N_u\}$

4.5 Performance Evaluation

In the present section, numerical results are presented to quantify the performance gains of the proposed SR maximization problem under various channel assumptions. Towards quantifying the gains of the proposed solution, the existing SPC solutions are re-scaled to respect the PACs, if and only if a constraint is over satisfied. Re-scaling is achieved by multiplying each row of the precoding matrix with the square root of the inverse level of power over satisfaction of the corresponding antenna, i.e.

$$\alpha = \sqrt{\max_{n}\{\mathbf{p}_{ant}\}/\left[\mathbf{W}\mathbf{W}^{\dagger}\right]_{nn}} \tag{4.25}$$

4.5.1 Multigroup Multicasting over Rayleigh Channels

Fairness optimization

The performance of multigroup multicasting under PACs is examined for a system with $N_t = 5$ transmit antennas, $G = 2$ groups and $N_u = 4$ users. Rayleigh fading is considered, thus the channels are generated as Gaussian complex variable instances with unit variance and zero mean. For every channel instance, the approximate solutions of the max-min fair SPC and the proposed PAC problems are evaluated using $N_{rand} = 100$ Gaussian randomizations [75]. The results are averaged over one hundred channel realizations, while the noise variance is normalized to one for all receivers and all SINR targets are assumed equal to one. The achievable minimum rate is plotted for the SPC and the PAC optimization in Fig. 4.2 with respect to the total transmit power in dBWs. These results are a system with $N_u = 4$ users, $N_t = 5$ antennas, $L = 2$ groups and $\rho = 2$ users per group. For a fair comparison, the total power constraint P_{tot} [Watts] is equally distributed amongst the transmit antennas when PACs are considered, hence each antenna can radiate at most P_{tot}/N_t [Watts]. The accuracy of the approximate solutions for both problems, given by comparing the actual solution to the relaxed upper bound [75], is clear across a wide range of SNR. Nevertheless, the accuracy due to the PACs is slightly reduced. This accuracy degradation is intuitively justified. A Gaussian randomization instance is less likely to approach the optimal point when the number of constraints is increased while the same number of Gaussian randomizations are performed ($N_{rand} = 100$). Towards exhibiting the gains of the proposed solution, the performance of the SPC solution

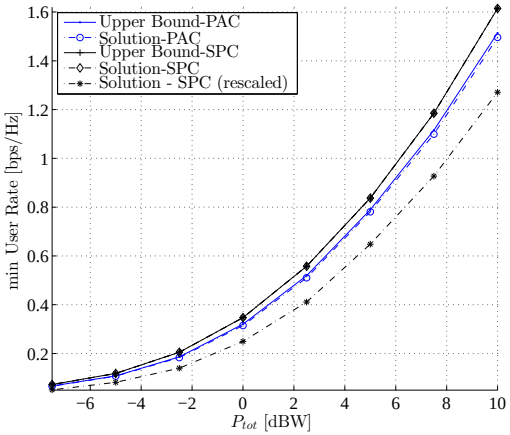

Figure 4.2: Minimum user rate with multicast multigroup beamforming under SPC and PAC, for Rayleigh channels.

re-scaled to respect the PACs is also included in Fig. 4.2, where it is clear that more than 1 dB of gain can be obtained by the proposed method over the suboptimal re-scaling approach.

A significant issue for the SDR techniques in multicast applications is the tightness of the approximate solution versus an increasing number of receivers per multicast. In the extreme case of one user per group (i.e. unicasting), it was proven in [57] that the relaxation provides an optimal solution. Thus the solution is no longer approximate but exact. However, the increasing number of users per group degrades the solution, as depicted in Fig. 4.3 for both problems, for $P_{tot} = 10$ dBW. It is especially noticed that the PAC system suffers more than the SPC of [75] as the number of users per multicast group increases. An attempt to solve this inaccuracy, but only under a sum power constraint, is presented in [79].

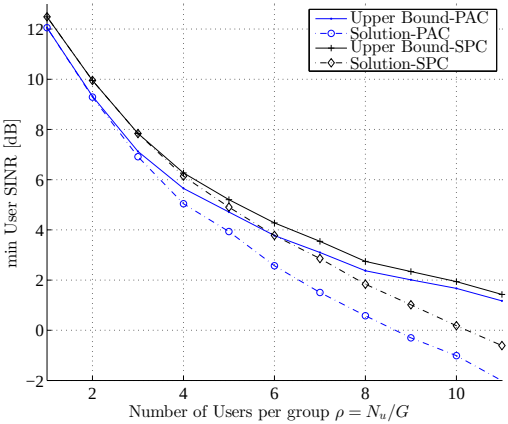

Figure 4.3: Minimum SINR under SPC and PAC versus an increasing ratio of users per group $\rho = N_u/G$, for Rayleigh channels.

Sum Rate Maximization

The performance of $\mathcal{SR}$ in terms of SR is compared to the performance of the solutions of [129] in a per-antenna constrained transmitter operating over Rayleigh channels in this paragraph. A system with $N_t = 4$ transmit antennas and $N_u = 8$ users uniformly allocated to $G = 4$ groups is assumed, while the channels are generated as Gaussian complex variable instances with unit variance and zero mean. For every channel instance, the solutions of the SPC [129] and the proposed PAC max SR are evaluated and compared to the weighted fair solutions of the previous section. The exact input parameters employed for the algorithmic solution are presented in Tab. 4.1. For fair comparison, the total power constraint P_{tot} [Watts] is equally distributed amongst the transmit antennas when PACs are considered, hence each antenna can radiate at most P_{tot}/N_t [Watts]. The results are averaged over one hundred channel realizations, while the noise variance is normalized to one for all receivers. The achievable SR is plotted in Fig. 4.4 with respect to the total transmit power P_{tot} in dBW. Clearly, in a practical PAC scenario, the proposed optimization problem outperforms existing solutions over the whole SNR

range. More significantly, the gains of the derived solution are more apparent in the high power region. In the low power noise limited region, interference is not an issue and the fair solutions perform close to the throughput maximizing solution. On the contrary, in the high power regime, the interference limited fairness solutions saturate in terms of SR performance. For $P_{tot} = 20$ dBW, the max SR solutions attain gains of more than 30% in terms of SR over the fair approaches. Interestingly, for the same available transmit power, the PAC optimization proposed herein, attains 20% gains over re-scaled to respect the per-antenna constraints max SR solutions. Finally, it clearly noted in Fig. 4.4 that the reported gains increase with respect to the transmit power.

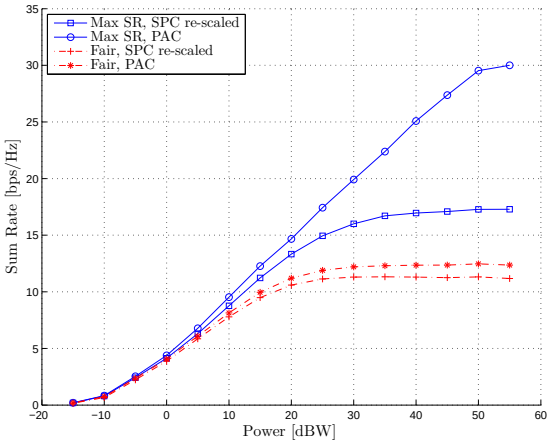

Figure 4.4: Sum rate under SPC and PACs, versus increasing total power P_{tot} [dBW], for Rayleigh channels.

A significant issue for the multicast applications is the scaling of the solution versus an increasing number of receivers per multicast. The increasing number of users per group degrades the performance for the weighted fair problems, as also shown in the previous section. For the case tackled herein, the max SR solutions are compared to the fairness solutions as depicted in Fig. 4.5 with respect to an increasing ratio of users per group $\rho = N_u/G$. According to these curves, the $\mathcal{SR}$ solution is

exhibiting a higher resilience to the increasing number of users per group, compared to the fair solutions. The re-scaled solutions remain suboptimal in terms of sum rate when compared to proposed solution for any user per group ratio.

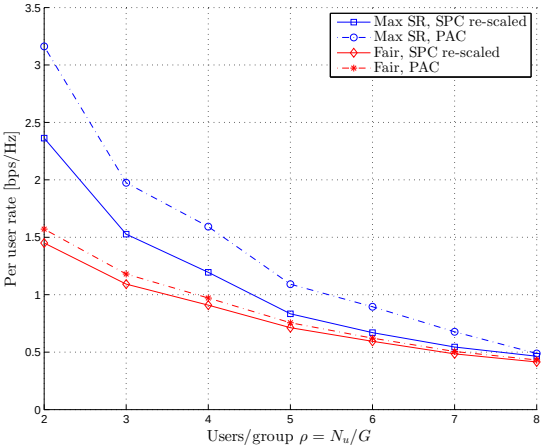

Figure 4.5: Sum rate under SPC and PAC versus an increasing ratio of users per group $\rho = N_u/G$, for Rayleigh channels.

4.5.2 Distributed Antenna Systems

The main difference between the SPC and the PAC optimization problems is the utilization of the available on board power in each system architecture. In [75], the sum power constraint is always satisfied with equality, since any remaining power budget can be equally distributed to the precoding vectors and the solution is further maximized. On the contrary, the PAC system includes N_t constraints which are coupled via the precoders. According to the relation between $\mathcal{F}$ and $\mathcal{Q}$, i.e. (4.5), the ratio of transmitted power over the power constraint (i.e. r) is one. Since this ratio applies for at least one of the N_t power constraints, if one is met with equality and the remaining $N_t - 1$ are not, then no more power can

be allocated to the precoders. Let us assume a channel matrix with one compromised transmit antenna, i.e. $\mathbf{H} =$

$$\begin{bmatrix} 2.94\angle 41^\circ & 11\angle -25^\circ & 4.4\angle 50^\circ & 6.6\angle -4^\circ \\ 13.2\angle -150^\circ & 4.8\angle 14^\circ & 15.2\angle -7^\circ & 4.8\angle -37^\circ \\ 12\angle -155^\circ & 1.5\angle 163^\circ & 13.5\angle -105^\circ & 3.9\angle -46^\circ \\ 0.02\angle -53^\circ & 0.03\angle -66^\circ & 0.03\angle 120^\circ & 0.03\angle -129^\circ \\ 5.66\angle 137^\circ & 9.2\angle 49^\circ & 13\angle -175^\circ & 2.45\angle 126^\circ \end{bmatrix}^{\mathrm{T}},$$

where 4 users, divided into 2 groups, are served by 5 antennas. One of the antennas (the 4-th antenna) has severely degraded gains towards all users. This practical case can appear in a DAS where the physical separation of the transmit antennas not only imposes per antenna constraints but can justify highly unbalanced channel conditions around the environment of the antennas. The power utilization of the solution of the optimization for each of the two problems is defined as the total transmitted power over the total available power P_{tot}, that is $P_u = \left(\sum_{k=1}^{G} \mathbf{w}_k{}^{\dagger}\mathbf{w}_k\right)/P_{tot}$, and is plotted versus an increasing power budget in Fig. 4.6. It is clear that in the low power regime the available power is not fully utilized. As the available power increases, however, the power consumption of the PAC increases. This result is in accordance with the optimality of equal power allocation in the high power regime and renders the PAC formulation relevant for power limited systems. Further insights for this PAC system are given in Fig. 4.7, where the power utilization of each antenna is shown, for different total power budgets. Interpreting these results, it can be concluded that the PAC problem is highly relevant for power-over-noise limited systems. Otherwise, in the high power regime, the solution of the SPC problem with less constraints could be also used as an accurate approximation.

4.5.3 Sensitivity to angular separation: Uniform Linear Arrays

Fairness

To the end of investigating the sensitivity of the proposed algorithm with respect to the angular separation of co-group users, a uniform linear array (ULA) transmitter is considered. Assuming far-field, line-of-sight conditions, the user channels can be modeled using Vandermonde matrices. For

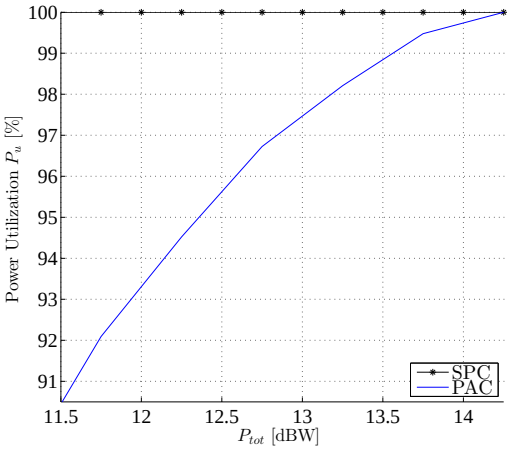

Figure 4.6: Total power consumption of a PAC system versus available power.

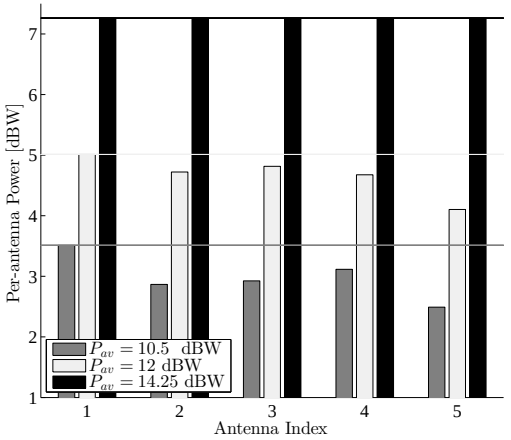

Figure 4.7: Per-antenna consumption in a PAC system.

this important special case, the SPC multicast multigroup problem was reformulated into a convex optimization problem and solved in [131,132]. These results where motivated by the observation that in ULA scenarios, the relaxation consistently yields rank one solutions. Thus, for such cases, the SDR is essentially optimal [76]. The fact that the SDR of the sum power minimization problem is tight for Vandermonde channels was established in [132]. Let us consider a ULA serving 4 users allocated to 2 distinct groups. In Fig. 4.8, its radiation pattern for co-group angular separation $\theta_a = 35^\circ$ is plotted. The symmetricity due to the inherent ambiguity of the ULA is apparent. Clearly, the multicast multigroup beamforming optimizes the lobes to reduce interference between the two groups. The SPC solution, re-scaled to respect the PACs are also included in Fig. 4.8. The superiority of the proposed solution is apparent.

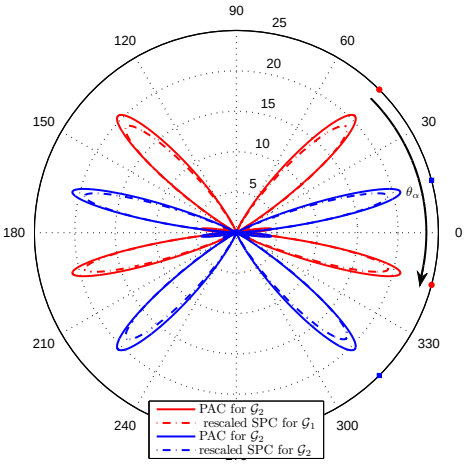

Figure 4.8: ULA beampattern for PAC and re-scaled SPC solutions.

The performance of the solution in terms of minimum user rate over the area with respect to an increasing angular separation, is investigated in Fig. 4.9. When co-group users are collocated, i.e. $\theta_a = 0^\circ$, the highest performance is attained. As the separation increases, the performance

is reduced reaching the minimum when users from different groups are placed in the same position, i.e. $\theta_a = 45^\circ$. In Fig. 4.9, the tightness of the relaxation for the SPC problem [132] is clear. However, the same does not apply for the proposed PAC. As co-group channels tend to become orthogonal, the approximation becomes less tight. Nevertheless, $N_{rand} = 200$ randomizations are sufficient to maintain the solution above the re-scaled SPC, as shown in Fig. 4.9. Consequently, the proposed solution outperforms a re-scaled to respect the per-antenna constraints, SPC solution, over the span of the angular separations.

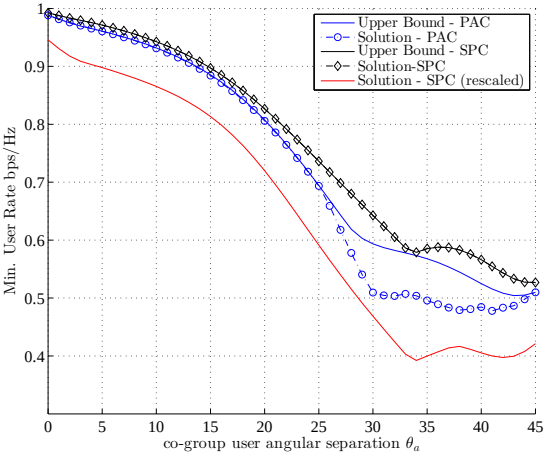

Figure 4.9: ULA performance for increasing co-group user angular separation.

Remark 4.4. *The semidefinite relaxation of the per-antenna power minimization problem in* ULA *transmitters is not always tight. For every optimum high rank set of matrices* $\{\mathbf{X}_k^{opt}\}_{k=1}^{G}$*, there exists a set of rank one positive semidefinite matrices* $\{\bar{\mathbf{X}}_k^{opt}\}_{k=1}^{G}$*, i.e.* $\text{rank}(\bar{\mathbf{X}}_k^{opt}) = 1, \forall k \in \{1 \dots G\}$*, which is equivalent with respect to the power received at each user, i.e* $\text{Tr}(\mathbf{X}_k^{opt}\mathbf{Q}_i) = \text{Tr}(\bar{\mathbf{X}}_k^{opt}\mathbf{Q}_i), \forall i \in \mathcal{G}_k, k, l \in \{1 \dots G\}$*. This result is based on the Riesz-Féjer theorem on real valued complex trigonometric polynomials [132]. Therefore, the Vandermonde channels impose a*

specific structure to the SPC *solution that allows for a convex reformulation. The difference in the case tackled herein lies in the* N_t PAC*s, i.e.* $\left[\sum_{k=1}^{G} \mathbf{X}_k\right]_{nn} \leq P_n, \forall n \in \{1 \dots N_t\}$*, in which the channel structure is not involved. Thus, a rank-1 matrix is equivalent in terms of per user received power [132] but not necessarily in terms of per-antenna consumed power, as shown herein.*

Sum Rate

Assuming far-field, line-of-sight conditions, the user channels can be modeled using Vandermonde matrices. Let us consider a ULA with $N_t = 4$ antennas, serving 4 users allocated to 2 distinct groups. The co-group angular separation is $\theta_1 = 5^\circ$ and $\theta_2 = 45^\circ$ for $\mathcal{G}_1$ and $\mathcal{G}_2$ respectively. In Fig. 4.10, the user positions and the optimized radiation pattern for this is transmitter plotted. The symmetry due to the inherent ambiguity of the ULA is apparent. Clearly, the fair beamforming design optimizes the lobes to provide equal service levels to all users. The three upper users (close to the 90° angle) receive higher power but also receive adjacent group interference. The fourth user, despite being in a more favorable in terms of interference position, is not allocated much power since its performance is constrained by the performance of the almost orthogonal, compromised user. Remembering that the noise level is equal to one and that the beam pattern is plotted in linear scale, all users achieve a SINR equal to 0.6, thus leading to a total SR of 1.2 [bps/Hz]. On the contrary, the max SR optimization, shuts down the compromised group (i.e. $\mathcal{G}_2$) and allocates the saved power to the well conditioned users of $\mathcal{G}_1$. This way, the system is interference free and each active user attains a higher service level. The achievable SNR is equal to 4 assuming normalized noise, (but only for the two active user of $\mathcal{G}_1$) and leads to a SR of more than 4.6 [bps/Hz]. Consequently, the proposed solution attains a 33% of increase in sum rate for the specific scenario, at the expense of sacrificing service availability to the ill conditioned users. In Fig. 4.11, the performance in terms of the SR optimization is investigated versus an increasing angular separation. When co-group users are collocated, i.e. $\theta = 0^\circ$, the highest performance is attained. As the separation increases, the performance is reduced reaching the minimum when users from different groups are placed in the same position, i.e. $\theta = 45^\circ$. The proposed solution outperforms a re-scaled to respect the per-antenna constraints, SPC solu-

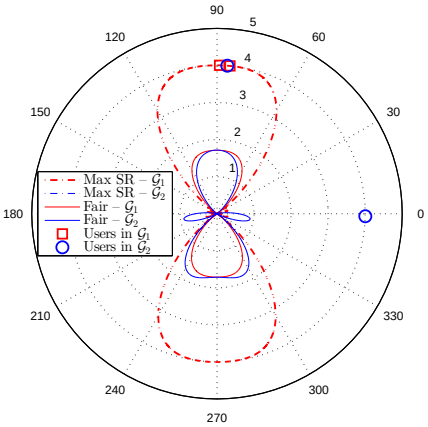

Figure 4.10: User positions and optimized antenna radiation pattern of ULA transmitter, under for max SR and fairness solutions.

tion, over the span of the angular separations. Also, the max SR solution performs equivalently to the fair solution under good channel conditions. However, when the angular separation of co-group users increases, the SR optimization exploits the deteriorating channel conditions and gleans gains of more than 25% over all other solutions.

4.5.4 Robustness to Imperfect Channel Information

In a practical system, robustness to imperfect CSI is of utmost importance. When beamforming under uncertainty is considered, three different designs can be realized. Namely, the probabilistic design, where acceptable performance is guaranteed for some percentage of time, the expectation based design that requires knowledge of the second order channel statistics but cannot guarantee any outage performance and the worst-case design [133]. The last approach guarantees a minimum QoS requirement for any error realization.

Focusing on a worst-case design, let us assume an elliptically bounded error vector. In this context, the actual channel is given as $\mathbf{h}_i = \bar{\mathbf{h}}_i + \mathbf{e}_i$

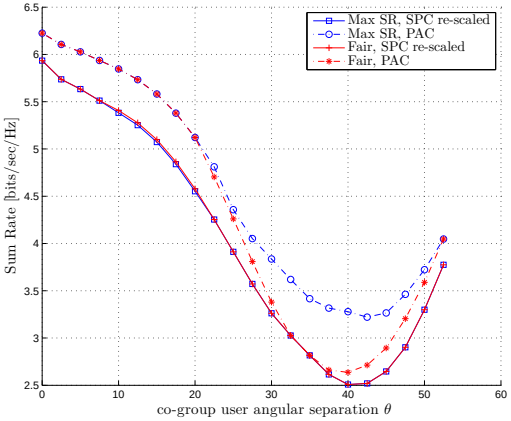

Figure 4.11: Achievable sum rates for ULA transmitter with respect to increasing co-group user angular separation.

where $\bar{\mathbf{h}}_i$ is the channel available at the transmitter and $\mathbf{e}_i$ is an error vector bounded by $\mathbf{e}_i^\dagger \mathbf{C}_i \mathbf{e}_i \leq 1$. The positive definite matrix $\mathbf{C}_i$ defines the shape and size of the ellipsoidal bound. For $\mathbf{C}_i = 1/\sigma_\epsilon^2 \mathbf{I}_{N_t}$, then $||\mathbf{e}_i||_2^2 \leq \sigma_\epsilon^2$ and the error remains in a spherical region of radius σ_ϵ [134]. This spherical error model is mostly relevant when the feedback quantization error of a uniform quantizer at the receiver is considered [135]. The proposed design is formulated as

$$\mathcal{F}_{\mathcal{RB}}: \max_{t,\ \{\mathbf{w}_k\}_{k=1}^G} t$$

$$\text{s. t. } \frac{1}{\gamma_i} \frac{|\mathbf{w}_k^\dagger (\mathbf{h}_i - \mathbf{e}_i)|^2}{\sum_{l \neq k}^G |\mathbf{w}_l^\dagger (\mathbf{h}_i - \mathbf{e}_i)|^2 + \sigma_i^2} \geq t, \quad \forall i \in \mathcal{G}_k, k, l \in \{1 \dots G\}, \tag{4.26}$$

$$\text{and to } \left[\sum_{k=1}^G \mathbf{w}_k \mathbf{w}_k^\dagger\right]_{nn} \leq P_n, \forall n \in \{1 \dots N_t\}, \tag{4.27}$$

and involves the channel imperfections only in the SNIR constraints. The novelty of $\mathcal{F}_{\mathcal{RB}}$ over existing robust multicast formulations lies in (4.27).

The SNIR constraints of $\mathcal{F}_{\mathcal{RB}}$, i.e. (4.26), are over all possible error realizations and cannot be handled. However, by applying the S-lemma [71], the error vector in (4.26) can be eliminated. This procedure is analytically described in [136]. Thus, $\mathcal{F}_{\mathcal{RB}}$ can be converted to a SDP and solved efficiently using the methods described in Sec. 4.3. The performance gain of the proposed robust design over 1000 error realizations is given in Fig. 4.12, versus an increasing error radius σ_ϵ, for a ULA with $N_t = 2$ transmit antennas, serving $N_u = 6$ users. These results exhibit the significant gains of the proposed technique as the error and the group sizes increase.

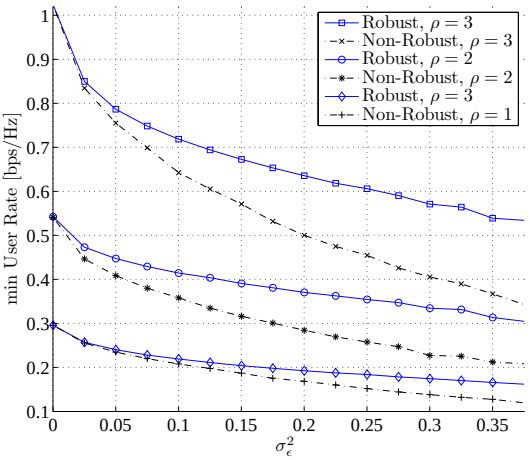

Figure 4.12: Minimum user rate versus increasing spherical CSI error radius, for different user per group configurations, ρ

To quantify the gains of the novel formulation, the performance of existing SPC solutions re-scaled to respect the per antenna constrains is also illustrated (see Sec. 4.5.1 for the re-scaling considerations). According to Fig. 4.13 the proposed robust PAC formulation outperforms existing solutions re-scaled to respect the practical constraints, for less than 0.15 squared error radius. It is therefore recommended for low to average error radius (less than 0.4). What is more, when compared to non-robust solutions, the proposed solution exhibits slightly less gains than the existing

ones. To gain better insights on the origin of this result, the accuracy of the proposed robust formulation is investigated in Fig. 4.14. It needs to be pointed out that in this figure, no re-scaling to respect the per-antenna constraints is applied and therefore the SPC seems to outperform the proposed methods.

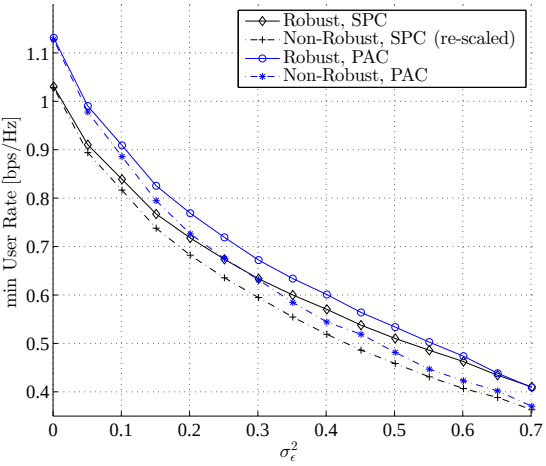

Figure 4.13: Minimum user rate versus increasing spherical CSI error radius.

Remark 4.5. *The semidefinite relaxation of robust optimization under* PAC*s yields non rank-1 solutions with higher probability than the relaxation of the robust* SPC *problems, as the error radius increases. Based on the simulation configuration of Fig. 4.13, Fig. 4.14 presents the accuracy of the proposed robust* PAC *design and the existing robust* SPC *versus an increasing error radius. In Fig. 4.14, it is clear that the existing robust* SPC *design consistently yields rank-1 solutions, since the solution attains the relaxation upper bound. However, the proposed robust* PAC *solution deviates from the upper bound for squared error radius values larger than 0.2. It is therefore exhibited that as the error radius increases, the relaxation of the robust* PAC *solution does not consistently yield rank-1 solu-*

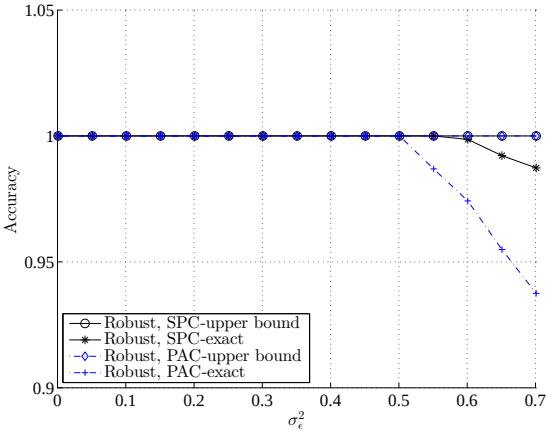

Figure 4.14: Accuracy of the SDR versus increasing CSI error.

tions. To exhibit this inaccuracy, only $N_{rand} = 50$ *gaussian randomizations have been employed. Despite these results, by increasing the number of gaussian randomizations, the upper bound can be further approached and the proposed* PAC *solution improved.*

4.6 Application Paradigm

Weighted Fairness

To the end of establishing the importance of the weighted optimization, a simple paradigm is elaborated herein. Under the practical assumption of a modulation constrained system, the weighted fair design can be exploited for rate allocation towards increasing the total system throughput. More specifically, the considered system employs adaptive modulation and allocates binary phase shift keying (BPSK) modulation if the minimum $\mathrm{SNIR_i}$ in the k-th group is less than the ratio for which the maximum modulation constrained spectral efficiency is achieved. This ratio is simply given by $\log_2 M$, where M is the modulation order. Hence for BPSK, $\gamma_2 = 0$ dB, and so forth. If for some group k, $\min_i \mathrm{SNIR_i} \geq \gamma_2,\ \forall i \in \mathcal{G}_k$,

then quaternary phase shift keying (QPSK) is used for all users in the group. Forward error correction is not assumed. Let there be a two antenna transmitter that serves four users grouped into two groups. The considered channel matrix reads as

$$\mathbf{H} = \begin{bmatrix} 0.2\angle 106^\circ & 90\angle -69^\circ & 0.5\angle -99^\circ & 0.5\angle 61^\circ \\ 0.8\angle 111^\circ & 120\angle -112^\circ & 1\angle 127^\circ & 1.5\angle 49^\circ \end{bmatrix}^{\mathrm{T}}.$$

The attributes of the specific channel matrix depict one possible instance of the system where one user with a good channel state (i.e. user two) is in the same group with a jeopardized user, namely user one. On the other hand, the second group contains relatively balanced users in terms of channel conditions. For an un-weighted optimization (i.e. $\mathbf{g} = [1\ 1\ 1\ 1]$) the spectral efficiency of each user is shown in Fig. 4.15. Baring in mind that each user is constrained by the minimum group rate, the actual rate at which all users will receive data is 0.52 [bps/Hz]. Both groups achieve the same spectral efficiency since the minimum SINRs and hence the minimum rates are balanced between the groups. Subsequently, a modulation constrained multicast transmitter will employ BPSK for all users. By heuristically choosing the constraint vector to be $\mathbf{g} = [1\ 1\ 5.3\ 5.3]$ each user rate is modified. As depicted in Fig. 4.15 both users in the second group are achieving adequate SINR to support a higher order modulation. This gain is achieved at the expense of the rates of the users of the first group. Following this paradigm, the weight optimization can lead to an improved modulation assignment and thus higher throughput in practical systems. Hence, the weighted formulation offers the substantial degrees of freedom to maximize the total throughput of a modulation constrained multicast system by properly allocating the rates amongst the groups.

Sum Rate Maximization

Towards exhibiting the differences between the weighted fair and the max SR designs in the multigroup multicasting context, the following small scale paradigm is elaborated. Let there be a ULA transmitter that serves eight users allocated into four groups, as depicted in Fig. 4.16. The attributes of the specific channel instance depict one possible instance of the system where one group, namely $\mathcal{G}_3$, has users with large angular separation while $\mathcal{G}_4$ has users with similar channels. The rate of each user is plotted in Fig. 4.16 for the case of a weighted fair optimization (equal

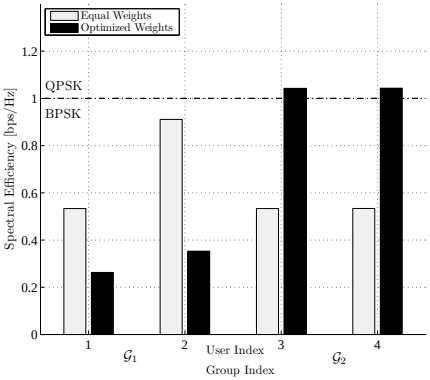

Figure 4.15: Modulation constrained paradigm.

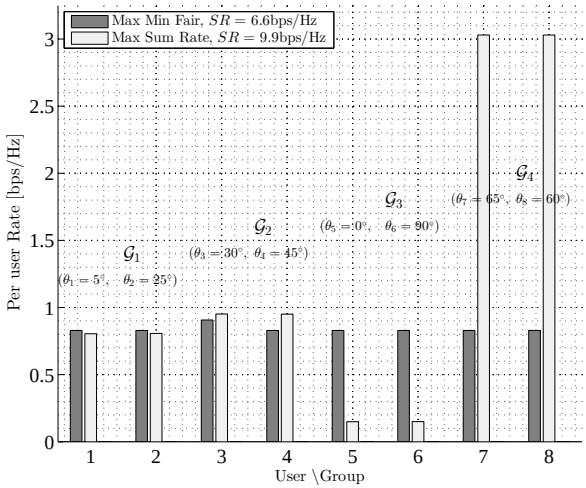

Figure 4.16: Achievable per user rates for weighted fair and max sum rate multicast multigroup optimization.

weights are assumed) and for the case of a SR maximizing optimization. Considering that each user is constrained by the minimum group rate, the sum rates are given in the legend of the figure. In the weighted fair case, the common rate at which all users will receive data is 0.83 [bps/Hz] leading to a sum rate of 6.64 [bps/Hz]. The minimum SINRs and hence the minimum rates are balanced between the groups since the fair optimization considers equal weights. The SR maximizing optimization, however, reduces the group that contains the compromised users in order to reallocate this power to the well conditioned group and therefore increase the system throughput to 9.9 [bps/Hz]. Consequently, a gain of almost 40% is realized in terms of total system rate. This gain is traded-off by driving users in $\mathcal{G}_3$ to the unavailability region.

4.7 Summary

In the present chapter, optimum linear precoding vectors have been derived under per antenna power constraints, when independent sets of common information are transmitted by an antenna array to distinct co-channel sets of users. Therefore, the weighted max–min fair multicast multigroup problem under PACs has been formulated. Following the novel problem formulation and the establishment of the non polynomial in complexity (NP) hardness of the problem, an approximate solution was presented based on the well established methods of semidefinite relaxation, Gaussian randomization and bisection. The performance of the weighted max–min fair multicast multigroup optimization has also been examined under various system parameters, thus leading to important system design insights. Moreover, an application paradigm of the new system design has been described while robust to imperfect CSI extensions have been given. Consequently, an important practical constraint towards the implementation of physical layer multigroup multicasting is alleviated.

Further extending the multicast multigroup literature, a novel sum rate maximization multicast multigroup problem under PACs has also been formulated. A detailed solution for this elaborate problem is given based on the well established methods of semidefinite relaxation, Gaussian randomization and sub-gradient power optimization. The performance of the SR maximizing multicast multigroup optimization is examined under various system parameters and important insights on the system design

are gained. Finally, an application paradigm of the new system design is examined. Consequently, an important practical constraint towards the implementation of throughput maximizing physical layer multigroup multicasting is alleviated.

As mentioned in the introduction of this chapter, multicasting becomes relevant when the objective is to optimize full frequency reuse multi-antenna transmitters without changing the framing structure of communication standards. Since beamforming techniques in frame based systems cannot rely on the conventional precoding design that assumes a different single user scheduled per transmission and multicast multigrouping needs to be considered. This problem is addressed in the following chapter.

Chapter 5

Frame based Precoding

A multibeam satellite that employs aggressive frequency reuse towards increasing the offered throughput is considered. Focusing on the forward link, the goal is to employ advanced signal processing techniques, namely precoding, towards mitigating the inter-beam interference. In this direction, the framing structure of satellite communication standards needs to be considered. Frame based precoding consists in precoding the transmit signals without changing the underlying framing structure of the system.

In the present chapter, the connection of the frame based precoding problem with the generic signal processing problem of conveying independent sets of common data to distinct groups of users is established. This model is known as physical layer multicasting to multiple co-channel groups, and has been in detail presented in the previous chapter. Building on the results of Ch. 4, the optimal per-antenna power constrained multicast precoders in the fairness sense are utilized for the frame based precoding problem. Fair multicast multigroup precoding is compared to multicast aware heuristic precoding methods over a realistic multibeam satellite scenario. The gains are quantified via extensive numerical results over realistic multibeam satellite channels.

Next, the SR maximizing design of Ch. 4 is applied in the multibeam scenario. Further on, to the end of trading-off the high performance of the SR optimal design with the stringent availability requirements of satellite systems, new optimization problems are proposed. The main novelty of these problems lies in the inclusion of availability constraints. Moreover,

towards leveraging the finite granularity of the system spectral efficiency function with respect to the receive SINR, a novel discretized optimization problem that acknowledges the finite granularity of the throughput function of practical adaptive link layer systems is formulated and solved.

Finally, numerical results over a realistic simulation environment are exhibiting that more than 30% gains over existing designs can be achieved for up to 6 users per frame, without modifying the framing structure of legacy communication standards.

5.1 Introduction

Aggressive frequency reuse schemes are currently being considered as the most promising way to enhance the spectral efficiency of wireless communication systems. In this context, linear precoding, a transmit signal processing technique that exploits the offered spatial degrees of freedom of multi-antenna transmitter, is brought into play to manage the induced interference. The most substantial enabler for such interference mitigation techniques and subsequently full frequency reuse configurations, is the availability of channel state information at the transmitter. However, the long Round Trip Time (RTT) of Geostationary (GEO) SatCom systems significantly burdens the real time channel acquisition process. Therefore, the focus herein is on FSS, where the relatively slow channel variations allow for a channel feedback process during which the channel remains quasi-static. In such scenarios, the incorporation of linear precoding techniques greatly depends on whether practical constraints imposed by the inherent characteristics of the satellite channel can be addressed [68]. The present contribution focuses on two fundamental constraints stemming from a practical satcom system implementation. Firstly, the framing structure of satcom standards, like the second generation digital video broadcasting for satellite standard DVB − S2 [19] and its most recent extensions DVB − S2X [23,112], and secondly, the conventional non flexible on-board payloads that prevent power sharing amongst the beams.

The physical layer design of DVB − S2X [19] [23] is optimized to cope with the inherent satellite channel characteristics. Long Forward Error Correction (FEC) codes and fade mitigation techniques that rely on an adaptive link layer design (adaptive coding and modulation – ACM) are employed for the noise limited with long propagation delays and intense fading phenomena satellite channel. The most recent definition of syn-

chronous across the multiple beams superframes in the latest evolution of DVB − S2X allows for the incorporation of advanced interference mitigation techniques (cf. annex E of [23]). A small-scale example of the application of linear precoding methods over existing satcom standards is depicted in Fig. 5.1. Function $f(\cdot)$ denotes the FEC coding operation over the data d_i that are addressed to the i-th user of the corresponding superframe (SF). Consequently, the transmitted sequence s_j needs to be received by all users in the SF. In SFs 3 and 4, multiple instances of d_a denote different un-coded data addressed to user α of each SF respectively, pointing out that the amount of data addressed to each user can vary. In this figure, it is illustrated that the existing framing structure hinders the calculation of a precoding matrix on a user-by-user basis. During one transmission period, one frame per-beam accommodates a different number of users, each with different data requirements. These unequal data payloads that correspond to each user, along with the application of FEC block coding over the entire frame requires that co-scheduled users decode the entire frame and then extract the relevant to them data. Consequently, despite the optimality, in the channel capacity sense, of channel-by-channel precoding [105], practical system implementations require precoding to be performed on a frame-by-frame basis.

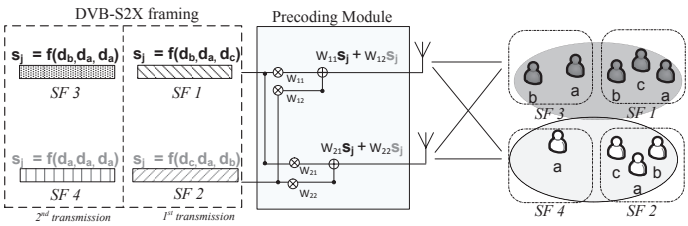

Figure 5.1: Frame-based precoding in DVB − S2X.

In frame based precoding, the framing constraint imposes one precoding matrix to apply over all users that belong in a frame. This leads to designing a precoder matched to more than one channel vectors. From a signal processing point of view, physical layer (PHY) multicasting to multiple co-channel groups [75] can provide the theoretically optimal precoders

when a multi-antenna transmitter conveys independent sets of common data to distinct groups of users. This scenario is known as PHY multicast multigroup beamforming (or equivalently precoding). Thus, the connection of the frame based precoding problem with the PHY multicast multigrouping is straightforward. In multicasting, the same symbol is transmitted to multiple receivers. This is the fundamental assumption of frame based precoding as well, since the symbols of one frame, regardless of the information they convey, are addressed to multiple users. These users need to receive the entire the frame, decode it and then extract the relevant to them information[1].

The second practical constraint tackled in the present work includes a maximum limit on the per-antenna transmitted power. Individual per-antenna amplifiers limit the flexibility in sharing the power resources amongst the antennas of the future full frequency reuse compatible payloads. On board flexible amplifiers, such as multi-port amplifiers and flexible TWTAs [103], come at high costs. Also, power sharing is impossible in distributed antenna systems (DAS), such as constellations of cooperative satellite systems (e.g. swarms of nano-satellites).

Considering the above discussed constraints, the incorporation of linear precoding in DVB − S2X is proposed, as depicted in Fig. 5.2. The design of an optimal -in a throughput maximizing sense- precoding matrix and a low complexity heuristic scheduling process is presented in the following. For the precoding matrix, optimal multicast multigroup precoders under per antenna constraints are proposed to maximize the throughput of a multibeam satellite system.

In the PHY multicast multigroup precoding literature, two fundamental optimization criteria, namely the sum power minimization under specific Quality of Service (QoS) constraints and the maximization of the minimum SINR (*max-min fair* criterion) have been considered in [75, 76, 80] under SPC.

Extending these works, a consolidated solution for the weighted *max–min fair* multicast multigroup beamforming under PACs has been derived in Ch 4. To this end, the well established tools of Semi-Definite Relaxation (SDR) and Gaussian randomization were combined with bisection

[1]This is the difference between broadcasting applications, where the same information is addressed to multiple users and interactive broadband applications where a point-to-point link with each individual user is established in the network layer. The latter application is addressed in the present work.

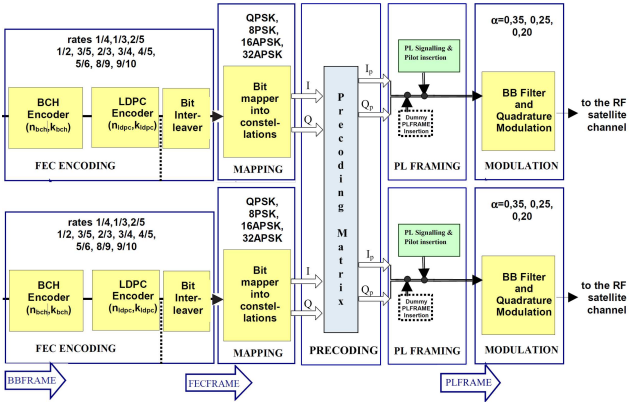

Figure 5.2: Extended functional block diagram of DVB-S2 [19], incorporating advanced interference mitigation techniques.

to obtain highly accurate and efficient solutions. For more details on *max–min fair* and SR maximizing multigroup multicast solutions, the reader is referred to Ch. 4.

Average User Throughput

By accounting the above link budget considerations, the achievable average user throughput is normalized over the number of beams, in order to provide a metric comparable with multibeam systems of any size. This normalized throughput is calculated as

$$C = \frac{2B_u}{1+\alpha}\frac{1}{N_t}\sum_{k=1}^{N_t} f_{\mathrm{DVB-S2X}}\left(\min_{i\in\mathcal{G}_k}\left\{\mathrm{SINR}_i\right\}, \mathbf{t}\right), \tag{5.1}$$

in [Gbps]. In (5.1) the spectral efficiency function $f_{\mathrm{DVB-S2X}}$ receives as input each users SINR as well as a threshold vector $\mathbf{t}$. Then, $f_{\mathrm{DVB-S2X}}$ performs a rounding of the input SINR to the closest lower floor given by the threshold vector $\mathbf{t}$ and outputs the corresponding spectral efficiency in [bps/Hz]. The mapping of receive SINR regions to a spectral efficiency achieved by a respective modulation and coding (MODCOD) scheme is

explicitly defined in the latest evolution of the satcom standards [23]. It should also be noted, that the conventional four color frequency reuse calculations are based on the exact same formula, with the only modifications being the input SINR, calculated under conventional four color reuse pattern and with the pre-log factor reduced by four times, due to the fractional resource reuse. The parameters of (5.1) are defined in Tab. 5.1

Contributions

In the present chapter, the focus is set on maximizing the total throughput of a frame based transmitter under PACs. The main contributions are summarized in the following points:

- Towards further addressing the practical constraints of multibeam SatComs, the max SR problem is extended to account for minimum rate constraints (MRCs).
- A novel modulation aware max SR optimization that considers the discretized throughput function of the receive useful signal power is proposed. A heuristic solution for this elaborate optimization problem is proposed.
- a low complexity user scheduling algorithm that considers the multicast multigroup nature of the frame based precoding system is envisaged.
- The developed techniques are applied over a multibeam satellite operating in full frequency reuse configuration, under realistic channel assumptions.

5.2 Fair vs Heuristic Solutions

5.2.1 Equivalent Channel Model

an alternative, simplified channel model in the fashion of [68] can also be adopted towards providing a more tractable representation. To facilitate the comprehension of system model, let us define multiple square channel matrices $\mathbf{H}_{[i]}, i = 1 \dots \rho$. Each matrix corresponds to a "a single user per beam" instance, which is the common assumption in satellite precoding

literature (e.g. [105] and the references therein). To model the frame based precoding constraint, the general input-output signal model can be defined as [68]:

$$\mathbf{y}_{[i]} = \mathbf{H}_{[i]}\mathbf{x}_{[i]} + \mathbf{n}_{[i]} = \mathbf{H}_{[i]}\mathbf{W}\mathbf{s}_{[i]} + \mathbf{n}_{[i]} \tag{5.2}$$

where $\mathbf{y}, \mathbf{x}, \mathbf{n}, \mathbf{s} \in \mathcal{C}^{N_t}$, with $\mathcal{E}||\mathbf{n}||^2 = \sigma^2$ and $\mathcal{E}||\mathbf{s}||^2 = 1$, while $\mathbf{H}_{[i]} \in \mathcal{C}^{N_t \times N_t}$ is a one-user-per-beam instance of the total non-square channel matrix. The index $[i]$ corresponds to the different UTs per beam that need to be served by the same frame, i.e. $i = 1, \dots \rho$, where $\rho = N_u/G$ is number of users per group. Also, due to the one group per antenna assumption, $N_u = \rho \cdot N_t$. The above definition allows for the calculation of one *equivalent* precoder $\mathbf{W} = f(\mathbf{H}_{[i]})$. The function f can be chosen according to the design criteria.

5.2.2 Multicast MMSE Precoding

5.2.3 Multicast Aware MMSE: Average Precoding

The optimal linear precoder $\mathbf{W} = f(\mathbf{H}_{[i]}), i = 1 \dots \rho$ in the minimum mean square error sense, with more users than transmit antennas is considered in this section. Under the constraint of designing a linear MMSE precoder $\mathbf{W} \in \mathbb{C}^{N_t \times N_t}$ for multiple channels, i.e. $\mathbf{H} \in \mathbb{C}^{N_u \times N_t}$ with $N_u > N_t$ the solution is not straightforward. Following the equivalent channel notation of Sec. 5.2.1, the problem of minimizing the MSE between the transmitted and the received signals over a noisy channel is formalized as

$$\begin{aligned} \mathbf{W} = \arg\min \mathcal{E} & \left|\left| \begin{bmatrix} \mathbf{H}_{[1]} \\ \mathbf{H}_{[2]} \\ \vdots \\ \mathbf{H}_{[\rho]} \end{bmatrix} \begin{bmatrix} \mathbf{W} \end{bmatrix} \begin{bmatrix} \mathbf{s} \end{bmatrix} + \begin{bmatrix} \mathbf{n}_{[1]} \\ \mathbf{n}_{[2]} \\ \vdots \\ \mathbf{n}_{[\rho]} \end{bmatrix} - \begin{bmatrix} \mathbf{s} \\ \mathbf{s} \\ \vdots \\ \mathbf{s} \end{bmatrix} \right|\right|^2 \\ s.t.\ \mathcal{E}||\mathbf{W}\mathbf{s}||^2 = P_n, & \end{aligned} \tag{5.3}$$

for the case that we need to serve $\rho = N_u/G$ users in each group using the same precoder. Problem (5.3) can be analytically solved, in the fashion

of [137], by noting that the cost function is the following sum:

$$\begin{aligned} C_{(5.3)} =& \mathrm{Tr}\left[(\mathbf{H}_{[1]}\mathbf{W}-\mathbf{I})(\mathbf{H}_{[1]}\mathbf{W}-\mathbf{I})^{\dagger}\right] + \beta \mathrm{Tr}\left[\mathbf{W}\mathbf{W}^{\dagger}\right] \\ &+ \dots \\ & \mathrm{Tr}\left[(\mathbf{H}_{[\rho]}\mathbf{W}-\mathbf{I})(\mathbf{H}_{[\rho]}\mathbf{W}-\mathbf{I})^{\dagger}\right] + \beta \mathrm{Tr}\left[\mathbf{W}\mathbf{W}^{\dagger}\right] \\ =& \sum_{i=1}^{\rho} \mathrm{Tr}\left[(\mathbf{H}_{[i]}\mathbf{W}-\mathbf{I})(\mathbf{H}_{[i]}\mathbf{W}-\mathbf{I})^{\dagger}\right] \\ &+ \rho\beta \mathrm{Tr}\left[\mathbf{W}\mathbf{W}^{\dagger}\right] \end{aligned}$$

where $\beta = \sigma^2/P_n$. By differentiation we get

$$\nabla_{\mathbf{W}} C(\mathbf{W}) = 0 \Leftrightarrow \tag{5.4}$$

$$\mathbf{W}\left(\sum_{i=1}^{\rho} \mathbf{H}_{[i]}^{\dagger}\mathbf{H}_{[i]} + \rho\beta\mathbf{I}\right) = \sum_{i=1}^{\rho} \mathbf{H}_{[i]}^{\dagger}, \tag{5.5}$$

Thus the general solution reads as

$$\mathbf{W} = \left(\frac{1}{\rho}\sum_{i=1}^{\rho} \mathbf{H}_{[i]}^{\dagger}\mathbf{H}_{[i]} + \rho\beta\mathbf{I}\right)^{-1} \frac{1}{\rho}\sum_{i=1}^{\rho} \mathbf{H}_{[i]}^{\dagger} \tag{5.6}$$

Following a different derivation methodology, this result was firstly reported in [80].

Remark 1: Under the assumption of Rayleigh fading, the elements of $\mathbf{H}$ are independent zero mean complex Gaussian instances. Subsequently, due to the central limit theorem, as the number of users per group ρ increases then the precoder will tend to zero:

$$\lim_{\rho\to\infty} \frac{1}{\rho}\sum_{i=1}^{\rho} \mathbf{H}_{[i]} = 0. \tag{5.7}$$

The implications of *Remark 1* can be seen when the system dimensions grow large and the channel matrices tend to be modeled as zero mean random variables. The main result is that the system performance will degrade as the number of users per group increases. Assuming a fixed number of groups, the degradation as the number of users increases has

only been examined hitherto via simulations [75,80]. Herein, an analytical proof for this result has been provided. Moreover, remembering that $\rho = N_u/G$, for a fixed number of users the performance is expected to degrade as the number of groups increases. Since each user belongs to only one group, the maximum number of groups is bounded by N_u. Hence, the best performance is expected for a one user per group configuration. In other words, multicasting is expected to perform worst, in terms of precoding gain, over unicasting. An expected result, if one considers that in multicasting the degrees of freedom at the transmit side are reduced.

The above results provide a multicast aware MMSE solution for the calculation of the precoding matrix. However, the main drawback of this solution is that it does not account for the practical per-antenna constraints. The simplest heuristic to overcome this obstacle is to re-scale the solution so that the per-antenna constraints are not violated [139]. Despite the fact that such an operation invalidates the MMSE optimality of the solution, it provides a low complexity heuristic method to design the precoder. Re-scaling is achieved by multiplying each line of the precoding matrix with the square root of the inverse level of power over satisfaction of the corresponding antenna.

5.2.4 Performance Evaluation

In the current section, extensive numerical results that exhibit the applicability of precoding in satellite communications are presented. To the end of providing accurate results, the simulation setup of [68] is employed. The simulation parameters are summarized in Tab. 5.1. The achievable spectral efficiency of the k-th user is directly linked with its SINR_k through the DVB-S2 achievable spectral efficiency. More importantly, to account for ACM and the fact that a single modulation and coding scheme (ModCod) is applied to each frame, the ρ users that are simultaneously served by the same frame are assumed to be using the ModCod corresponding to lowest SNIR value out of the ρ. This consideration is inline with the common multicast consideration that the user with the lowest rate in each group will determine the performance of the group. The multibeam satellite antenna pattern has been provided by ESA [84]. From the 245 beams used to cover Europe, the focus herein is on a cluster of 9 beams, as depicted in Fig. 2.3. This assumption is inline with future multi-GW considerations, where precoding will be performed in each GW separately [103]. Perfect

Table 5.1: Frame Based Precoding Satellite System: Link Budget Parameters

Parameter	Value
Frequency Band	Ka (20 GHz)
User terminal clear sky temp, T_{cs}	235.3K
User Link Bandwidth, B_u	500 MHz
Output Back Off, OBO	5 dB
On board Power, P	50 dBW
Roll off, α	0.20
User terminal antenna Gain, G_R	40.7 dBi
Multibeam Antenna Gain, G_{ij}	Ref: [84]

channel state information is assumed throughout this work. The complex channel coefficients are generated as described in Sec. 2.4.2, where only the phases due to different propagation paths between the satellite and users are assumed [85]. Herein, the interference from adjacent clusters is not accounted for, since the purpose is to give a relative comparison between the possible precoding methods rather than an absolute evaluation of the total system throughput. For ease of reference, however, the results are given on a per beam basis.

The per beam achievable throughput with respect to an increasing on board available power budget for the conventional 4 color frequency reuse scheme and the two proposed precoding methods is given in Fig. 5.3. Clearly, the weighted fair solution achieves 42% improvement over the conventional system, while the heuristic average precoder 21%, for a nominal on board power of 55 dBW. In the same figure, the substantial gain of the proposed techniques with respect to an increasing power budget is also presented. This is gain identical for both precoding methods. Fig. 5.4 presents the per beam throughput when four users per group are considered (i.e. $\rho = 4$). For this setting, the heuristic sub-optimal system performs worst than the conventional systems. However, the multicast approach still manages to achieve some gains (6%). To investigate the sensitivity of all methods to the frame dimensions, the per beam throughput is plotted with respect to an increasing number of users per group in Fig. 5.5, for $P = 55$ dBW.. The performance degradation of all precoding methods with the increasing number of users per group is apparent. This expected result [108] is justified by the inherent constraints of linear precoding methods. As the number of users increases, the transmit spatial degrees of freedom do not suffice to manage interference and the performance is degraded. Nevertheless, the optimal multicast scheme manages to maintain gains over the conventional systems for up to five users per

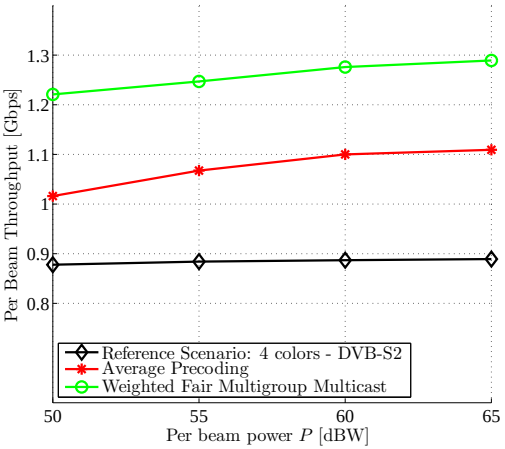

Figure 5.3: Per beam throughput versus increasing on board power for $\rho = 2$ users per group.

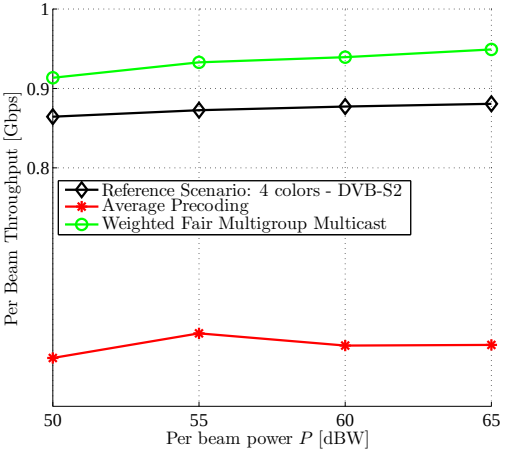

Figure 5.4: Per beam throughput versus increasing on board power.

group. The heuristic scheme however, cannot provide any gains for more than two users per group. In Figs. 5.6 and 5.7 the per user rate distribu-

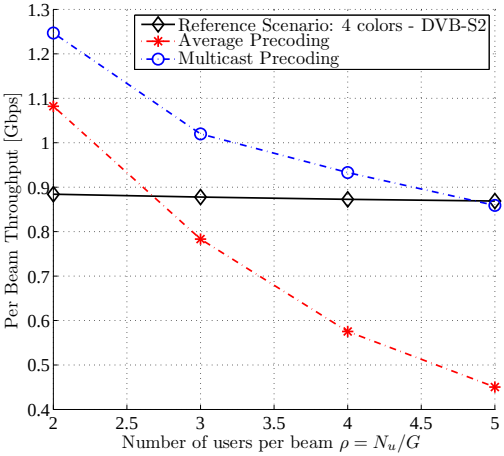

Figure 5.5: Per beam throughput versus number of users per group.

tion over the coverage area for two and four users per group respectively is plotted, for $P = 55$ dBW. In these figures, insights on the origins of the gains of the optimal multicast approach are gleaned. The fairness optimization, reduces the variability of the SNIR across the coverage area and consequently inside each frame. This results in better utilization of resources since users with relatively equal SNIRs are served by the same frame. On the contrary, the MMSE precoding approach exhibits high SNIR variability. Hence, users with different SNIRs are scheduled in the same frame and their performance is compromised by the performance of the worst user. Additionally, many users are driven to the unavailability region, since their SNIR is lower than the minimum value that the available ModCods can support. As depicted in Figs. 5.6 and 5.7, with heuristic MMSE precoding, more than 15% and 30% of users experience unavailability incidents over the coverage area respectively and therefore receive zero rate.

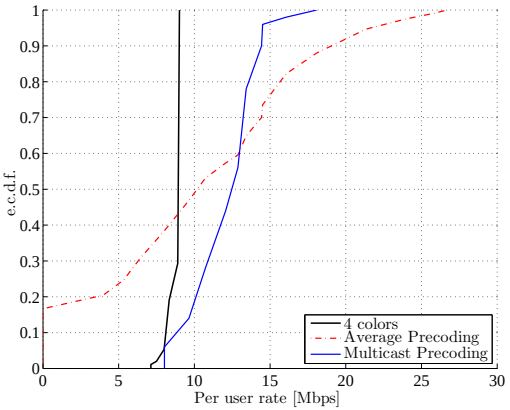

Figure 5.6: Per user rate distribution over the coverage for 2 users per group.

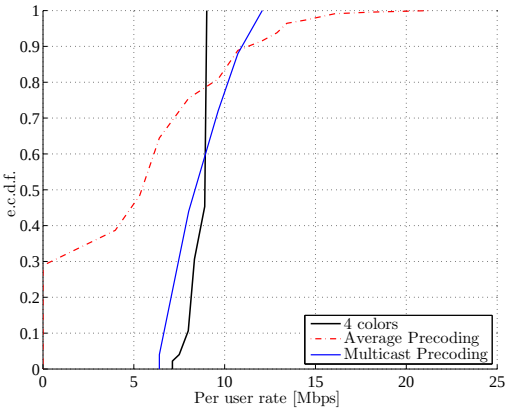

Figure 5.7: Per user rate distribution over the coverage for 4 users per group.

5.3 Max Sum Rate vs Fair Solutions

5.3.1 System Driven Optimization

Increased scepticism over spectrally efficient, aggressive frequency reuse multibeam satellites stems from the effects of such configurations on the SINR distribution across the coverage.

In full frequency reuse scenarios, the useful signal power at the receiver is greatly reduced due to the intra-system interference. Despite the throughput gains due to the increased user link bandwidth and the adequate management of interference by linear precoding, the mean and variance of the SINR distribution over the coverage area is reduced. Intuitively, this will lead to a higher utilization of lower MODCODs and increase the probability of service unavailability over the coverage (outage probability). Retransmissions that incur in these outage instances, burden the system in terms of efficiency. As a result, the probability of compromised users to experience long outage periods, needs to be considered. What is more, by acknowledging the multiuser satellite environment and exploiting user scheduling to maximize the system throughput (cf. Sec. 6.2), these outage periods can potentially become comparable to the inherent long propagation delay of GEO SatCom systems. Such a case will render the overall delay experienced by the user, unacceptable. Consequently, in the present work the introduction of minimum rate constraints over the all the users in the coverage area is proposed as a means to guarantee the availability requirements, typically accustomed in SatComs. To the end of tackling this problem, the practical constraint of guaranteeing a minimum level of service availability is introduced for the first time in a system dependent sum rate optimization.

Sum Rate Maximization under Minimum Rate Constraints

To the end of guaranteing a minimum level of availability, the high gains of the sum rate optimization can be traded-off. This trade-off mostly depends on the minimum MODCOD supported by the ACM. For instance in DVB − S2X under normal operation over a linearized channel, the most robust modulation and coding rate can provide quasi error free communications (frame error probability lower than 10^{-5}) for as low as -2.85 dB of user SINR, thus achieving a minimum spectral efficiency of 0.4348

[bps/Hz] [23][2]. Beyond this value, which is lower than the DVB − S2 [19], a service outage occurs. Thus the evolution of communication standards can guarantee higher availability levels. More importantly, by reducing the availability threshold, the throughput losses from guaranteeing a minimum rate over the coverage can be reduced.

Since an intermediate solution between the fairness and the sum rate optimizations is of high engineering interest, a novel optimization problem, namely the throughput maximization under availability constraints, is proposed. The innovation lies in the incorporation of minimum rate constraints (MRCs) in the PAC sum rate maximizing problem (equivalently minimum SINR constraints). Formally, the new optimization problem is defined as

$$
\begin{aligned}
&\mathcal{SRA}: \max_{\{\mathbf{w}_k\}_{k=1}^{G}} \sum_{i=1}^{N_u} \log_2\left(1+\gamma_i\right) \\
&\text{s. t. } \gamma_i = \min_{m\in\mathcal{G}_k} \frac{|\mathbf{w}_k^{\dagger}\mathbf{h}_m|^2}{\sum_{l\neq k}^{N_t}|\mathbf{w}_l^{\dagger}\mathbf{h}_m|^2+\sigma_m^2}, \qquad (5.8)\\
&\quad \forall i\in\mathcal{G}_k, k, l\in\{1\dots N_t\}, \\
&\text{a.t } \left[\sum_{k=1}^{N_t}\mathbf{w}_k\mathbf{w}_k^{\dagger}\right]_{nn} \leq P_n, \qquad (5.9)\\
&\quad \forall n\in\{1\dots N_t\}, \\
&\text{and to } \gamma_i \geq \gamma_{min},\ \forall i\in\{1\dots N_u\}. \qquad (5.10)
\end{aligned}
$$

In the availability constrained max SR, the power allocation needs to account for the MRC. This can be achieved by modifying the constraints of the sub-gradient search [130], which are imposed via the projection of the current power vector onto the convex set of constraints. Therefore, an additional constraint can be introduced in the projection method, as long as it does not affect the convexity of the optimization problem. Subsequently, to solve $\mathcal{SRA}$ a new projection that includes the minimum rate constraints needs to be performed. The new subset, that is the min SINR

[2]This value can be further reduced to up to -9.9 dB in DVB-S2X under short frame operation but such a technicality is not included in the present work. Therefore, the results presented hereafter can be considered as worst case since possible reduction of the minimum rate would increase the gains of the minimum rate constrained sum rate maximization.

constrained set, is a convex subset of the initially convex set. The availability constrained projection reads as

$$\begin{aligned}
&\mathcal{PA}: \min_{\mathbf{p}} ||\mathbf{p}-\mathbf{x}||_2^2 \\
&\text{subject to}: \frac{p_k|\mathbf{v}_k^\dagger \mathbf{h}_i|^2}{\sum_{l\neq k}^{G} p_l|\mathbf{v}_l^\dagger \mathbf{h}_i|^2+\sigma_i^2} \geq \gamma_{min}, \qquad (5.11)\\
&\qquad \forall i \in \mathcal{G}_k, k, l \in \{1\dots N_t\}, \\
&\text{and to}: \left[\sum_{k=1}^{G} p_k \mathbf{v}_k \mathbf{v}_k^\dagger\right]_{nn} \leq P_n, \qquad (5.12)\\
&\qquad \forall n \in \{1\dots G\},
\end{aligned}$$

which is a convex optimization problem, that includes one additional linear constraint, i.e. (5.11), over $\mathcal{P}$. Provided that $\mathcal{SRA}$ is feasible, i.e. (12) is satisfied, then a solution for $\mathcal{PA}$ always exists. Similarly to $\mathcal{P}$, this problem can be solved using standard methods [71].

Subsequently, the solution of $\mathcal{SRA}$ is derived following the steps of Alg. 2 but with a modification in the sub-gradient method (Step 3), where the projection is calculated by solving problem $\mathcal{PA}$ instead of $\mathcal{P}$. As intuitively expected, the introduction of MRCs is bound to decrease the system throughput performance. However, this trade-off can be leveraged towards more favorable conditions, by considering other system aspects, as will be discussed in the following.

Throughput Maximization via MODCOD Awareness

A modulation constrained practical system employs higher order modulations to increase its rate with respect to the useful signal power. The strictly increasing logarithmic cost functions describe communications based on Gaussian alphabets and provide the Shannon upper bound of the system spectral efficiency. Therefore, the sum rate maximization problems solved hitherto fail to account for the modulation constrained throughput performance of practical systems. The complication lies in the analytically intractable, at least by the methods considered herein, nature of a step cost function. In the present section, an attempt to leverage this cost function in favor of the system throughput performance is presented. In more detail, benefiting from the finite granularity of the rate function

(5.1) over the achieved SINR, an extra system level optimization can be defined as

$$\mathcal{SRM}: \max_{\{\mathbf{w}_k\}_{k=1}^{G}} \sum_{i=1}^{N_u} f_{\text{DVB-S2X}}(\gamma_i)$$

$$\text{s. t. } \gamma_i = \min_{m \in \mathcal{G}_k} \frac{|\mathbf{w}_k^{\dagger}\mathbf{h}_m|^2}{\sum_{l \neq k}^{N_t} |\mathbf{w}_l^{\dagger}\mathbf{h}_m|^2 + \sigma_m^2}, \tag{5.13}$$

$$\forall i \in \mathcal{G}_k, k, l \in \{1 \dots G\},$$

$$\text{a.t} \left[\sum_{k=1}^{N_t} \mathbf{w}_k \mathbf{w}_k^{\dagger}\right]_{nn} \leq P_n, \tag{5.14}$$

$$\forall n \in \{1 \dots N_t\},$$

$$\text{and to } \gamma_i \geq \gamma_{min}, \ \forall i \in \{1 \dots N_u\}, \tag{5.15}$$

where $f_{\text{DVB-S2X}}(\cdot,\cdot)$ is the finite granularity step function defined in (5.1). The realization of a non-strictly increasing cost function inhibits the application of gradient based solutions. and necessitates a different solution process. To provide a solution for this elaborate -yet of high practical value- problem, a heuristic iterative algorithm is proposed. More specifically, Alg. 3 receives as input the availability constrained precoders $\{\mathbf{w}_k^{\mathcal{SRA}}\}_{k=1}^{G}$ calculated as described in Sec. 5.3.1, and calculates an initial SINR distribution. Then, it calculates new precoding vectors under minimum SINR constraints given by the closest lower threshold of the worst user in each group, according to the discrete throughput function. Therefore, the resulting system throughput is not decreased while power is saved. This power can now be redistributed. Also, in this manner, the solution guarantees a minimum system availability. Following this step, an ordering of the groups takes place, in terms of minimum required power to increase each group to the next threshold target. For this, the power minimization problem is executed for each group. Next, each of the available groups, starting from the group that requires the least power, is sequentially given a higher target. With the new targets, the power minimization problem is again solved. This constitutes a feasibility optimization check. If the required power satisfies the per antenna constraints, then these precoders are kept. Otherwise the current group is given its previous feasible SINR target and the search proceeds to the next group.

Remark: A further improved solution can be attained when dropping the constraint of a single step increase per group. Herein, such a consideration is avoided for complexity reasons. Since each of the G groups can take at most N_m possible SINR values, where N_m denotes the number of MODCODs, by allowing each group to increase more than one step, the number of possible combinations can be as much as $(N_m)^G$. As a result, the complexity of the optimal solution found by searching the full space of possible solutions, grows exponentially with the number of groups. In the present work, the high number of threshold values for $f_{\text{DVB-S2X}}$ prohibits such considerations.

The summary of this algorithm is given in Alg. 3. Since it is an iterative algorithm over the number of available groups, convergence is guaranteed. Also, since it receives as input the $\mathcal{SRA}$ solution, its complexity is dominated by the complexity of Alg. 2, as described in Sec. 4.3.2.

5.3.2 Performance Evaluation

Based on an accurate simulation model defined in [84] the performance of a frame based precoding full frequency reuse broadband multibeam satellite is compared to conventional four color reuse configurations. Results in terms of normalized average throughput given by (5.1) are given to quantify the potential gains of frame based precoding. The rate distribution over the coverage before and after precoding is investigated. Finally, the performance all discussed methods versus an increasing number of users per frames is presented. For accurate averaging, 900 users are considered uniformly distributed across the footprint of the 9 beams depicted in Fig. 2.3. The throughput results are given via (5.1), averaged over all transmissions required to serve all 900 users. This consideration provides a fair comparison when user scheduling methods are considered. Since the grids of user positions over the coverage are finite, very large user pools will render the results biased. Also, serving less users than the available for selection would drastically improve the results but not in a fair manner from a system design perspective, since this would imply that some users are denied service for an infinite time.

Input: $\mathbf{H}, P_{tot}, \sigma_i^2\ \forall i \in \{1 \dots N_t\}, \{\mathbf{w}_k^{(0)}\}_{k=1}^G = \{\mathbf{w}_k^{\mathcal{SRA}}\}_{k=1}^G$, $r^{(0)}$, γ_{min}

Output: $\{\mathbf{w}_k^{out}\}_{k=1}^G$

begin

$j = 0$; $q = 1$; $\{\mathbf{w}_k^{out}\}_{k=1}^G = \{\mathbf{w}_k^{(0)}\}_{k=1}^G$;

Step 1: Solve $r^{*,(0)} = \mathcal{Q}(\mathbf{g}^{(0)}, \mathbf{p}_{ant})$ to calculate $\{\mathbf{w}_k^{\mathcal{Q},(0)}\}_{k=1}^G$. The input SINR targets are given by the minimum threshold SINR per group, i.e.

$\mathbf{g}^{(0)} : \gamma_i = \lfloor \min_{m \in \mathcal{G}_k} \{\text{SINR}_m\} \rfloor_{\mathbf{t}}, \forall i, m \in \mathcal{G}_k, k = 1, \dots, G.$

for $j = 1 \dots G$ **do**

Step 2: Solve $r^{*,(j)} = \mathcal{Q}(\mathbf{g}^{(j)}, \mathbf{p})$ to calculate $\{\mathbf{w}_k^{\mathcal{Q},(j)}\}_{k=1}^G$. The targets of the current j-th group are increased by one level: $\gamma_i = \lceil \min_{m \in \mathcal{G}_j} \{\text{SINR}_m\} \rceil_{\mathbf{t}}, \forall i \in \mathcal{G}_j$;

Order the groups in terms of increasing $r^{*,(j)}$.

end

while $r^{*,(q)} < 1$ **do**

Step 3: For each group, in a sequence ordered by the previous step, increase the target by one level;

Solve $r^{*,(q)} = \mathcal{Q}(\mathbf{g}^{(q)}, \mathbf{p})$ with input targets from the previous iteration: $\mathbf{g}^{(q)} = \mathbf{g}^{(q-1)}$; $q = q + 1$

end

$\{\mathbf{w}_k^{out}\}_{k=1}^G = \{\mathbf{w}_k^{\mathcal{Q},(q)}\}_{k=1}^G$

end

Algorithm 3: Discretized sum rate maximization.

Throughput Performance

In Fig. 5.8, the per beam throughput of the considered multibeam satellite is plotted versus an increasing total on board available power. Two users per group are considered. Clearly, across a wide region of operation, the proposed methods outperform conventional systems. The proposed max SR problem achieves more than 30% gains over the fair solutions of [109]. These gains are reduced when the max SR under MRCs is considered. This is the price paid for guaranteeing service availability over the coverage. Finally, the maximum gains are observed when the modulation aware max SR precoding is employed, which also guarantees service availability. Consequently, the best performance is noted for the proposed $\mathcal{SRM}$ with more than 30% of gains over [109] and as much as 100% gains over conventional systems in the high power region, for 2 users per group.

The distribution of the SINRs over the coverage area is given in Fig. 5.9. Clearly, conventional systems achieve higher SINRs by the means of the fractional frequency reuse. This value is around 17 [dB], in line with the results of [84]. However, this does not necessarily translate to system throughput performance. To guarantee increased SINRs, the PHY resources allocated per user are four times reduced. On the other hand, aggressive frequency reuse reduces the average SINR values and increases its variance, as seen in Fig. 5.9. This, however, allows for more efficient resource utilization and thus the improved system throughput performance, as presented in Fig. 5.8. Moreover, the superiority of the max SR techniques proposed herein, over the fair solutions is also evident. Amongst these methods, the best on is $\mathcal{SRM}$ as already shown. In Fig. 5.9, it is clear that the proposed optimization manages to adapt each users SINR to the throughput function since the SINR distribution shows higher granularity than the distributions of the rest of the methods. According to these results, 40% of the users operate utilizing the first three available MODCODs. Also, a minimum SINR is guaranteed.

Fig. 5.10 provides insights for the above reported gains. The rate cumulative distribution functions (CDFs) of the conventional and the fair systems is justified by the very low variance of their receive SINR. However, the max SR optimization achieves very high rates but also drives some users to the unavailability region. A 5% outage probability is noted for this precoding scheme. This is not the case for the $\mathcal{SRA}$ and $\mathcal{SRM}$ problems, which guarantee at least 0.3 Gbps to all users. The superiority

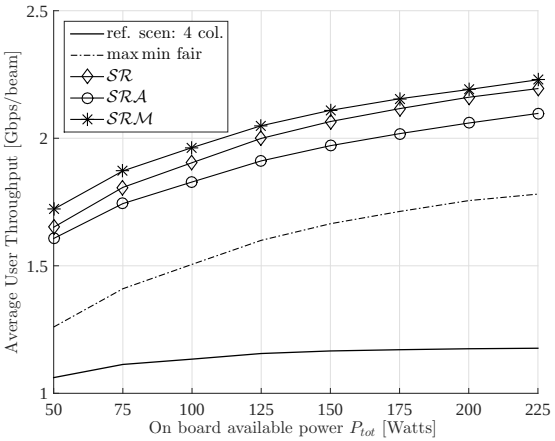

Figure 5.8: Average user throughput of frame based precoding, versus transmit power.

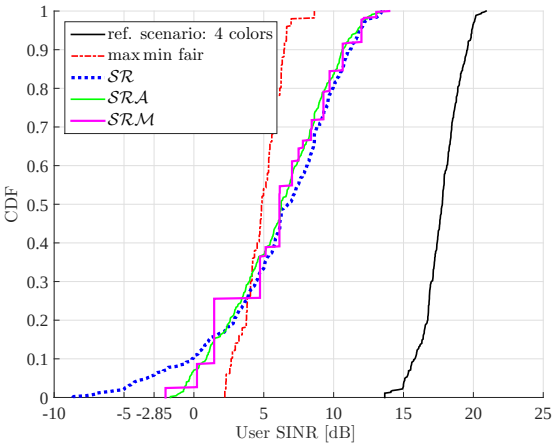

Figure 5.9: Average user throughput CDF over the coverage.

of the latter is also clear, since higher rates are achieved with greater probability. To gain better insights into the reported gains, the SINR CDFs are plotted in Fig. 5.9. An important discussion involves the performance

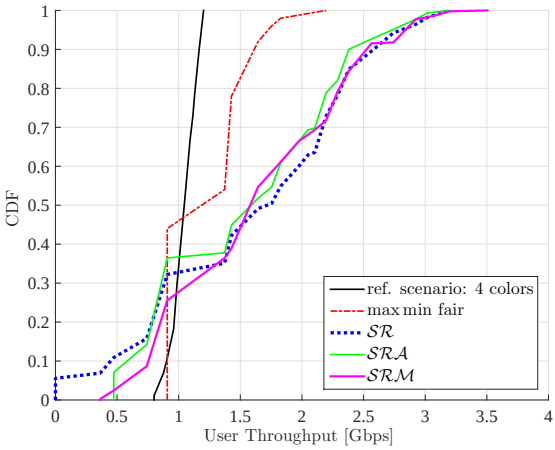

Figure 5.10: Per-user rate CDF.

of the developed methods with respect to an increasing number of users per group. As presented in Fig. 5.11, the $\mathcal{SRM}$, manages to provide gains over the conventional systems even for 6 users per group unlike all other techniques. These results are given for a nominal on board available power of 50 dBWs. This performance is compromised by the random user scheduling since users with very different SINRs are co-scheduled and thus constrained by the performance of the worst user.

Paradigm

To the end of exhibiting the differences of the max SR optimization with the fair optimization of [109], a small scale simple paradigm is presented. Let us assume 2 users per group (i.e. $\rho = 2$). The throughput of each user is plotted in Fig. 5.12 for the case of a conventional system, a full frequency reuse satellite under weighted fair optimization (equal weights are assumed) and a modulation aware max SR design. The sum rates

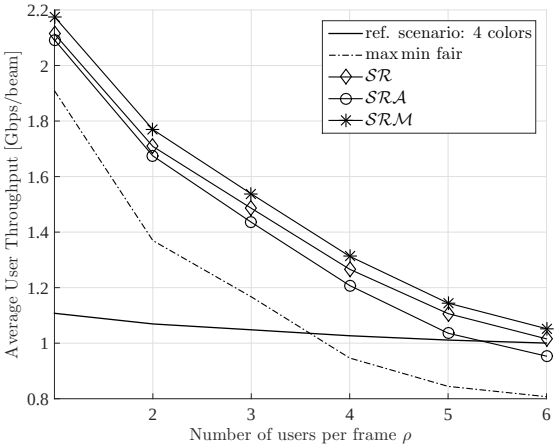

Figure 5.11: Per-beam throughput with respect to an increasing number of users per frame.

are given in the legend of the figure. In the conventional system, the common rate at which all users will receive data is 1.2 Gbps leading to a sum rate of 10.8 Gbps. By the fair optimization of [109] 12.4 Gbps of are attained, while the minimum SINRs and hence the minimum rates are again balanced between the groups. Finally, the sum-rate maximizing optimization, reduces the group that contains the compromised users in order to reallocate this power to the balanced group and therefore increase the system throughput to 13.6 Gbps, whilst simultaneously keeping all users above the outage threshold.

5.4 Summary

In the present work, full frequency reuse combined with linear precoding has been proposed for the optimization of broadband multibeam satellite systems in terms of throughput performance. Different than before, two fundamental practical constraints, namely the rigid framing structure of satcom standards and the per antenna maximum power limitations have been considered.

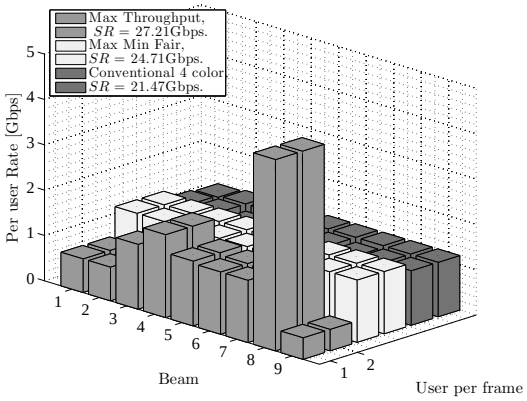

Figure 5.12: Per-user rates for each beam.

In the first part of the chapter, the optimal in a fairness sense, per antenna power constrained, multicast multigroup linear precoding vectors have been considered for the application of frame based precoding. The performance of the proposed precoding technique is compared to the heuristic methods of re-scaled to respect the PACs MMSE precoding. Simulation results over an multibeam satellite operating in full frequency reuse configuration exhibit the optimality of the multicast multigroup solution over heuristic precoding methods. Insights on the origin of this result are provided by examining the SINR and rate distributions over the coverage. Also, a sensitivity analysis with respect to system design parameters, namely the number of users per group, reveals the limits of the herein fair precoding methods.

Towards improving the previously established limitations, in the second part of the chapter, the SR optimal multicast multigroup design have been proposed for frame based transmitters with per-antenna power constraints. Moreover, to better establish frame based precoding over satellite, the optimization has been extended to account for availability constraints as well as the modulation constrained throughput performance of the system.

In summary, the gains reported herein are up to 100% in terms of throughput performance compared to conventional four color frequency reuse schemes. These gains are achieved without loss in the outage performance of the system, while following the most advanced design, up to 6 users per group can be accommodated without losses over conventional systems.

Chapter 6

User Scheduling in Cooperative SatComs

In the present chapter, the application of user scheduling in the context of cooperative multibeam SatComs is discussed. The main goal is to establish the importance of multiuser scheduling in satellite systems. To this end, two exemplary systems that can benefit from advanced user scheduling methods are described. For these systems, the development of heuristic user scheduling algorithms is described in full detail. The performance gains gleaned by the application of the proposed algorithms are quantified over accurate simulation environments. Consequently, the attained gains constitute a significant incentive for the incorporation of multiuser scheduling in next generation cooperative multibeam satellites.

6.1 Introduction

The constantly increasing demand in interactive broadband SatComs is driving current research to explore novel transmission techniques and system architectures. The spatial degrees of freedom offered by the multibeam antenna constitute a substantial interference mitigation resource. To fully exploit this spatial separation, advanced signal processing techniques, namely precoding, are herein examined. Consequently, the scarce user link bandwidth can be efficiently utilized by higher frequency reuse schemes. In terms of novel system architectures, aggressive frequency

reuse can come into play between physically separated satellites or even between hybrid satellite/terrestrial systems. In the present chapter, the term cooperative multibeam SatComs, will refer to both above mentioned concepts. Hence, a satellite bearing a multiple antenna driven by a communications payload compatible with aggressive frequency reuse configurations is called cooperative. Additionally, a cooperative dual satellite system refers to two cooperative satellites that can operate as one, by exchanging a large amount of information. A relaxation of the later constraint results in coordinated satellite systems. Coordination involves the exchange of a small amount of data and therefore trades-off the high gains of inter-system cooperation for a reduced implementation complexity. More details on these concepts will be provided in the respective sections.

The information theoretic capacity bounds of the multiuser satellite channel can be approached by exploiting the underlying rich multiuser environment. The high number of users served by one satellite can offer significant multiuser diversity gains. In this direction, the topic of user scheduling is developed in the present chapter. In spite of the fact that cooperation between co-existing systems is expected to highly impact the satcom industry, user scheduling can enhance the performance of the cooperative systems in two manners. Firstly, it can boost the performance of each cooperative satellite by exploiting the multiuser gain. Secondly, it can reduce the level of interference between coordinated systems, that is systems that exchange only a reduced amount of data between them.

In the following sections, the application of user scheduling in the context of full frequency reuse multibeam SatComs is discussed. The importance of multiuser scheduling in joint processing systems is pointed out by two major applications. Firstly, in Sec. 6.2 a multicast aware user scheduling policy, based on the orthogonality of the user vector channels, is developed to glean the gains offered by the rich multiuser environment of satellite systems. Consequently, the frame based precoding system presented in Ch. 5 is completed by the application of advanced user scheduling. Extensive numerical results over an accurate satellite scenario are substantiating the above claims.

Secondly, an exemplary cooperative dual satellite system that can benefit from advanced user scheduling methods is described. In this scenario, a low complexity user scheduling algorithm customized for the proposed system is developed. The performance gains gleaned by the application

of the proposed algorithm are exhibited via simulation results. Consequently, a preliminary study to quantify the potential gains of multiuser scheduling in cooperative multibeam SatComs is presented.

6.2 User Scheduling for Frame Based Precoding

Multibeam satellite networks typically cover vast areas by a single satellite illuminating a large pool of users requesting service. Therefore, a satcom system inherently operates over a very rich in terms of multiuser diversity gains environment. In current satcom standards, user scheduling is based on the demanded traffic and the channel conditions of each user [19]. Thus DVB − S2 schedulers require knowledge of each users specific SINR value. Given this value, users with relatively similar requirements are scheduled in the same frame and a specific link layer mode (assuming ACM) is employed to serve them. An diagram with the necessary operations performed at the transmitter is illustrated in Fig. 6.1 (a) for conventional systems.

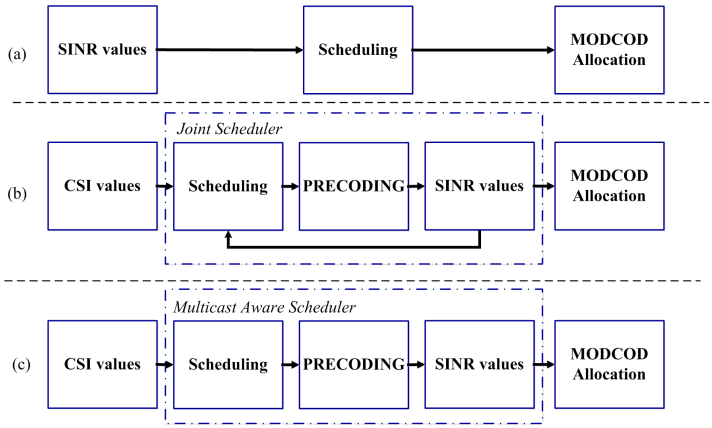

Figure 6.1: Scheduling over satellite: (a) Conventional DVB − S2 (b) Optimal joint precoding and scheduling (c) Proposed multicast aware heuristic scheduling.

In the frame based precoding methods presented in the previous sections, a precoding design over a randomly defined group of users is assumed. Since all co-scheduled users are served by the link layer mode imposed by the worst user in each group, significant performance losses from a system design perspective will be realized by a random user grouping. Acknowledging that CSI is readily available at the transmit side, since it is a requisite for the application of interference management, the optimization of the system in any required sense can be achieved by advanced scheduling methods. These methods, as shown in Fig. 6.1 (b) and (c) are based on the exact CSI. As it will be shown hereafter, by accounting the vector CSI in the scheduling process, the multiuser gains can be exploited towards further maximizing the system throughput performance.

The most intrinsic attribute of a joint scheduling and precoding design lies in the coupled nature of the two designs. Since precoding drastically affects the useful signal power at the receive side, scheduling cannot be simply based of the receive SINR value. On the other hand, the performance of precoding depends on the user vector channels. The block diagram (b) of Fig. 6.1 presents the optimal joint scheduler. This module jointly performs precoding and scheduling by including a feedback from the output of the precoder to the scheduler. Based on an initial user scheduling, a precoding matrix calculated by the methods of Sec. 5.3.1 is applied and each users SINR is calculated. Then this value is fed back to the scheduler where a new user selection is performed. Based on this scheduling, a new precoding matrix is calculated and applied thus leading to a new SINR distribution. Clearly, this procedure needs to be iterative and can be performed until all the possible combinations of users are examined. Thus the implementation complexity of such a technique is considered unappealing and will not be considered for the purposes of the present work.

6.2.1 Multicast Aware User Scheduling

As described in the previous paragraph, the precoding is affected by scheduling and vice versa. To the end of providing a solution to this causality dilemma, a multicast aware approach is illustrated in Fig. 6.1 (c). Based on such an architecture, an advanced low complexity CSI based scheduling method that does not require knowledge of the resulting SINR is developed. The key step in the proposed method lies in mea-

suring the similarity between users based on the readily available CSI. The underlying intuition is that users scheduled in the same frame should have co-linear (i.e. similar) channels since they need to receive the same symbols. On the contrary, interfering users, scheduled in adjacent synchronous frames, should be orthogonal to minimize interference [53]. In the parlance of MU − MIMO communications the level of similarity between the users can be measured in terms of orthogonality of the complex vector channels. To maximize the similarity of two vectors, one needs to maximize their projection, that is the dot product of the two vectors. On the contrary, to maximize their orthogonality the projection needs to be minimized.

Assuming a fixed pool of users, the optimal allocation into orthogonal groups of parallel users can be found by examining all the possible combinations. Since the optimal user scheduling policy would require a full search over all possible combinations of users, its implementation complexity easily becomes prohibitively large. Therefore, in the present section a heuristic iterative user scheduling algorithm that reduces the co-channel interference between the different multicast groups by the means of multiuser diversity and simultaneously maximizes the multicast gains by allocating highly parallel users in the same frames, is developed.

The multicast aware user scheduling algorithm, presented in detail in Alg. 4 is a low complexity heuristic iterative algorithm that allocates orthogonal users in different frames and simultaneously parallel users with similar channels in the same frame. In more detail, this two step algorithm operates as follows. In the first step of the process, one user per group is allocated according to the semi-orthogonality criteria originally proposed in [53]. This semi-orthogonality criterion was originally derived for zero-forcing ZF precoding, to the end of finding the users receiving the minimum interference and thus maximize the performance of ZF. These results are herein employed for the first step of the proposed algorithm since the goal is to find the optimal allocation of non-interfering users amongst different groups. Next, a novel second step provides the multicast awareness of the herein proposed algorithm. Thus, in Step 2, for each of the groups sequentially, the most parallel users to the previously selected first user are selected. Subsequently, the similarity of the channels that are to be sent the same information is maximized.

Input: $\mathbf{H}$
Output: User allocation sets $\mathcal{I}$
begin
Step 1: $\forall\ l = 1, 2 \dots G$ allocate semi-orthogonal users to different groups: Let $\mathcal{I} = \emptyset$ denote the index set of users allocated to groups, $\mathcal{J} = \{1, \dots N_u\} - \{\mathcal{I}\}$ the set of unprocessed users and $g_{(1)} = \max_k ||\mathbf{h}_k||_2$.
while $|\mathcal{I}| < G$ **do**
forall the $m \in \mathcal{J}$, $l = 1 \dots N_t$ **do**
$\mathbf{g}_m^\dagger = \mathbf{h}_m^\dagger \left(\mathbf{I}_{N_t} - \sum_{q=1}^{l} \frac{\mathbf{g}_{(q)} \mathbf{g}_{(q)}^\dagger}{||\mathbf{g}_{(q)}||_2^2} \right)$ calculate the orthogonal component (rejection) of each unprocessed user's channel, onto the subspace spanned by the previously selected users.
end
Select the most orthogonal user to be allocated to the l-th group: $\mathcal{G}_l = \arg\max_m ||\mathbf{g}_m||$, $\mathbf{g}_{(l)} = \mathbf{g}_{\mathcal{G}_l}$ and update the user allocation sets $\mathcal{I} = \mathcal{I} \cup \{\mathcal{G}_l\}$, $\mathcal{J} = \mathcal{J} - \{\mathcal{G}_l\}$.
end
Step 2: for each group select the most parallel users.
for $l = 1 \dots G$ **do**
while $|\mathcal{G}_l| \leq \rho$ **do**
forall the $m \in \mathcal{J}$ **do**
$\mathbf{u}_m = \mathbf{h}_k^\dagger \frac{\mathbf{h}_j \mathbf{h}_j^\dagger}{||\mathbf{h}_j^\dagger||^2}, j = [\mathcal{G}_l]_1$; calculate the projection of each users channel, onto the first user of each group.
end
Select the user that is most parallel to the first user of each group. $\pi_l = \arg\max_m \{||\mathbf{u}_m||\}$ and update the user allocation sets $\mathcal{G}_l = \mathcal{G}_l \cup \{\pi_l\}$, $\mathcal{I} = \mathcal{I} \cup \{\mathcal{G}_l\}$, $\mathcal{J} = \mathcal{J} - \{\mathcal{G}_l\}$
end
end
end

Algorithm 4: Multicast Aware User Scheduling Algorithm

6.2.2 Performance Evaluation

Assuming a fixed user pool, as in the previous results, the formulated groups are no longer randomly formulated. Instead, the multicast aware user scheduling algorithm is employed. In Fig. 6.2 the performance of the algorithm for 2 users per group is given versus an increasing on-board power budget. In this figure, slight improvements of the system performance are realized. However, the gains of user scheduling are revealed when advancing to higher numbers of users per group. In Fig. 6.3 it is clear that by employing user scheduling methods, the degradation of the system performance with respect to an increasing number of users per group is significantly improved. The same initial group of users as before is employed regardless of the frame size, excluding a small rounding error cut off. For instance, when 3 users per frame are assumed, the total number of users served is reduced to 891. The most important result is that by employing multicast aware user scheduling methods, as much as 14 users per frame can be accommodated in the frame based precoding, without negative gains over conventional frequency reuse payload configurations.

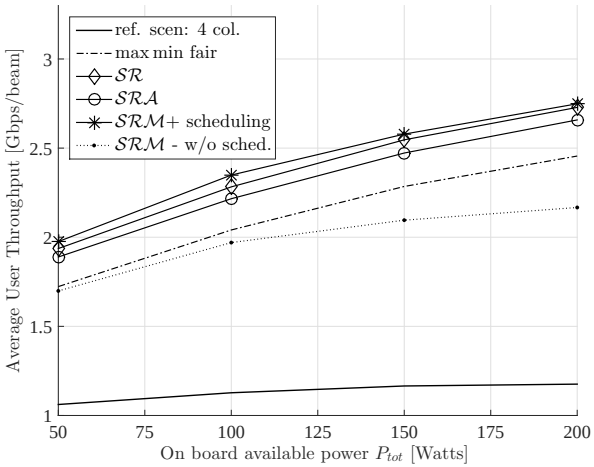

Figure 6.2: Average throughput versus an increasing on board available transmit power, with scheduling.

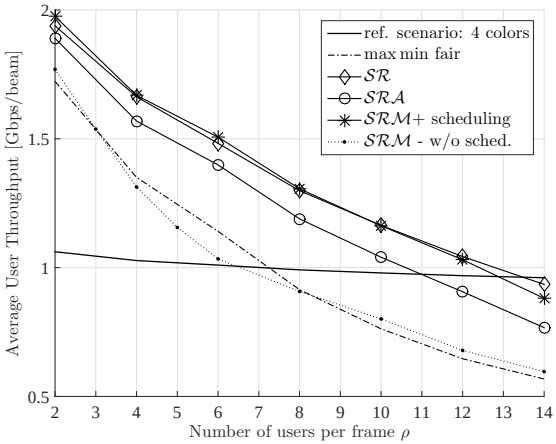

Figure 6.3: Per-beam throughput versus the number of users per frame.

Finally, to exhibit the dependence of the performance with respect to the available for selection user pool, in Fig. 6.4, the average user throughput for three users per frame with respect to an increasing user pool is plotted. Almost 20% gains are noticed when doubling the user pool.

6.3 Co-Existing Multibeam Satellite Systems

Towards the next generation of broadband multibeam SatCom systems, innovative system architectures need to be considered in order to meet the highly increasing demand for throughput and close the digital divide. Spectrum scarcity is a major obstacle, especially in a satellite context where the higher frequency bands exhibit challenging channel impairments. In this direction, the investigation of full frequency reuse techniques that exploit the spatial degrees of freedom offered by the multibeam satellite antenna comes into play. The consideration of co-existing multibeam satellite architectures is necessitated by the following facts:

- In the evolution of GEO satellite systems, orbital slot congestion is an uprising problem. In this context, co-operation between multi-

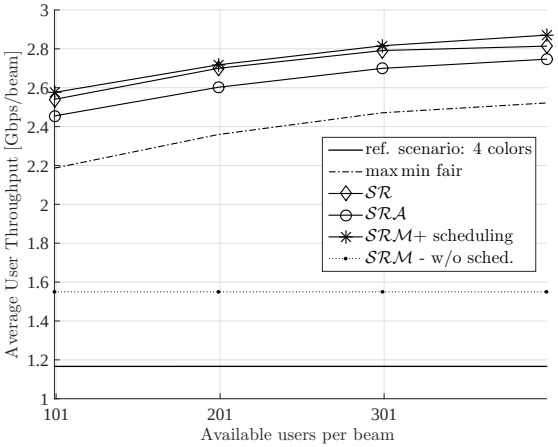

Figure 6.4: Average throughput with respect to an increasing number of available for selection users.

beam satellites has the potential of overcoming the major issue of Adjacent Satellite Interference (ASI).

- Unpredictable changes in the traffic demand can dictate the launch of secondary satellites to support existing ones. The optimal co-existence of such systems has the potential to realized significant gains.

- Aggressive frequency reuse increases the communication payload size since a single TWTA cannot be shared by multiple beams. Hence, the payload required to drive a large number of beams that cover large regions (e.g. pan-European coverage) can only be accommodated by multiple co-existing satellites. There, cooperation amongst satellites also becomes relevant.

- Last but not least, long periods of coexisting satellites appear during the replacement phase of old satellites.

6.3.1 Co-located Satellites

The system under investigation consists of two collocated multibeam satellites with overlapping coverage areas, serving fixed single antenna users (Fixed Satellite Services, FSS). A large number of users uniformly distributed in each beam is assumed and a Time Division Multiple Access (TDMA) scheme is realized, leading to one user per beam served, during each time slot. An overview of the considered system is depicted in Fig. 6.5, where the focus is on the FL downlink of the satellites (i.e. the link between the satellite and the users), while the FL uplink, or feeder link (i.e. the link between each satellite and the earth GW station), is considered ideal. The channel model of Sec. 2.4.1 is considered.

Each satellite is served by a dedicated GW that has full CSI over the channels between the corresponding satellite and each user. The information that each GW handles defines the architecture of the system. As seen in Fig. 6.5, the level of cooperation between two co-located satellites might vary from none up to full cooperation, with of course increasing implementation complexity. The technique proposed herein, namely coordination, attempts to balance performance gains and implementation complexity. More details on the level of required information will be given in Sec. 6.3.2.

Dual Satellite System Signal Model

Extending the system model considerations of Ch. 2 to a dual satellite scenario, the resulting channel needs to be modeled. In this direction, two overlapping clusters of N_1 and N_2 spot-beams covering K_1 and K_2 fixed user terminals respectively, are considered (Fig. 6.5) . The users, each equipped with a single antenna, are uniformly distributed over the coverage area. Despite the fact that in each satellite separately, a MU MISO BC is realized, the whole system operates over an interference channel. The equivalent equation for the second satellite is straightforward to deduce by substituting index 1 with 2. The k-th user now has two vector channels, one towards each satellite, denoted using the indices 1 and 2 respectively. The channel vectors $\mathbf{h}_{k1}^{\dagger}, \mathbf{h}_{k2}^{\dagger}$ are the rows of a total channel matrix $\mathbf{H}_{tot}$ of $(K_1 + K_2) \times (N_1 + N_2)$ dimensions, that models the satellite antenna gains of the two satellites.

Considering each multibeam satellite separately, linear precoding is employed to cancel out inter-beam interference. More specifically, ZF

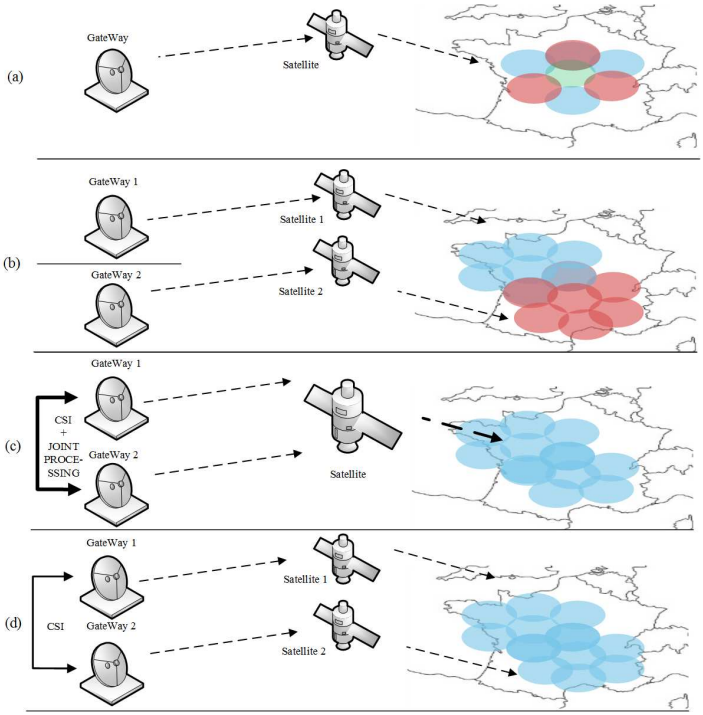

Figure 6.5: Different levels of cooperation between collocated satellite systems: (a) Independent (b) Coordinated and (c) Fully cooperative dual satellite systems

precoding is performed in each satellite, while the power allocation is optimized under max SR criteria subject to realistic PACs, as described in Sec. 2.3.1. To formalize the precoding problem, each time slot only one user per beam is scheduled leading to $K_1 = N_1$ users to be served from the first satellite using ZF, and $K_2 = N_2$ for the second system. Despite the complete mitigation of per-satellite inter-beam interference, each user still receives interference from the adjacent satellite. Using indices 1 and 2 to distinguish between the parameters of each satellite, the resulting SINR in a user served by the first satellite will read as

$$\hat{\mathrm{SINR}}_k = \frac{p_{1k}|\mathbf{h}_{k1}^{\dagger}\mathbf{w}_{k1}|^2}{1+\sum_{j=1}^{K_2} p_{2j}|\mathbf{h}_{k2}^{\dagger}\mathbf{w}_{j2}|^2}. \tag{6.1}$$

In (6.1), the interference from the adjacent satellite is apparent in the denominator, while inter-satellite multiuser interference is completely mitigated by the precoding. The equivalent relations for the users allocated to the second satellite, are straightforward to deduce, by exchanging indices 1 and 2.

6.3.2 User Scheduling for Dual Satellite Systems

Despite the extensive literature on linear precoding and user selection, in the present chapter the optimal allocation of the selected users in two coexisting groups that interfere with each other is also considered. The novelty of the presented results lies in the fact that user selection and allocation, not only optimizes the ZF performance of each system but also considers the interaction between the two transmitters, i.e. the inter-satellite interference. The procedure of selecting users out of a large pool and allocating them to specific sets is referred to as user scheduling.

As it will be further explained in the remainder of the chapter, the allocation of one user in a set not only affects the performance of the current user group but also the performance of the second group due to the interference this user will induce to the other set.

The derived algorithm selects users from a large user set -since only one user is served in each timeslot by each antenna- with the aim of maximizing the orthogonality between the selected users in each set (optimal selection for each satellite separately to maximize ZF performance) but at the same time trying to minimize the level of interference this user is receiving and inducing from and to the second user set.

However, this selection will not take into account the inter-system interference, thus orthogonalization in the frequency domain will be necessary and each system will operate over the half of the available spectrum. The optimal solution to this problem is the full cooperation between the two systems, where interference can be mitigated by ZF over the total channel matrix of both systems. However, the distributed nature of the systems makes full cooperation unrealistic, especially in SatComs where each satellite is served by a specific GW. The large amount of data and CSI that needs to be exchanged for an interactive broadband network, the feeder link limitations and signal synchronization issues are the main prohibitive factors. An interesting solution to this fundamental problem is the partial cooperation between the two GWs. The nature of this cooperation is studied herein.

As proven in [82], user selection can significantly improve the performance of ZF in an individual system. However, considering the coexistence of two separate transmitters, as is the case in a dual satellite system, partial cooperation, namely coordination, can be employed to solve the problem of high intersatellite interference. To this end, this contribution proposes an algorithm that selects users and allocates them to each satellite. Intuitively, the two basic criteria that need to be considered for this procedure are: a) the maximization of the performance of each satellite separately, and b) the minimization of the interference between the two sets.

As a result of this procedure, each GW will only process the data of the users allocated to the corresponding satellite, thus the amount of information that needs to be exchanged will only rely on the nature of the proposed algorithm as will be explained further on.

The performance of each satellite separately is optimized by constructing a semi-orthogonal user group from a vast number of users [53]. Extending this result, the creation of two user sets under the semi-orthogonality criterion is straightforward since the channel gain of each user can be projected to the orthogonal complement of the channels of the previously selected users. In each iteration of the algorithm, the user with the maximum projection is allocated to the corresponding set. This simplistic approach has been considered for comparison reasons.

The novel proposed algorithm accounts for the effects of the interference between the two sets. It should first be mentioned that the exact calculation of the level of interference in each iteration is not possible

since the exact user set is still undetermined. To exactly calculate the interference, one would need to solve the beamforming problem for each and every possible combination of users. Under the assumption of large number of users, this would lead to unaffordable computational complexity. However, based on a basic advantage of ZF beamforming, which is the decoupled nature of the precoder design and the power allocation optimization problems, an approximation of the interference can be made. In this direction, the precoding vectors of the users selected in the previous iterations can be utilized to provide an indicative measure of the interference between the user sets. This implies that an equal power allocation is assumed. This assumption becomes asymptotically exact in the high SNR regime, where the powers allocated to each user are approximately equal. Incorporating all the above, a heuristic, iterative Semi-orthogonal Interference aware User Allocation algorithm (SIUA) has been developed and will be presented in the following.

The SIUA algorithm, presented in full detail in Algo. 5 works as follows. During the initialization procedure, i.e. Step 1, the strongest user towards each satellite is allocated to the equivalent group. While the two sets are not full, Steps 2 and 3 are executed. In Step 2, for each of the unallocated users, the following metrics are calculated: a) In accordance to [53], $\mathbf{g}_{1k}$ and $\mathbf{g}_{2k}$ represent the orthogonal component of each unallocated user's channel to the orthogonal subspace of the already allocated users, for the two sets respectively. In b) I_{k1}^{r} and I_{k2}^{r} are equivalent measures for the interference each user would receive if equal power allocation is employed. It is calculated as the squared norm of the product of the users' channel with the power of the transmit signal of the second user set and the channel of each user. Finally, in c) I_{k1}^{i} and I_{k2}^{i} are approximations of the interference that the allocation of each user can potentially induce to the second set, if this user is allocated in the respective set. It is calculated as the product of the interference this user induces to every user that belongs to the second set. Since the goal is to find the most orthogonal users that at the same time receive and induce the least possible interference, the measure to be maximized is the fraction of the orthogonality metric over the product of the interference metrics. At the last stage of each iteration, two maximum fractions μ_1 and μ_2 are calculated over the hole user set and compared between them. The user that corresponds to the largest measure among the two, is allocated to the equivalent satellite.

The described heuristic, iterative, optimization algorithm requires full

SIUA algorithm
Output: $\mathcal{S}_1$ & $\mathcal{S}_2$
Step 1: $\forall\ k = 1, 2 \dots M$ allocate the strongest channel norm to each satellite:
$\pi_{1(1)} = \arg\max ||\mathbf{h}_{k1}||$, $\mathbf{g}_{1(1)} = \mathbf{h}_{\pi_1 1}$
$\pi_{2(1)} = \arg\max ||\mathbf{h}_{k2}||$, $\mathbf{g}_{2(1)} = \mathbf{h}_{\pi_2 2}$
$\mathcal{S}_1 = \pi_{1(1)}$, $\mathcal{S}_2 = \pi_{2(1)}$
$\mathcal{T} = \{1, \dots M\} - \{\pi_{1(1)}, \pi_{2(1)}\}$ set of unprocessed users
$i = 1$ iteration counter
while $(|\mathcal{S}_1| < M_1)\,\&\,(|\mathcal{S}_2| < M_2)$
do
  Step 2: **forall the** *elements of* $\mathcal{T}_{(i)}$ **do**
    (a) $\mathbf{g}_{1k} = \mathbf{h}_{1k}\left(\mathbf{I}_K - \sum_{j=1}^{i-1} \frac{\mathbf{g}_{1(j)}^{\dagger}\mathbf{g}_{1(j)}}{||\mathbf{g}_{1(j)}||^2}\right)$
    $\mathbf{g}_{2k} = \mathbf{h}_{k2}\left(\mathbf{I}_K - \sum_{j=1}^{i-1} \frac{\mathbf{g}_{2(j)}^{\dagger}\mathbf{g}_{2(j)}}{||\mathbf{g}_{2(j)}||^2}\right)$
    (b) $\mathrm{I}_{1k}^{r} = \mathbf{h}_{k2}\left(\mathbf{W}_2\mathbf{W}_2^{\dagger}\right)\mathbf{h}_{k2}^{\dagger}$
    $\mathrm{I}_{2k}^{r} = \mathbf{h}_{k1}\left(\mathbf{W}_1\mathbf{W}_1^{\dagger}\right)\mathbf{h}_{k1}^{\dagger}$
    (c) $\mathrm{I}_{1k}^{i} = \prod_{l\epsilon\ \mathbf{t}}^{l\neq k}\left(\mathbf{h}_{l1}\left(\mathbf{W}_{1k}\mathbf{W}_{1k}^{\dagger}\right)\mathbf{h}_{l1}^{\dagger}\right)$
    $\mathrm{I}_{2k}^{i} = \prod_{l\epsilon\ \mathbf{t}}^{l\neq k}\left(\mathbf{h}_{l2}\left(\mathbf{W}_{2k}\mathbf{W}_{2k}^{\dagger}\right)\mathbf{h}_{l2}^{\dagger}\right)$
    where $\mathbf{W}_n, n = 1, 2$ is the ZF precoding matrix of each satellite with users allocated from previous iterations and $\mathbf{W}_{nk}, k\epsilon\ \mathbf{t}$ is the same matrix but with the kth user added.
  end
  Step 3: $\mu_{1(i)} = \max\{||g_{1k}||/\left(\mathrm{I}_{1k}^{r} \cdot \mathrm{I}_{1k}^{i}\right)\}$,
  $\mu_{2(i)} = \max\{||g_{2k}||/\left(\mathrm{I}_{2k}^{r} \cdot \mathrm{I}_{2k}^{i}\right)\}$
  if $\mu_{1(i)} \geq \mu_{2(i)}$ *&* $|\mathcal{S}_1| < M_1$ **then**
    $\pi_{(i)} = \arg\mu_{1(i)}$; $\mathcal{S}_1 = \mathcal{S}_1 \cup \{\pi_{(i)}\}$;
    $\mathbf{g}_{1(i)} = \mathbf{h}_{\pi_{(i)}}$;
  else
    $\pi_{(i)} = \arg\mu_{2(i)}$; $\mathcal{S}_2 = \mathcal{S}_2 \cup \{\pi_{(i)}\}$;
    $\mathbf{g}_{2(i)} = \mathbf{h}_{\pi_{(i)}}$;
  end
  $i = i + 1$;
  $\mathcal{T}_{(i)} = \mathcal{T}_{(i-1)} - \{\pi_{(i-1)}\}$;
end

Algorithm 5: Semiorthogonal Interference aware User Allocation algorithm (SIUA)

Table 6.1: Dual Satellite System Link Budget Parameters (identical for both satellites)

Parameter	Value
Orbit	GEO
Frequency band	Ka (20 GHz)
User link bandwidth	500 MHz
Number of beams	7
Beam diameter	600 Km
TWTA RF power @ saturation	+21 dBW
Max satellite antenna gain G_T	+52 dBi
Max user antenna Gain G_R	+40 dBi
Free space loss	−210 dB
Signal Power S	−97 dBW
Receiver noise power N	−118 dBW
SNR S/N	21 dB

knowledge of the CSI of all users. Consequently, coordination reduces the amount of data that needs to be exchanged since each GW handles only the data of the users allocated to the corresponding satellite. Moreover, SIUA runs only as many times as the number of transmit antennas and thus compromises a scalable solution that can be extended for larger multibeam systems. Another advantage of this solution is that the power optimization in each satellite, a convex optimization problem that requires some computational complexity, is decoupled from the algorithm execution. Additionally, despite the fact that the solution is heuristic and not optimal, it is considerably less complex since the optimal user allocation would require exhaustive search of all possible combinations of the users. Finally, SIUA, can be executed in a centralized location or run in parallel at the GWs that share CSI.

6.3.3 Performance Evaluation

To evaluate the performance of the proposed algorithm, two satellites each with seven beams where assumed. The low number of beams is only chosen to reduce the simulation time of the convex optimization beamforming problem and has no effect on the algorithm, as discussed in Sec. 6.3.2. It is however inline with the future considerations for the terabit satellites, where each GW is expected to handle between 5 and 8 beams. Additionally, the simulations are performed according to the link budget calculations described in Tab. 6.1, where it can be noted that the normal SNR operating point of current satellite systems is 21dB.

In Fig. 6.6, the results of Monte Carlo simulations that calculate the

performance in terms of system Sum Rate (SR) of the coexisting systems with and without cooperation, are presented. Due to random user positioning, 100 iterations where executed, each with a different user position pattern so that the average performance can be evaluated. The upper bound for the system performance is deduced assuming full cooperation amongst the transmitters. For this case two curves show the SR in bps/Hz: one for the average performance of random user positioning and one employing the algorithm developed in [53], namely the Semi-orthogonal User allocation (SUS) algorithm, which allocates users without regarding the coexistence of the systems. Subsequently, an average gain of 25% is noted by employing a simple user selection scheme, instead of randomly selecting users. Since in the fully cooperative system, interference is completely mitigated, SIUA is unnecessary.

The substantial performance gain from SIUA is proven in Fig. 6.6 for the more realistic case of coordinated systems. In this figure, SIUA is compared to SUS and also to an independent interfering system. From these curves, it is concluded that in the low SNR region, the SUS algorithm performs better, as expected since the noise limited regime is almost interference free. In the SNR region of interest, however, it is clear that the SIUA algorithm, by reducing the level of interference, provides substantial gains: more than 52% of improvement in terms of SR, over a non cooperative system and 28% of improvement over a coordinated system employing simple user selection. It is therefore concluded that the SIUA sacrifices some low SNR performance to provide substantial gains in the SNR region of interest. A simple switching scheme between the two algorithms can provide good performance over the whole SNR region of interest.

For each setting, ZF beamforming was performed in each satellite and the aggregate SR of the two independent interfering transmitters was calculated via (6.1). For this calculation the average total system SR is depicted versus the receive SNR in Fig. 6.6.

The SR, measured in bits per transmission since we assume fixed bandwidth, is calculated by assuming only interference from the adjacent satellite using (6.1)[1]. Additionally, the simulations are performed according to the link budget calculations described in Tab. 6.1, where it can be

[1]It should be clarified that under the common assumption of normalized noise, the terms transmit SNR and total on board available power P_{tot} describe the same quantity.

noted that the normal SNR operating point of current satellite systems is 21dB. Moreover, 100 users per beam are generated leading to a total pool of 1400 users over which the SIUA algorithm is executed. In Fig. 6.6, the system SR when the SIUA algorithm is executed is presented and also compared to the SR of a fully cooperative system.

By closely examining the results presented in Fig. 6.6 the performance of the proposed algorithm can be evaluated. The following conclusions about the performance of the SIUA algorithm are drawn: In the SNR region of interest, i.e. around 21dB, the coordination amongst the interfering satellites, can lead to more than 52% of improvement in terms of SR, over a non cooperative system, when the proposed SIUA algorithm is applied. As expected, the full cooperation of the two systems (data and CSI exchange) totally mitigates interference and leads to almost double performance of the system but at high implementation costs.

In Fig. 6.7, a coordinated system using SIUA, is compared to an ideal non interfering dual satellite system that employs frequency orthogonalization to allow the operability of the two coexisting satellites. This approach models the currently employed techniques of bandwidth splitting. In this plot it is proven that around the SNR area of interest, the proposed algorithm outperforms the conventional techniques (25% gain). Therefore, the SIUA comprises a candidate tool for handling ASI. As the SNR increases, the gain decreases as expected, since the conventional system operates under the ideal assumption of zero interference.

Finally, in Fig. 6.8, the behavior of the algorithm with respect to the size of the user pool is investigated. To this end, the achievable SR for a given value of SNR, i.e. 20dB, is calculated as the total number users increases and also compared to the performance of the SUS algorithm. In this figure it is proven that the algorithm reaches close to its maximum performance for a finite number of total users (600 users) and further increase of the user pool has little effects. From the same figure we note that the rate of convergence of the proposed technique to the saturation point is very similar to the SUS algorithm.

6.4 Summary

In the first part of the chapter, novel multicast aware scheduling methods are developed for the frame based precoding problem of Ch. 5. In summary, the gains due to multicast aware scheduling are more than 30%

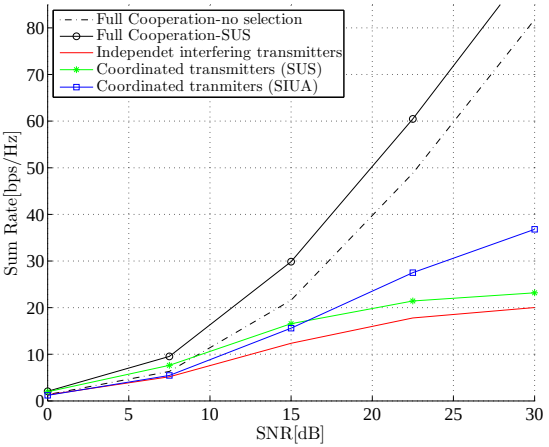

Figure 6.6: Evaluation of SIUA algorithm in terms of system sum rate, by comparison with optimal and interfering systems.

terms of throughput performance compared to conventional four color frequency reuse schemes. These gains also allow for up to 14 users per frame to be accommodated without losses over conventional systems.

The topic of dual satellite systems has been addressed in the second part of the chapter, where a suboptimal, simple scheduling method was proposed. This low complexity, heuristic algorithm that minimizes the interference between the two groups, while maintaining the orthogonality between the users of the same group, allows for the coexistence of two separate multibeam, joint processing, coordinated satellites. Thereby the overall system spectral efficiency can be increased. The cost of the proposed solution is the CSI exchange between the GWss. According to simulation results, the algorithm achieves 52% of spectral efficiency improvement over non-cooperative full frequency reuse systems and 25% improvement over non-cooperative conventional orthogonalized in the frequency domain systems. Subsequently, co-existing satellites that are coordinated can successfully exploit the spatial orthogonalization of users and operate over all the same spectrum.

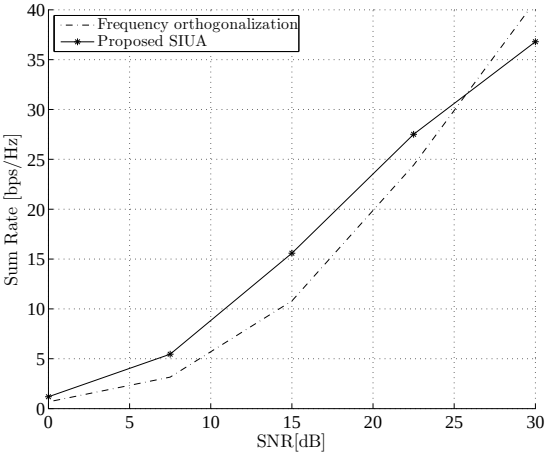

Figure 6.7: Comparison of the proposed coordinated system, with a conventional frequency orthogonalization system.

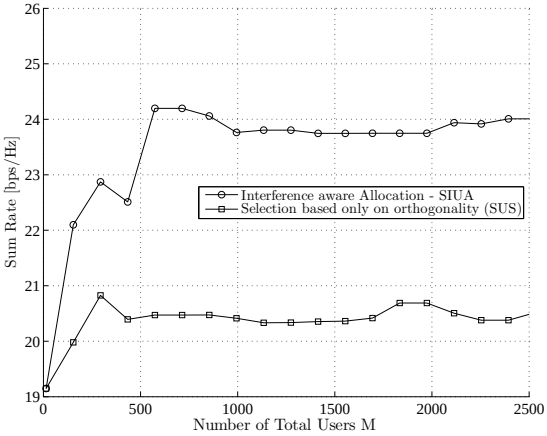

Figure 6.8: Algorithm performance with respect to the number of available for selection users.

Chapter 7

Conclusions

7.1 Conclusions

The present thesis has provided novel arguments supporting the application of multibeam joint processing techniques in SatComs. From a signal processing perspective, the practical barriers of applying advanced interference mitigation techniques, namely linear precoding for the FL and MUD for the RL of multibeam aggressive frequency reuse satellite systems, have been identified and tackled in this work. Both the forward and the return links of these systems have been examined under realistic assumptions and accurate simulation environments. Hence, the proposed signal processing techniques have shown great potential to be incorporated in the next generation High Throughput Satellite (HTS) systems. It has also been shown herein that the technology readiness level of the proposed methods allows for their consideration in existing satellite communications payloads with minor modifications on the ground segments, in the existing SatCom standards and in the capacity of the feeder link. However, such approaches are not expected to provide detrimental gains. By assuming more sophisticated payloads, compatible with aggressive frequency reuse configurations, the following techniques are proposed herein for the next generation SatComs.

Multibeam joint processing in the RL can potentially achieve more than twofold gains over current system architectures. These results has been supported by novel, closed form derivations for the spectral efficiency

of the RL multibeam channel under realistic assumptions. In more detail, the ergodic capacity of composite Rician/lognormal channels has been studied and analytically lower bounded. Also, accurate approximations for the MMSE of MU SIMO channels that exhibit full receive correlation have been derived. Therefore, an analytic framework straightforwardly extendable to account for various propagation parameters that provides important system design insights is established. Consequently, the adoption of multibeam decoding techniques in next generation satellite systems has the potential to surpass current performance limitations.

Concerning the FL, aggressive frequency reuse supported by linear precoding can provide substantial throughput gains. These gains are supported even with only minor modifications over existing SatCom standards. Focusing on one of the most critical limitations of precoding in DVBS2X based systems, that is the statistical multiplexing of users in a frame, the novel topic of frame based precoding is introduced and modeled. To provide an optimal solution to this problem and inspired by the practical per antenna power limitations, the SoA in multicast multigroup literature has been extended to optimally account these practical constraints in the design. What is more, user selection is proposed to optimize the performance of frame based precoding systems by gleaning the rich multiuser gains of the rich multiuser satellite environment. When compared to current conventional architectures, the proposed frame based precoding methods offer more than twofold gains. Consequently, it is proven that even with simple methods, the practical barrier of user framing can be overcome and the potential gains of precoding could be gleaned in next generation multibeam HTS systems.

7.2 Future Work

The main open topics to be addressed in the immediate extensions of this work include:

1. **Frame based precoding for non-linear satellite channels**: Peak-to-average power ratio (PAPR) constrained optimization has the potential to reduce the effects of the non-linear satellite channel. The main challenge of this direction lies in the dependence of the PAPR on the signal constellation and the baseband filtering. Furthermore, the optimal combination of precoding with channel

linearization methods (e.g. signal pre-distortion) is an open topic left for future extensions of this work.

2. **Modulation constrained optimal beamforming: Finite signal alphabets instead of Gaussian** Starting from the recent considerations of [138], optimal multicast multigroup precoder design with finite discrete code-books still remains an open topic. Any solutions on this problem can then further enhance the performance of frame based precoding.

3. **Channel acquisition for frame based precoding** While this work has been focused in providing solutions when CSI is readily available, in some sense (perfect or imperfect), the means to acquire such information have not been addressed. Hence, in the context of multibeam joint processing, techniques to measure and feedback the channel coefficients of the vector channels still remain to be explored.

4. **Rank-1 approximations for multicast multigroup beamforming under PACs**: The investigation of alternatives to Gaussian randomization towards reducing the implementation complexity and increasing the accuracy of the approximation are an on-going research topic with great potential. This direction will eventually simplify the transmitter design and reduce the implementation cost of the herein discussed methods.

Bibliography

[1] [Online]. Available: http://sslmda.com

[2] [Online]. Available: http://www.telesat.com

[3] [Online]. Available: http://www.eutelsat.com

[4] [Online]. Available: http://www.viasat.com

[5] J.-D. Gayrard, "Terabit satellite: Myth or reality?" in *Advances in Satellite and Space Communications, 2009. SPACOMM 2009. First International Conference on.* IEEE, 2009, pp. 1–6.

[6] D. Mignolo, R. Emiliano, A. Ginesi, A. Alamanac, P. Angeletti, and M. Harverson, "Approaching terabit/s satellite capacity: A system analysis," in *Proc. Ka Broadband Conf*, 2011.

[7] B. Evans and P. Thompson, "Key issues and technologies for a terabit/s satellite," in *28th AIAA International Communications Satellite Systems Conference (ICSSC-2010)*, 2010.

[8] P. Thompson, B. Evans, L. Castenet, M. Bousquet, and T. Mathiopoulos, "Concepts and technologies for a terabit/s satellite," in *SPACOMM 2011, The Third International Conference on Advances in Satellite and Space Communications*, 2011, pp. 12–19.

[9] O. Vidal, G. Verelst, J. Lacan, E. Alberty, J. Radzik, and M. Bousquet, "Next generation high throughput satellite system," in *Satellite Telecommunications (ESTEL), 2012 IEEE First AESS European Conference on.* IEEE, 2012, pp. 1–7.

[10] M. Angelone, N. Alagha, and A. Ginesi, "Advanced physical layer techniques: Performance limits within future multi-spot Ka-band networks," in *Satellite Telecommunications (ESTEL), 2012 IEEE First AESS European Conference on*, Oct. 2012, pp. 1–6.

[11] P.-D. M. Arapoglou, K. P. Liolis, M. Bertinelli, A. D. Panagopoulos, P. G. Cottis, and R. D. Gaudenzi, "MIMO over satellite: A review," *IEEE Communication Surveys and Tutorials*, vol. 13, no. 1, pp. 27–51, Mar. 2011.

[12] P.-D. Arapoglou, B. Shankar, A. Panagopoulos, and B. Ottersten, "Gateway diversity strategies in Q/V band feeder links," 2013.

[13] A. Gharanjik, B. S. M. R. Rao, P.-D. Arapoglou, and B. Ottersten, "Large scale transmit diversity in Q/V band feeder link with multiple gateways," in *Personal Indoor and Mobile Radio Communications (PIMRC), 2013 IEEE 24th International Symposium on*, Sept 2013, pp. 766–770.

[14] A. Gharanjik, B. Rao, P.-D. Arapoglou, and B. Ottersten, "Gateway switching in q/v band satellite feeder links," *Communications Letters, IEEE*, vol. 17, no. 7, pp. 1384–1387, Jul. 2013.

[15] E. Amyotte, Y. Demers, L. Hildebrand, M. Forest, S. Riendeau, S. Sierra-Garcia, and J. Uher, "Recent developments in Ka-band satellite antennas for broadband communications." in Proc. of *Europ. Conf. on. Antennas and Propagation (EuCAP), IEEE* pp.1,5, Apr. 2010

[16] ETSI TR 102 376 V1.1.1, "Digital video broadcasting (DVB); user guidelines for the second generation system for broadcasting, interactive services, news gathering and other broad-band satellite applications (DVB-S2)." Feb. 2005, tR Patent 102,376.

[17] ETSI TS 101 545-1 V1.1.1 (2012-05), "Second generation DVB interactive satellite system (DVB-RCS2)."

[18] M. Angelone, A. Ginesi, and A. Chowdhary, "Performance of an alternative SSPA-based payload for next generation broadband multi-spot beam systems."

[19] ETSI EN 302 307 V1.1.2, "Digital video broadcasting (DVB); second generation framing structure, channel coding and modulation systems for broadcasting, interactive services, news gathering and other broad-band satellite applications (DVB-S2)."

[20] A. Morello and V. Mignone, "DVB-S2: the second generation standard for satellite broad-band services," *Proc. IEEE*, vol. 94, no. 1, pp. 210–227, 2006.

[21] H. Bischl, H. Brandt, T. de Cola, R. De Gaudenzi, E. Eberlein, N. Girault, E. Alberty, S. Lipp, R. Rinaldo, B. Rislow *et al.*, "Adaptive coding and modulation for satellite broadband networks: From theory to practice," *Int. J. of Satell. Commun. and Netw.*, vol. 28, no. 2, pp. 59–111, 2010.

[22] E. Alberty, S. Defever, C. Moreau, R. De Gaudenzi, A. Ginesi, R. Rinaldo, G. Gallinaro, and A. Vernucci, "Adaptive coding and modulation for the DVB-S2 standard interactive applications: capacity assessment and key system issues," *IEEE Wireless Commun. Mag.*, vol. 14, no. 4, pp. 61–69, 2007.

[23] DVB Blue Book A83-2, "Second generation framing structure, channel coding and modulation systems for broadcasting, interactive services, news gathering and other broadband satellite applications; part II: S2-extensions (S2X)."

[24] G. Zheng, S. Chatzinotas, and B. Ottersten, "Multi-gateway cooperation in multibeam satellite systems," in *Proc. of 23rd IEEE symp. on Person. Indoor Mob. Radio Commun.*, 2012.

[25] S. V. Hanly and P. A. Whiting, "Information-theoretic capacity of multi-receiver networks," *Telecommun. Syst.*, vol. 1, pp. 1–42, 1993.

[26] A. Wyner, "Shannon-theoretic approach to a Gaussian cellular multiple-access channel," *IEEE Trans. Inf. Theory*, vol. 40, no. 6, pp. 1713–1727, Nov 1994.

[27] O. Somekh and S. Shamai, "Shannon-theoretic approach to a Gaussian cellular multiple-access channel with fading," *IEEE Trans. Inf. Theory*, vol. 46, no. 4, pp. 1401–1425, July 2000.

[28] S. Chatzinotas, M. Imran, and C. Tzaras, "On the capacity of variable density cellular systems under multicell decoding," *IEEE Commun. Lett.*, vol. 12, no. 7, pp. 496–498, July 2008.

[29] S. Chatzinotas, M. A. Imran, and C. Tzaras, "Optimal information theoretic capacity of the planar cellular uplink channel," in *IEEE 9th Workshop on Signal Processing Advances in Wireless Communications (SPAWC'08)*, Pernambuco, Brazil, Jul. 2008, pp. 196–200.

[30] D. Aktas, M. Bacha, J. Evans, and S. Hanly, "Scaling results on the sum capacity of cellular networks with MIMO links," *IEEE Trans. Inf. Theory*, vol. 52, no. 7, pp. 3264–3274, July 2006.

[31] S. Chatzinotas, M. A. Imran, and C. Tzaras, "Uplink capacity of MIMO cellular systems with multicell processing," in *IEEE International Symposium on Wireless Communication Systems (ISWCS'08)*, Reykjavik, Iceland, Oct 2008, pp. 453–457.

[32] S. Chatzinotas, M. Imran, and R. Hoshyar, "On the multicell processing capacity of the cellular MIMO uplink channel in correlated Rayleigh fading environment," *IEEE Trans. Wireless Commun.*, vol. 8, no. 7, pp. 3704–3715, July 2009.

[33] O. Simeone, O. Somekh, H. Poor, and S. Shamai, "Distributed MIMO in multi-cell wireless systems via finite-capacity links," in *Communications, Control and Signal Processing, 2008. ISCCSP 2008. 3rd International Symposium on*, Mar. 2008, pp. 203–206.

[34] N. Jindal, "MIMO broadcast channels with finite-rate feedback," *IEEE Trans. Inf. Theory*, vol. 52, no. 11, pp. 5045–5060, 2006.

[35] R. Bhagavatula and R. W. H. Jr., "Adaptive limited feedback for sum-rate maximizing beamforming in cooperative multicell systems," *CoRR*, vol. abs/0912.0962, 2009.

[36] E. Bjornson, R. Zakhour, D. Gesbert, and B. Ottersten, "Cooperative multicell precoding: Rate region characterization and distributed strategies with instantaneous and statistical CSI," *IEEE Trans. Signal Process.*, vol. 58, no. 8, pp. 4298 –4310, 2010.

[37] T. M. Cover and J. A. Thomas, *Elements of information theory*, 2nd ed. New York, NY, USA: Wiley, 2006.

[38] M. K. Varanasi and T. Guess, "Optimum decision feedback multiuser equalization with successive decoding achieves the total capacity of the Gaussian multiple-access," in *Thirty-First Asilomar Conference on Signals, Systems and Computers*, vol. 2, Nov 1997, pp. 1405–1409.

[39] I. E. Telatar, "Capacity of multi-antenna Gaussian channels," *Eur. Trans. Telecommun.*, vol. 10, no. 6, pp. 585–595, Nov. 1999.

[40] A. M. Tulino and S. Verdú, "Random matrix theory and wireless communications," *Commun. Inf. Theory*, vol. 1, no. 1, pp. 1–182, 2004.

[41] S. Verdú and S. Shamai, "Spectral efficiency of CDMA with random spreading," *IEEE Trans. Inf. Theory*, vol. 45, no. 2, pp. 622–640, Mar 1999.

[42] S. Shamai and S. Verdú, "The impact of frequency-flat fading on the spectral efficiency of CDMA," *IEEE Trans. Inf. Theory*, vol. 47, no. 4, pp. 1302–1327, May 2001.

[43] W. Hachem, O. Khorunzhiy, P. Loubaton, J. Najim, and L. Pastur, "A new approach for mutual information analysis of large dimensional multi-antenna channels," *IEEE Trans. Inf. Theory*, vol. 54, no. 9, pp. 3987–4004, Sept. 2008.

[44] J. Hoydis, A. Kammoun, J. Najim, and M. Debbah, "Outage performance of cooperative small-cell systems under Rician fading channels," in *Proc. IEEE Int. Work. Signal Process. Advances Wireless Commun. (SPAWC)*, June 2011, pp. 551–555.

[45] D. Kaltakis, M. Imran, and C. Tzaras, "Information theoretic capacity of cellular multiple access channel with shadow fading," *IEEE Trans. Commun.*, vol. 58, no. 5, pp. 1468–1476, May 2010.

[46] M. Matthaiou, N. D. Chatzidiamantis, and G. K. Karagiannidis, "A new lower bound on the ergodic capacity of distributed MIMO systems," *IEEE Signal Process. Lett.*, vol. 18, no. 4, pp. 227–230, Apr. 2011.

[47] W. Roh and A. Paulraj, "MIMO channel capacity for the distributed antenna systems," in *Proc. IEEE Veh. Tech. Conf. (VTC)*, vol. 2, Sept. 2002, pp. 706–709.

[48] W. Roh and A. Paulraj, "Outage performance of the distributed antenna systems in a composite fading channel," in *Proc. IEEE Veh. Tech. Conf. (VTC)*, vol. 3, Sept. 2002, pp. 1520–1524.

[49] D. Wang, X. You, J. Wang, Y. Wang, and X. Hou, "Spectral efficiency of distributed MIMO cellular systems in a composite fading channel," in *Proc. IEEE Int. Conf. Commun. (ICC)*, May 2008, pp. 1259–1264.

[50] C. Zhong, K.-K. Wong, and S. Jin, "Capacity bounds for MIMO Nakagami-m fading channels," *IEEE Trans. Signal Process.*, vol. 57, no. 9, pp. 3613–3623, Sep. 2009.

[51] M. Matthaiou, N. Chatzidiamantis, G. Karagiannidis, and J. Nossek, "On the capacity of generalized-K fading MIMO channels," *IEEE Trans. Signal Process.*, vol. 58, no. 11, pp. 5939–5944, Nov. 2010.

[52] S. Al-Ahmadi and H. Yanikomeroglu, "The ergodic and outage capacities of distributed antenna systems in generalized-k fading channels," in *Proc. IEEE Int. Symp. Personal Indoor Mob. Radio Commun. (PIMRC)*,, Sept. 2010, pp. 662 –666.

[53] T. Yoo and A. Goldsmith, "On the optimality of multi-antenna broadcast scheduling using zero-forcing beamforming,," *IEEE J. Select. Areas Commun.*, vol. 24, Mar. 2006.

[54] M. Costa, "Writing on dirty paper," *IEEE Trans. Inf. Theory*, vol. 29, no. 3, pp. 439–441, 1983.

[55] H. Weingarten, Y. Steinberg, and S. Shamai, "The capacity region of the Gaussian multiple-input multiple-output broadcast channel," *IEEE Trans. Inf. Theory*, vol. 52, no. 9, pp. 3936–3964, 2006.

[56] W. Yu and T. Lan, "Transmitter optimization for the multi-antenna downlink with per-antenna power constraints," *IEEE Transactions on Signal Processing*, vol. 55, no. 6, pp. 2646–2660, Jul. 2007.

[57] M. Bengtsson and B. Ottersten, "Optimal and suboptimal transmit beamforming," in *Handbook of Antennas in Wireless Communications*. CRC Press, 2001, pp. 18–1–18–33, qC 20111107.

[58] M. Bengtsson and B. Ottersten, "Optimal downlink beamforming using semidefinite optimization," in *Proc. of Annual Allert. Conf. on Commun. Control and Computing*, vol. 37. Citeseer, 1999, pp. 987–996.

[59] M. Schubert and H. Boche, "Solution of the multiuser downlink beamforming with individual SINR constraints," *IEEE Trans. Veh. Technol.*, vol. 53, no. 1, pp. 18–28, 2004.

[60] W. Yu and T. Lan, "Transmitter optimization for the multi-antenna downlink with per-antenna power constraints," *IEEE Trans. Signal Process.*, vol. 55, no. 6, pp. 2646–2660, June 2007.

[61] E. Bjornson, M. Bengtsson, and B. Ottersten, "Optimal multi-user transmit beamforming: Difficult problem with a simple solution structure," *IEEE Signal Processing. Mag.*, vol. 31, no. 4, pp. 142–148, Jul. 2014.

[62] H. Viswanathan, S. Venkatesan, and H. Huang, "Downlink capacity evaluation of cellular networks with known-interference cancellation," *IEEE J. Select. Areas Commun.*, vol. 21, no. 5, pp. 802–811, 2003.

[63] G. Caire and S. Shamai, "On the achievable throughput of a multiantenna Gaussian broadcast channel," *IEEE Trans. Inf. Theory*, vol. 49, no. 7, pp. 1691–1706, July 2003.

[64] A. Wiesel, Y. C. Eldar, and S. Shamai, "Zero forcing precoding and generalized inverses," *IEEE Trans. Signal Process.*, vol. 56, no. 9, pp. 4409–4418, Sept. 2008.

[65] B. Hochwald, C. Peel, and A. Swindlehurst, "A vector-perturbation technique for near-capacity multiantenna multiuser communication - part ii: perturbation," *IEEE Trans. Commun.*, vol. 53, no. 3, pp. 537–544, 2005.

[66] C. Peel, B. Hochwald, and A. Swindlehurst, "A vector-perturbation technique for near-capacity multiantenna multiuser communication - part i: channel inversion and regularization," *IEEE Trans. Commun.*, vol. 53, no. 1, pp. 195–202, 2005.

[67] R. Muharar and J. Evans, "Downlink beamforming with transmit-side channel correlation: A large system analysis," in *Communications (ICC), 2011 IEEE International Conference on*, june 2011, pp. 1 –5.

[68] D. Christopoulos, P.-D. Arapoglou, S. Chatzinotas, and B. Ottersten, "Linear precoding in multibeam SatComs: Practical constraints," in *31st AIAA International Communications Satellite Systems Conference (ICSSC)*, Florence, IT, Oct. 2013.

[69] G. Dartmann, X. Gong, W. Afzal, and G. Ascheid, "On the duality of the max min beamforming problem with per-antenna and per-antenna-array power constraints," *IEEE Trans. Veh. Technol.*, vol. 62, no. 2, pp. 606–619, Feb 2013.

[70] K. Karakayali, R. Yates, G. Foschini, and R. Valenzuela, "Optimum zero-forcing beamforming with per-antenna power constraints," in *Information Theory, 2007. ISIT 2007. IEEE International Symposium on*. IEEE, 2008, pp. 101–105.

[71] S. Boyd and L. Vandenberghe, *Convex optimization*. Cambridge Univ. Press, 2004.

[72] B. L. Ng, J. Evans, S. Hanly, and D. Aktas, "Distributed downlink beamforming with cooperative base stations," *IEEE Trans. Inf. Theory*, vol. 54, no. 12, pp. 5491 –5499, dec. 2008.

[73] Y. Huang, G. Zheng, M. Bengtsson, K.-K. Wong, L. Yang, and B. Ottersten, "Distributed multicell beamforming with limited intercell coordination," *IEEE Trans. Signal Process.*, vol. 59, no. 2, pp. 728 –738, feb. 2011.

[74] M. J. Lopez, "Multiplexing, scheduling and multicasting strategies for antenna arrays in wireless networks," Ph.D. dissertation, Dept. of Elect. Eng. and Comp. Sci., MIT Cambridge, MA, Mar. 2002.

[75] E. Karipidis, N. Sidiropoulos, and Z.-Q. Luo, "Quality of service and max-min fair transmit beamforming to multiple cochannel multicast groups," *IEEE Trans. Signal Process.*, vol. 56, no. 3, pp. 1268–1279, 2008.

[76] N. Sidiropoulos, T. Davidson, and Z.-Q. Luo, "Transmit beamforming for physical-layer multicasting," *IEEE Trans. Signal Process.*, vol. 54, no. 6, pp. 2239–2251, 2006.

[77] E. Karipidis, N. Sidiropoulos, and Z.-Q. Luo, "Transmit beamforming to multiple co-channel multicast groups," in *Proc. of 1st Int. Workshop on Comput. Adv. in Multi-Sensor Adapt. Process. (CAMSAP)*, 2005, pp. 109–112.

[78] Y. Gao and M. Schubert, "Group-oriented beamforming for multistream multicasting based on quality-of-service requirements," in *Proc. of 1st Int. Workshop on Comput. Adv. in Multi-Sensor Adapt. Process. (CAMSAP)*, 2005, pp. 193–196.

[79] A. Schad and M. Pesavento, "Max-min fair transmit beamforming for multi-group multicasting," in *Proc. of Int. ITG Workshop on Smart Ant. (WSA)*, 2012, pp. 115–118.

[80] Y. C. B. Silva and A. Klein, "Linear transmit beamforming techniques for the multigroup multicast scenario," *IEEE Trans. Veh. Technol.*, vol. 58, no. 8, pp. 4353–4367, 2009.

[81] Z. Xiang, M. Tao, and X. Wang, "Coordinated multicast beamforming in multicell networks," *IEEE Trans. Wireless Commun.*, vol. 12, no. 1, pp. 12–21, 2013.

[82] T. Yoo and A. Goldsmith, "Optimality of zero-forcing beamforming with multiuser diversity," in *IEEE International Conference on Communications (ICC 2005)*, vol. 1, May 2005, pp. 542–546.

[83] M. Diaz, N. Courville, C. Mosquera, G. Liva, and G. Corazza, "Non-linear interference mitigation for broadband multimedia satellite systems," in *Proc. Int. Work. Sat. Space Commun. (IWSSC)*, Sept. 2007, pp. 61–65.

[84] Satellite Network of Experts (SatNEx) 3, "Call of order 2-task 1: Fair comparison and combination of advanced interference mitigation techniques," ESA Contract 23089/10/NL/CPL.

[85] G. Zheng, S. Chatzinotas, and B. Ottersten, "Generic optimization of linear precoding in multibeam satellite systems," *IEEE Trans. Wireless Commun.*, vol. 11, no. 6, pp. 2308 –2320, Jun. 2012.

[86] D. Christopoulos, S. Chatzinotas, M. Matthaiou, and B. Ottersten, "Capacity analysis of multibeam joint decoding over composite satellite channels," in *Proc. of 45th Asilomar Conf. on Signals, Systems and Computers*, Pacific Grove, CA, Nov. 2011, pp. 1795 –1799.

[87] N. Letzepis and A. Grant, "Capacity of the multiple spot beam satellite channel with Rician fading," *IEEE Trans. Inf. Theory*, vol. 54, no. 11, pp. 5210–5222, Nov. 2008.

[88] M. Moher, "Multiuser decoding for multibeam systems," *IEEE Trans. Veh. Technol.*, vol. 49, no. 4, pp. 1226–1234, Jul. 2000.

[89] R. M. M. Debbah, G. Gallinaro, R. Rinaldo, and A. Vernucci, "Interference mitigation for the reverse-link of interactive satellite networks," in *9th International Workshop on Signal Processing for Space Communications (SPSC 2006)*, Noordwijk, The Netherlands, 2006.

[90] G. Alfano, A. De Maio, and A. M. Tulino, "A theoretical framework for LMS MIMO communication systems performance analysis," *IEEE Trans. Inf. Theory*, vol. 56, no. 11, pp. 5614–5630, Nov. 2010.

[91] P. Dharmawansa and M. McKay, "Extreme eigenvalue distributions of Gamma-Wishart random matrices," in *Communications (ICC), 2011 IEEE International Conference on*, june 2011, pp. 1 –6.

[92] D. Tse and S. Hanly, "Linear multiuser receivers: effective interference, effective bandwidth and user capacity," *IEEE Trans. Inf. Theory*, vol. 45, no. 2, pp. 641–657, Mar 1999.

[93] K. Kumar, G. Caire, and A. Moustakas, "Asymptotic performance of linear receivers in MIMO fading channels," *IEEE Trans. Inf. Theory*, vol. 55, no. 10, pp. 4398 –4418, Oct. 2009.

[94] J. Arnau and C. Mosquera, "Performance analysis of multiuser detection for multibeam satellites under rain fading," in *6th Adv. Satellite Multimedia Syst. Conf. (ASMS) and 12th Sig. Process. for Space Commun. Workshop (SPSC)*, Baiona, Spain, Sep 2012, pp. 197–204.

[95] D. Guo, S. Shamai, and S. Verdu, "Mutual information and minimum mean-square error in Gaussian channels," *IEEE Trans. Inf. Theory*, vol. 51, no. 4, pp. 1261 –1282, Apr. 2005.

[96] M. McKay, I. Collings, and A. Tulino, "Achievable sum rate of MIMO MMSE receivers: A general analytic framework," *IEEE Trans. Inf. Theory*, vol. 56, no. 1, pp. 396 –410, Jan. 2010.

[97] S. Jin, X. Gao, and X. You, "On the ergodic capacity of rank-1 Ricean-fading MIMO channels," *IEEE Trans. Inf. Theory*, vol. 53, no. 2, pp. 502–517, Feb. 2007.

[98] G. Gallinaro, G. Caire, M. Debbah, L. Cottatellucci, R. Mueller, and R. Rinaldo, "Perspectives Of Adopting Inteference Mitigation Techniques In The Context Of Broadband Multimedia Satellite Systems," in *Proc. ICSC 2005*.

[99] L. Cottatellucci, M. Debbah, E. Casini, R. Rinaldo, R. Mueller, M. Neri, and G. Gallinaro, "Interference mitigation techniques for broadband satellite system," in *24th AIAA International Communications Satellite Systems Conference (ICSSC 2006)*, San Diego, USA, 2006.

[100] N. Zorba, M. Realp, and A. Perez-Neira, "An improved partial CSIT random beamforming for multibeam satellite systems," in *10th International Workshop on Signal Processing for Space Communications (SPSC 2008)*, 2008, pp. 1 –8.

[101] M. Poggioni, M. Berioli, and P. Banelli, "BER performance of multibeam satellite systems with Tomlinson-Harashima precoding," in *IEEE International Conference on Communications (ICC 2009)*, 2009, pp. 1 –6.

[102] S. Chatzinotas, G. Zheng, and B. Ottersten, "Energy-efficient mmse beamforming and power allocationin multibeam satellite systems," in *Asilomar Conference on Signals, Systems and Computers (ACSSC'11)*, Nov 2011.

[103] S. Chatzinotas, G. Zheng, and B. Ottersten, "Joint precoding with flexible power constraints in multibeam satellite systems," in *IEEE Global Telecommunications Conference (GLOBECOM 2011)*, Houston, Texas, 2011.

[104] B. Devillers, A. Perez-Neira, and C. Mosquera, "Joint linear precoding and beamforming for the forward link of multi-beam broadband satellite systems," in *IEEE Global Telecommunications Conference (GLOBECOM 2011)*, Houston, Texas, Dec 2011.

[105] D. Christopoulos, S. Chatzinotas, G. Zheng, J. Grotz, and B. Ottersten, "Linear and non-linear techniques for multibeam joint processing in satellite communications," *EURASIP J. on Wirel. Commun. and Networking 2012, 2012:162.* [Online]. Available: http://jwcn.eurasipjournals.com/content/2012/1/162

[106] D. Christopoulos, J. Arnau, S. Chatzinotas, C. Mosquera, and B. Ottersten, "MMSE performance analysis of generalized multibeam satellite channels," *IEEE Commun. Lett.*, vol. 17, no. 7, pp. 1332–1335, 2013.

[107] D. Christopoulos, S. Chatzinotas, J. Krause, and B. Ottersten, "Multiuser detection for mobile satellite systems: A fair performance evaluation," in *Proc. of 77th IEEE Vehic. Technol. Conf.*, 2013.

[108] D. Christopoulos, S. Chatzinotas, and B. Ottersten, "Multicast multigroup beamforming under per-antenna power constraints," in *Proc. of IEEE International Communications Conference (ICC)*, Sydney, AU, Jul. 2014, *preprint:* arXiv:1407.0004 [cs.IT].

[109] D. Christopoulos, S. Chatzinotas, and B. Ottersten, "Weighted fair multicast multigroup beamforming under per-antenna power constraints," *IEEE Trans. Signal Process.*, vol. 62, no. 19, pp. 5132–5142, Oct. 2014.

[110] D. Christopoulos, S. Chatzinotas, and B. Ottersten, "Frame based precoding in satellite communications: A multicast approach," in *Proc. of IEEE Adv. Satellite Multimedia Syst. Conf. (ASMS)*, Livorno, IT, Sep. 2014, *preprint:* arXiv:1406.6852 [cs.IT].

[111] D. Christopoulos, S. Chatzinotas, and B. Ottersten, "Sum rate maximizing multigroup multicast beamforming under per-antenna power constraints," in *Proc. of IEEE Glob. Commun. Conf.*, Austin,TX, USA, Dec. 2014, *preprint:* arXiv:1407.0005 [cs.IT].

[112] D. Christopoulos, S. Chatzinotas, and B. Ottersten, 'Multicast Multigroup Precoding and User Scheduling for Frame-Based Satellite Communications," *IEEE Trans. Wireless Commun.*, vol. PP, no. 99, pp. 1–1, 2015, *DOI: 10.1109/TWC.2015.2424961.*

[113] D. Christopoulos, S. Chatzinotas, and B. Ottersten, "User scheduling for coordinated dual satellite systems with linear precoding," in *Proc. of IEEE Int. Commun. Conf.* Budapest, HU, 2013.

[114] J. Arnau, D. Christopoulos, S. Chatzinotas, C. Mosquera, and B. Ottersten, "Performance of the multibeam satellite return link with correlated rain attenuation," *IEEE trans. in Wirel. Commun.*, vol. 13, no. 11, pp. 6286–6299, Nov. 2014.

[115] A. Zohair, B. Shankar, D. Christopoulos, and P.-D. Arapoglou, "Timing and frequency synchronisation for multiuser detection on the return link of interactive mobile satellite networks," in *31st AIAA International Communications Satellite Systems Conference (ICSSC)*, Florence, IT, Oct. 2013.

[116] S. K. Sharma, D. Christopoulos, S. Chatzinotas, and B. Ottersten, "New generation cooperative and cognitive dual satellite systems: Performance evaluation," in *32st AIAA International Communications Satellite Systems Conference (ICSSC)*, San Diego, US, Sep. 2014.

[117] S. Chatzinotas, D. Christopoulos, and B. Ottersten, "Coordinated multi-point decoding with dual-polarized antennas," in *Proc. of 7th Int. Wirel. Commun. and Mobile Comput. Conf.*, Jul. 2011, pp. 157 –161.

[118] D. Christopoulos, S. Chatzinotas, G. Taricco, M. A. Vazquez, A. Perez-Neira, P.-D. Arapoglou, and A. Ginesi, *Cooperative and Cognitive satellite systems*. Elsevier, 2014, ch. Multibeam Joint Precoding: Frame Based Design.

[119] D. Christopoulos, S. Chatzinotas, and B. Ottersten, *Cooperative and Cognitive satellite systems*. Elsevier, 2014, ch. User Scheduling in Cooperative Satellite Systems.

[120] N. Letzepis and A. Grant, "Information capacity of multiple spot beam satellite channels," in *Proc. Australian Commun. Th. Work.*, Feb. 2005, pp. 168–174.

[121] O. Oyman, R. Nabar, H. Bölcskei, and A. Paulraj, "Characterizing the statistical properties of mutual information in MIMO channels," *IEEE Trans. Signal Process.*, vol. 51, no. 11, pp. 2784 – 2795, Nov. 2003.

[122] A. Lapidoth and S. Moser, "Capacity bounds via duality with applications to multiple-antenna systems on flat-fading channels," *IEEE Trans. Inf. Theory*, vol. 49, no. 10, pp. 2426–2467, Oct. 2003.

[123] S. Moser, "Duality-based bounds on channel capacity," Ph.D. dissertation, Swiss Federal Institute of Technology (ETH), Switzerland, Oct. 2004.

[124] B. Vucetic and J. Du, "Channel modeling and simulation in satellite mobile communication systems," *IEEE J. Select. Areas Commun.*, vol. 10, no. 8, pp. 1209–1217, Oct. 1992.

[125] S. Verdú, *Multiuser Detection*. UK: Cambridge University Press, 1998.

[126] Z.-Q. Luo, W.-K. Ma, A.-C. So, Y. Ye, and S. Zhang, "Semidefinite relaxation of quadratic optimization problems," *IEEE Signal Processing Mag.*, vol. 27, no. 3, pp. 20–34, 2010.

[127] Y. E. A. Wiesel and S. Shamai, "Linear precoding via conic optimization for fixed MIMO receivers," *IEEE Trans. Signal Process.*, vol. 54, no. 1, pp. 161–176, Jan. 2006.

[128] Y. Ye, *Interior point algorithms: theory and analysis.* John Wiley & Sons, 2011, vol. 44.

[129] M. Kaliszan, E. Pollakis, and S. Stanczak, "Multigroup multicast with application-layer coding: Beamforming for maximum weighted sum rate," in *Wireless Communications and Networking Conference (WCNC), 2012 IEEE*, 2012, pp. 2270–2275.

[130] S. Stanczak, M. Wiczanowski, and H. Boche, *Fundamentals of resource allocation in wireless networks: theory and algorithms.* Springer Publishing Company, Incorporated, 2009.

[131] E. Karipidis, N. Sidiropoulos, and Z.-Q. Luo, "Convex transmit beamforming for downlink multicasting to multiple co-channel groups," in *Proc. of IEEE Int. Conf. on Acoustics, Speech and Signal Proc. (ICASSP)*, vol. 5, May 2006.

[132] E. Karipidis, N. Sidiropoulos, and Z.-Q. Luo, "Far-field multicast beamforming for uniform linear antenna arrays," *IEEE Trans. Signal Process.*, vol. 55, no. 10, pp. 4916–4927, Oct 2007.

[133] A. Gershman, N. Sidiropoulos, S. Shahbazpanahi, M. Bengtsson, and B. Ottersten, "Convex optimization-based beamforming," *IEEE Signal Processing Mag.*, vol. 27, no. 3, pp. 62–75, 2010.

[134] M. Shenouda and T. Davidson, "Convex conic formulations of robust downlink precoder designs with quality of service constraints," *IEEE J. Select. Topics Signal Process.*, vol. 1, no. 4, pp. 714–724, Dec. 2007.

[135] N. Jindal, S. Vishwanath, and A. Goldsmith, "On the duality of Gaussian multiple-access and broadcast channels," *IEEE Trans. Inf. Theory*, vol. 50, no. 5, pp. 768–783, May 2004.

[136] Z. Chen, W. Zhang, and G. Wei, "Robust transmit beamforming for multigroup multicasting," in *IEEE Vehic. Tech. Conf. (VTC Fall)*, Sept 2012, pp. 1–5.

[137] R. L.-U. Choi and R. Murch, "New transmit schemes and simplified receivers for MIMO wireless communication systems," *IEEE Trans. Wireless Commun.*, vol. 2, no. 6, pp. 1217–1230, 2003.

[138] M. Wang, W. Zeng, and C. Xiao, "Linear precoding for MIMO multiple access channels with finite discrete inputs," *IEEE Trans. Wireless Commun.*, vol. 10, no. 11, pp. 3934 –3942, Nov. 2011.

[139] G. Taricco, "Linear precoding methods for multi-beam broadband satellite systems," in *European Wireless 2014; 20th European Wireless Conference; Proceedings of*, May 2014, pp. 1–6.

[140] P.-D. Arapoglou, A. Ginesi, G. Taricco, D. Christopoulos, S. Chatzinotas, B. Ottersten, M.-Á. Vázquez, A.-I. Pérez-Neira, S. Andrenacci, A. Vanelli-Coralli "Joint Transmitter Signal Processing in Multi-Beam Satellite Systems," in *European Space Agency Patent: 641 - 205628EP TE/BD*, 2014